UNIVERSITÀ
DEGLI STUDI
DI PADOVA

PhD in ECONOMICS AND MANAGEMENT
ECONOMICS CURRICULUM
XXXI CYCLE
Department of Economics and Management
University of Padova

Essays on Energy Markets

Head of the PhD Program: Prof. Antonio Nicolò

Supervisor: Prof. Tiziano Vargiolu

PhD Candidate: Maria Flora

30 September 2018

Acknowledgments

Pursuing a Ph.D. is a venture: the path seems long and perilous, and you start with a vague idea of what to expect. However, the journey can be incredible, and like Ulysses in pursuing his quest for knowledge, "much have I seen and known; [...] myself not least". I wasn't alone along this journey; thus, I wish to thank all the people who made this work possible.

First and foremost, I would like to thank my supervisor, Tiziano, for always being there for me and for guiding my research. Your constant help, advice and support have been fundamental to my research, you helped me grow as a researcher, and I am thankful for all the wonderful opportunities you gave me (including a random David Guetta concert in the middle of Asia). A profound gratitude also goes to Álvaro, working with you in Oxford has been an amazing experience. You've been the Virgilio to my wavery path in the *selva oscura* of stochastic control theory. Without your guidance, I'd be probably still wandering somewhere in the Wrath Circle. Special thanks to Michael as well, and our (predictable) tennis matches and (serendipitous) conversations. Marco, thank you for your incredibly valuable help and useful suggestions throughout this thesis work. I'd also like to thank Michele Moretto, who helped me in the early stages of my Ph.D. career, and Antonio Nicolò, the head of the Ph.D. program, for his support and useful advice during seminars and throughout my doctoral work.

I also owe my family, you taught me the love and curiosity about life in all aspects and to look beneath the surface. Thank you for your constant support, love and help. Federica, thank you for always being there, even when it means having to listen (or pretending to being listening) to boring rants about codes not working the way they should. In the vastitude of space and time, I feel blessed we are both sharing the here and now. Leandro, you are the (positive) Black Swan event of the "heartiness of people in Finance" index, and the best buddy I could hope for. You and Oxford will always hold a special place in my heart. Thank you Giuliana, Giulia and Sabrina: my expected value of Padova conditional on Venezia was pretty low, but you proved my model was misspecified. You are family to me. I'd also like to thank Lara, for being an amazing friend, and my fellow companions of Ph.D. adventures: Rossella, Matin, Jasmine, Elham, Costantino (and Frevd) and everyone in Padova and in Oxford I have shared part of my life with. I owe you all.

30 September 2018 Maria Flora

Contents

List of Figures

List of Tables

Chapter 1

Introduction

During the last decades, the energy sector, and in particular the electricity one, have undergone a remarkable transition around the world. The increasing competition in the market, the growing penetration of renewable generation and the pressure for decarbonisation are all part of the process. Moreover, in Europe, the recent market coupling initiatives are paving the road for an integrated European electricity market, and the aim is to enable the free movement of electricity across the different power regions.

This thesis builds from this paradigm and investigates some of the most recent changes relative to the energy market, in the general context of the European region.

In particular, Chapter 2 investigates the relationship between the European electricity market and the EU ETS, namely the European Union Emission Trading System. This chapter assesses the ability of the scheme in delivering low-carbon investments at the firm level in the electricity generation sector, by modeling, in a real option framework, a price taker electricity producer subject to the EU ETS jurisdiction. It also investigates the effects of a carbon price stabilization mechanism on the timing of the investment decision.

Chapter 3 instead looks into the so-called Capacity Remuneration Mechanisms, and in particular into the pricing of the reliability option, which is a market mechanism used to ensure security of supply in electricity markets. This tool is about to be introduced in the Italian electricity market, and this chapter develops methodologies for its modeling and shows that, in the sim-

plest contract design, the reliability option can be written as the integral of call options on the power price, with a strike price that can be modeled either as a fixed quantity or as a stochastic process itself (so that it represents the marginal cost of the marginal technology used to produce electricity). The value of the Reliability Option is simulated under a real-market calibration, using data of the Italian power market. A sensitivity analysis finally highlights the impact of the power and strike price levels and of their volatility, mean reversion speed and correlation on the Reliability Option valuation.

Finally, Chapter 4 aims at analyzing electricity flows between interconnected locations in the EU, and their effect on electricity prices in the different locations. Building from this endeavor, we then solve the optimal control problem of an agent who uses the interconnectors to take positions in a subset of locations that are part of the interconnected network. A real-market simulation finally shows the performance of the trading strategy.

Conference presentations and Awards. Chapters 2, 3 and 4 constitute three different papers, and each one of them has been presented at different seminars and conferences. In particular, I am thankful to conference and seminar participants for the helpful comments and remarks they provided me with at the Association for Mathematics Applied to Social and Economic Sciences 2017 meeting (AMASES), the Energy Finance Italia III conference (EFI), and the BOMOPAV workshop, where I presented the paper relative to Chapter 2; the University of Padova, the Energy Finance Christmas 2017 workshop (EFC17), the Workshop on Stochastics and Optimization in Energy at King's College London, the Commodity and Energy Markets Annual Meeting (CEM18), and the 29$^{\text{th}}$ European Conference on Operational Research (EURO18), where I presented the paper relative to Chapter 4.
Moreover, the paper relative to Chapter 4 (*Optimal cross-border electricity trading*) is the result of my visiting periods at University of Oxford, where I have been working with Professor Álvaro Cartea on this project. This intense and engaging period culminated with an official recognition at the Commodity and Energy Markets 2018 Annual Meeting, where the paper was awarded the General Prize for best paper.

1.1 The electricity market

After it is produced by an electricity generator, electricity flows through transmission networks, which are run by Transmission System Operators (TSOs). Each country can have one or more TSOs; Italy and France, for example, have one (Terna and RTE, respectively), while Germany has four (50 Hertz, Amprion, TenneT and TransnetBW). Finally, DSOs (Distribution System Operators) distribute the electricity across the various households and businesses. In Italy, for example, ENEL is the biggest DSO.

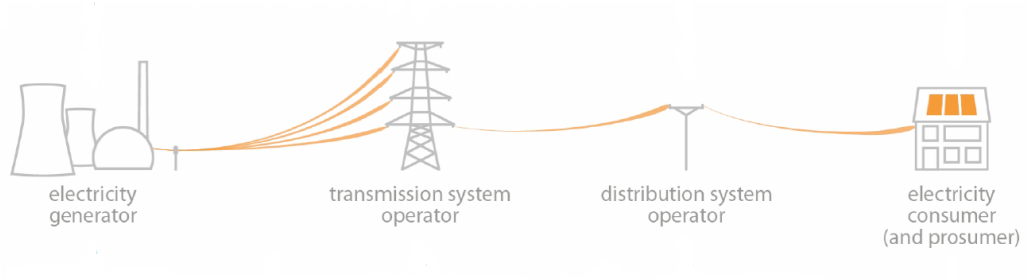

Figure 1.1: *Source: Understanding electricity markets in the EU.* European Parliament briefing (2016).

National transmission grids can be interconnected, meaning that electricity can flow across national borders into another country's grid. The physical structures enabling this connection between two different grids are called "interconnectors". The recent market coupling initiatives are aimed at integrating the European wholesale electricity markets, thus increasing security of supply while reducing price volatility across Europe, and interconnectors are at the core of the market coupling process.

The term "electricity market", intended as a virtual space where anyone can trade this commodity, is a relatively new concept. Citing Edwards (2009),

> Prior to deregulation, only power plants owned by utilities could sell power into a power grid. After deregulation, anyone could build a power plant, produce power, and offer that power for sale. In deregulated markets, utilities have shifted away from running power plants to concentrating on operating transmission grids. There are power plants now owned by power traders and operated by specialized service companies. These changes revolu-

tionized the power industry - they created a market for electrical power.

Electricity transactions can be done over-the-counter (OTC), that is off-exchange, directly between two parties, or on an exchange. One of the biggest exchanges where electricity can be traded in Europe is EPEX Spot, the European power exchange for spot trading, covering Germany, France, the United Kingdom, the Netherlands, Belgium, Austria, Switzerland and Luxembourg.

EPEX Spot operates the power *spot* markets for short-term trading, i.e. the day-ahead and intra-day markets. However, another important piece of the energy market is the *forward* one. The main difference among these three markets is that, in each one of them, one can trade contracts on electricity with a specific range of delivery times.

The forward and future market is mainly intended for hedging purposes, and it can be over-the-counter (OTC) or a centralized exchange market. In the latter case, it is a continuous trading market, where you can trade contracts where the delivery of electricity is sometime in the future: weeks, months, quarters, seasons, years.

The day-ahead market in Europe is a uniform auction system, where electricity contracts with delivery on the following day are traded. Each different hour of delivery is a different product, so that the price of electricity delivered at, for example, 4 p.m. on the following day, is different from the one of electricity delivered at 5 p.m. of the following day. Moreover, electricity can also be traded in blocks, so that there are additional products, such as Block Baseload (covering hours 1 to 24), Block Peakload (covering hours 9 a.m. to 8 p.m.), Block Off-Peak (covering hours 9 p.m. to 8 a.m), among others. This market closes at midday of the day before delivery is scheduled, and demand and supply curves determine the price. In such a way, each electricity producer has incentive to bid the marginal cost of production, because if somebody else bids higher, and their aggregate supply is met by demand, that higher bid will be the final price they both will receive.

Finally, the intra-day market in EPEX is a pay-as-bid system with continuous trading, where one can trade electricity contracts with delivery on the following or on the same day. In fact, starting from 3 p.m. on a certain day, all hours of the following day can be traded, and each contract can be traded until 30 minutes before delivery begins.

As Creti and Fontini (2018) note, the two different systems governing these last two markets, the continuous trading system and the auction one, each have their own advantages and shortcomings. Continuous trading systems are more efficient in presence of high liquidity, since they facilitate the order matching. However, if liquidity is limited, they are riskier. An auction system, on the contrary, provides a reference price, but can be inefficient as it forces agents to wait until the end of the auction period.

1.2 Black & Gold

Oil and sunlight are two important sources of power in energy markets. These are going to be the subject of the case study in Chapter 2.

Oil, compared to hydrocarbon gases, contains a lot of energy per unit of volume. There are a lot of varieties of crude oil, and the most common oil benchmarks, and most liquid, are Brent and WTI. Figure 1.2 and 1.3 show the world total primary energy supply (TPES) by source, over different years. Even if it decreased from 1971 to 2016, oil is still the dominant fuel.

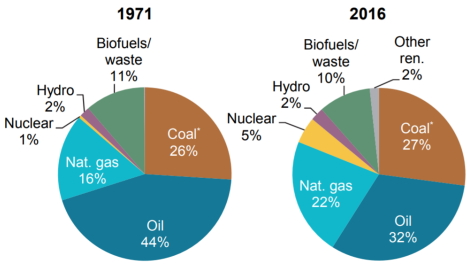

Figure 1.2: 1971 and 2016 World total primary energy supply (TPES) by source. *Source:* IEA (2018).

Fossil fuel power plants can burn oil to produce steam, which drives a generator to produce electrical power. A common measure of the efficiency of fossil fuel power plants is the so-called 'heat rate', expressed as a ratio of heat input to work output. Oil-fired power plants are typically not very efficient, when compared to natural gas-fired ones. As for their emissions, they also produce more CO_2 than natural gas-fired plants, although they have a better emission factor than coal-fired ones (IPCC (2006)). Fossil fuel power plants are the most influential in energy trading, since they are the marginal producers. As such, they usually set the clearing price for power in auction markets, such as the EPEX day-ahead one. In fact, as mentioned in the last section, in auction markets, all winning bidders get paid the same price for the electricity they sell, regardless of their bids.

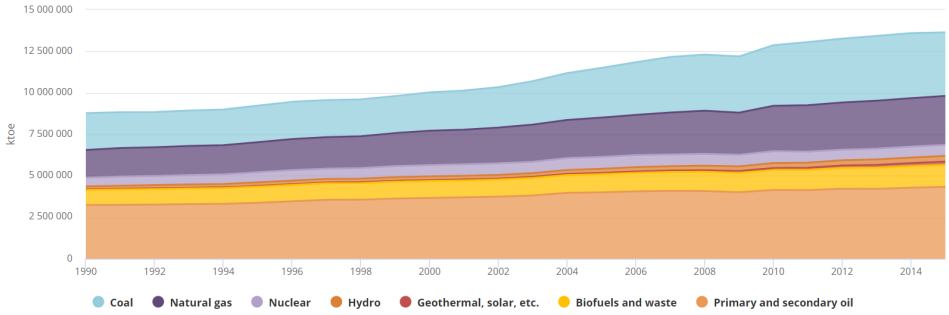

Figure 1.3: World total primary energy supply (TPES) by source, 1990-2015. *Source:* IEA (2017b).

Solar power plants, instead, are always going to bid low in auction markets: they require a considerable initial investment, but are very cheap to operate. There are two types of solar power plants - photovoltaic (PV) and thermal ones. The former are the most commonly referred to when discussing solar power. PV plants produce direct current electricity using a sheet of solar cells made of specialized semiconductors. In several countries in Europe, thanks to governmental support schemes, this technology has been deployed rapidly and, over the last few decades, there was a considerable growth in PV power. The advantage, of course, is that they do not need any fuel to operate, and thus they do not emit greenhouse gases.

1.3 Emission trading

Carbon emissions are another important commodity in the energy market. Moreover, they are also a fairly recent one. In fact, over the last few years, environmental regulation has tried to integrate the social costs entailed by environmental pollution into the price of the products, and this was done essentially in two ways: through command-and-control instruments or using market-based ones.

The former instruments are the least efficient: they impose a quantitative restriction on individual players, without taking into account the different marginal abatement costs. On the other hand, market-based methods represent a more cost-effective alternative. Among these latter instruments, cap-and-trade markets offer the promise of finding the lowest cost way to decrease emissions.

In a cap-and-trade scheme, the cap on the total emissions is set by the regulator, while the price of the tradable emission permits, or carbon allowances, is determined by the market. In such a way, the right to create pollution becomes a tradable commodity.

Some of the first examples of these kind of systems can be traced back to the 1980s in the US, when the Environmental Protection Agency offered states such tools in order to control localized air pollutants. Then, in 1990, Title IV of Clean Air Act amendments established a sulfur dioxide allowance trading program, in order to control the acid rain issue. This was indeed one of the first cases of successful implementation of an emission trading system on a large scale.

Europe had to wait a bit more to have its own emission trading market, but it can now boast the biggest one in the world, the European Emission Trading Scheme (EU ETS), accounting for more than 75% of international carbon trading. This was established by the European Directive 2003/87/EC, and was launched in 2005. It covers a range of different greenhouse gases: CO_2 emitted from power and heat generation, energy-intensive industry sectors and civil aviation, N_2O (nitrous oxide) from the production of acids and PFCs (perfluorocarbons) from aluminum production.

During the first two phases of the EU ETS, allowances were freely allocated among players, while Phase 3 (2013-2020) employs auctioning as the preferred primary allocation method. Each European Union allowance (EUA) grants the right to emit one tonne of CO_2 equivalent. The price of these permits, however, has been very fluctuating and subject to spikes and jumps, as it can be seen in Figure 1.4.

Despite the extensive literature (see Chapter 2) advocating for a regulatory intervention in the market, this has never been implemented. Chapter 2 analyses the historical behavior of carbon prices and provides tools for evaluating the effectiveness of the EU ETS in encouraging environmentally conscious investments in the power generation sector. Specifically, it models the choice of a price taker electricity producer to switch from her current carbon-intensive power production technology to a cleaner one. This choice is evaluated as a real option, via Least Squares Monte Carlo methods. Moreover, it also investigates the effects of a carbon price stabilization mechanism on the electricity producer's choice. The envisaged regulatory intervention is

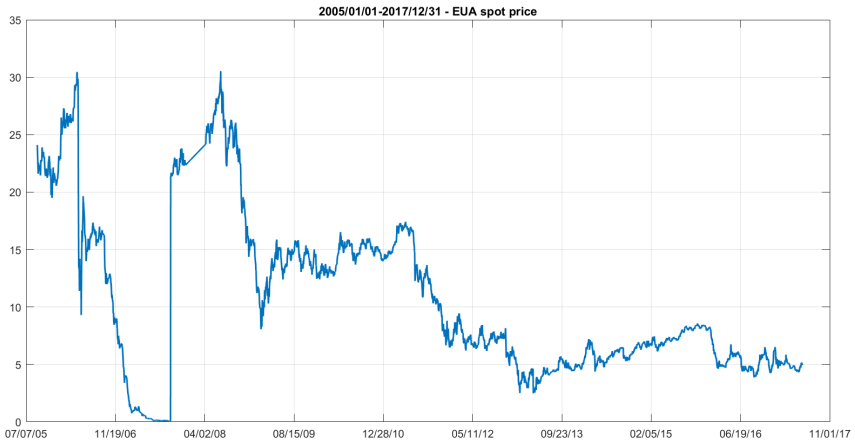

Figure 1.4: European Union Allowance spot price 2005-2017.

a price floor on carbon, and the scope of different floor levels is evaluated in this context.

1.4 Capacity markets

Capacity markets (or capacity mechanisms) represent another policy tool used to tackle the daunting challenge of decarbonizing electricity production. Their goal is that of ensuring reliability needs are met in the power system during the low-carbon transition. Moreover, these markets mitigate the problems caused by the fact that electricity demand is highly inelastic to prices.

There are two types of capacity mechanisms: targeted ones (for instance, strategic reserves) and market-wide ones (reliability options). The former mechanisms do not provide additional revenues, they are instead the only source of revenues for the contracted capacity. The latter instead complement revenues from the sale of electricity, and are, in principle, the most efficient ones. The largest and most complex capacity mechanism in the United States is the PJM Reliability Pricing Model (RPM), which is a market-wide mechanisms.

The US, and the American continent in general, have a long history of capacity remuneration mechanisms, while in Europe they have become a priority for the regulator only in recent years (see Mastropietro et al. (2016)

and references therein). As mentioned above, Chapter 3 will focus on the Italian experience, as Italy is planning to implement a market-wide mechanisms, namely a reliability option one. These contacts grant their owner the right, but not the obligation, to buy electricity from the option's seller at a predetermined strike price. In such a way, the sellers of a reliability option obtain a stable revenue in exchange for which they forego possible rents from price peaks. Thus, reliability options reduce supplier risk, while also hedging load from high prices. These tools are particularly efficient in that they avoid market price distortions, as they lower regulatory risk, and can be easily adapted to meet national needs.

1.5 Cross-border transmission networks

In the perspective of a low carbon transition in the power market, investing in new transmission projects is a cost-efficient means of facilitating the integration of high shares of intermittent renewable energy sources, and of securing electricity supply. This is why interconnecting different electricity markets is very high in the political agenda of the European Commission.

According to IEA (2014b), an investment of 546 billion dollars in transmission networks is needed in OECD countries by 2035, making up 37% of the total investment foreseen in renewables, networks and conventional generation. In fact, the present lack of fully interconnected macro regions also causes the need to sometimes curtail the generation of electricity from renewable sources, simply because it cannot be distributed to a wider area (IEA (2016)). The technology mix for electricity production varies a lot across Europe. For example, hydroelectricity shares are high in Norway (96.3% of total electricity generated in the country in 2016), Iceland (72.6%) and Austria (61.2%), wind production is substantial in Germany (77.4 TWh in 2016) and Spain (48.9 TWh in 2016), while Germany (38.2 TWh in 2016) and Italy (22.9 TWh in 2016) account for most of solar PV power production in Europe (IEA (2017a)). Thus, having a fully interconnected market could be very beneficial for the system, as it would increase the security of supply and decrease overall costs.

Even if the urge for new interconnecting infrastructures is felt at the European Commission level, the literature on interconnectors valuation is still scarce. To our knowledge, the papers by Rosenberg et al. (2010) and Cartea

and González-Pedraz (2012) are the first having undertaken this task. In their works, they suggested to value interconnectors as a strip of real options written on the price spread between interconnected power markets, so that, each day, each spread option can be exercised or not, depending on its convenience. However, their analysis is static, in the sense that the way the interconnector is used on a given day does not affect the way it will be used on the following one. In Chapter 4, instead, we first show that traded volumes have a direct and indirect effect on the electricity price in the different countries, and then we provide a valuation framework based on optimal stochastic control theory, computing the total cash flows an agent can obtain by trading electricity contracts across interconnected locations. We do so by considering the intra-day market.

In fact, as mentioned earlier in Section 1.1, the day-ahead and the intra-day markets, in the European region, present a lot of different features. Moreover, they also differ in their level of interconnectedness. In fact, the day-ahead market is an integrated market, and prices are coupled, meaning that, provided that the interconnector capacity is enough, the price of electricity in the two interconnected countries will be the same. Moreover, imports and exports are implicit, in the sense that they are determined by an algorithm. The intra-day market, instead, is not as integrated, and agents can decide to go and buy electricity in another country, so that there could be arbitrage opportunities. These opportunities will be explored in Chapter 4.

Chapter 2

Price dynamics in the European Emission Trading System and evaluation of its ability to boost emission-related investment decisions *

In this chapter, we assess the effects of the European Union emission trading scheme (EU ETS) in delivering low-carbon investments at the firm level, by modeling a price taker electricity producer subject to the EU ETS jurisdiction. We compute, via Least Squares Monte Carlo (LSMC) methods, the value of the real option the greenhouse gas emitter has, consisting in the opportunity to switch from its current high-carbon technology to a cleaner one. We evaluate this real option by proposing a Brennan-Schwarz model, which exhibits positive mean-reverting prices, for fuel and a Variance Gamma (VG) specification for carbon prices. Moreover, we further analyze the investment decision problem, in case of a CO_2 price stabilization mechanism, by explicitly computing the expected value of the investment project by means of Fourier

*This paper is a joint work with Tiziano Vargiolu (Università degli Studi di Padova). This paper is currently under revision for an international journal.

methods. Our results show that the introduction of a price stabilization mechanisms, in this case a carbon floor price, significantly affects the timing of the investment decision, supporting emission related investments.

2.1 Introduction

In the past decades, it has become increasingly clear that a development model heavily based on fossil fuels is hardly sustainable on the long term. This is why the recent international environmental agreements (UNFCCC, Kyoto Protocol) have urged countries to adopt emission reduction measures and to invest in alternative energy projects. One of the policy tools of newest implementation, aimed at reducing greenhouse gas (GHG) emissions, is emission trading. Such a tool is aimed at internalizing the negative externalities generated through the production processes, by making the polluting private firms buy a number of emission allowances, corresponding to the tons of GHG they emit in the atmosphere.

Emission trading systems (ETS) are usually cap-and-trade schemes, in which the regulator sets the maximum amount of CO_2 and other polluting gases that can be emitted in the system, and then firms buy and trade the emission permits on the base of their needs. Each emission permit (or emission allowance) grants its owner the right to emit one ton of GHG.

The aim of this chapter is to give a quantitative view on the evolution of the EU ETS (European Union Emission Trading Scheme) carbon market, analyzing the emission reduction problem from the point of view of an electricity producer running a fossil fuel-fired power plant, who is confronted with the choice of either submitting to the ETS jurisdiction, as opposed to changing the production model, by switching production to low carbon sources of energy.

In order to do this, taking into account the uncertainty involving future EUA (European Union Allowance) prices and the irreversible costs connected to a new PV plant investment, we considered the opportunity of switching production method as a real option. Computing the price of such a real option gives a measure of how convenient it is for the GHG emitter to shut down the fossil fuel-fired power plant and to invest in a renewable energy

project. We focused on an oil-fired power plant, and we chose PV energy as the alternative source of energy considered.

Section 2.2 places this work in the relevant literature on the subject. The first part of Section 2.3 presents the model and the methodology. Pricing a real option requires consistently defining the price dynamics of the underlying assets, and this is why the second part of Section 2.3 is devoted to analyzing the EUA spot prices, in order to define a stochastic process able to consistently replicate their trend over time. Section 2.4 presents the results and conducts a sensitivity analysis. Section 2.5 concludes.

2.2 Relevant Literature

Since the European Union carbon market was established, in 2005, the uncertainty related to the magnitude of compliance costs and to the impact of this type of climate policy on the power sector has motivated some research on this field. Some of the early contributions can be traced back to Laurikka and Koljonen (2006) and Szolgayova et al. (2008). Both papers use stochastic carbon and electricity prices and deterministic fuel prices. While the former investigates how emission-related uncertainty affects the value of an option to invest in a coal powered plant as opposed to that of investing in a gas-fired power plant, the latter analyzes the effects of a cap on the carbon price, concluding that it would jeopardize the incentive to phase in low-carbon technologies. Both of them investigated the implications of the EU ETS by means of a real option analysis, but did so at a time when the EU carbon market was still very young and unstable, so historical data were relatively short.

As time went by, the magnitude of the downward risk in the EU ETS started to motivate some research aimed at discussing the effects of bounding carbon prices by means of a regulatory minimum price for EU allowances. The theoretical studies by Weber and Neuhoff (2010), Grüll and Taschini (2011) and Wood and Jotzo (2011) act in this sense, analyzing the possibility of enhancing the incentives provided by the EU ETS, by introducing a CO_2 price floor. Their results suggest that establishing a regulatory minimum price would be advisable in many respects.

The papers by Abadie et al. (2011) and Brauneis et al. (2013) incorporate

the possibility of such a political intervention in their real option analysis, to assess its effects on the firm-level investment decisions. The former employs a binomial lattice model to compute the value of the option to abandon a coal-fired power plant and advocates a price stabilization mechanisms in the form of floor price. The latter, instead, uses the least-squares Monte Carlo approach to solve the optimization problem of decision making in case of an electricity producer who has the option to replace the existing coal-fired power plant with a "clean" nuclear one. Brauneis et al. (2013), moreover, compute the floor price required to trigger investment in the new low-carbon plant, and propose a number of different designs for the floor price.

In this work, we propose an extension to the model by Brauneis et al. (2013), introducing a different stochastic process, both for fuel and carbon prices, in place of the geometric brownian motion (GBM). In fact, unlike other financial products, which all fall into a precise asset category (equity, fixed income, FX, commodities, derivatives), carbon is a special asset which may resemble energy commodities in some aspects but differentiates itself in others, in the sense that its price somewhat depends on an exogenous political decision, which caps the total supply of the product. This aspect reflects in the price distribution, featuring extreme events such as jumps in the price process, as well as heavy tails and leptokurtic behavior in the distribution. The majority of the papers on the ETS subject have used, for ease of modeling, GBM processes to describe the EUA price behavior (cfr. Szolgayova et al. (2008), Abadie et al. (2011), Yang et al. (2008), Brauneis et al. (2013), among others). Instead, we propose a different specification for the allowances price, namely a Variance Gamma (VG) process, which, to our knowledge, has never been used to model carbon prices. Moreover, we further analyze the investment decision problem in case of a CO_2 price stabilization mechanism, by explicitly computing the expected value of the investment project by means of Fourier methods.

2.3 Methodology

We consider a price taker and risk neutral power generating firm, operating a "dirty" electricity generation technology in Italy.[1] Being subject to the EU

[1] Choosing a specific geographic region where to base our project is just a tool for consistently defining the technical characteristics and output of the new plant, powered by renewable sources. Nevertheless, our model can be used for different geographical

ETS jurisdiction, the firm has either to buy the necessary EUAs to run its business, or it can decide to switch production model towards more sustainable energy sources, in order to avoid the compliance costs. Specifically, we decided to choose photovoltaic (PV) technology as a case study. In fact, solar production has experienced a consistent growth in Italy over the last years, accounting for the highest share of incremental production from renewable energies in the period 2002-2015, going from only 677 GWh in 2009, topping 22,900 GWh in 2015 (GSE (2017)). In order to reduce the dimensionality of the problem, we suppose that the two alternative plants, the "clean" and the "dirty" one, produce the same amount of electricity per year. In this way, when evaluating the real option, we get rid of the electricity price variable. We thus chose to model the firm as an oil-fired plant with a comparable capacity to that of the alternative solar one. The technical characteristics of the firm at $t = 0$ are reported in Table 2.1.[2]

2.3.1 The investment decision problem

At the beginning of each period, until the end of its economic life, the company can choose to replace the existing power plant with another one, based on PV technology, with no carbon emissions. Given the fact that this decision (1) can be taken at any moment in time prior to the end of the economic life of the oil-fired power plant, (2) is irreversible in that it implies high sunk costs (decommissioning of the existing plant and construction of the PV one), and (3) is affected by the uncertainty related to some key variables, such as the price of CO_2 and that of fuels, this choice can be modeled as a real option, to which a value can be given, in a very similar way to the one in which financial options are priced. The pricing process of a real option has received an in depth treatment in the seminal text by Dixit and Pindyck (1994) on real option theory. It is possible to use two different methods: dynamic programming, in which the investment problem is formulated in terms of a Hamilton-Jacobi-Bellman equation and solved by backward induction, using a discount rate reflecting the opportunity cost of capital for similarly risky investments, or contingent claims analysis, which consists in constructing a riskless replicating portfolio of existing traded assets able to indeed replicate

locations.

[2]We refer the reader to Appendix A.1 for the computation of some of the values in the table.

Table 2.1: Technical characteristics of the oil-fired power plant.

Variable	Unit	Value
Capacity	MW	10
Residual lifetime	years	25
Capacity factor*	rate	80%
Efficiency¶	rate	40%
Electricity produced	kWh/year	$7.01 \cdot 10^7$
Fuel consumption	tons/year	$1.48 \cdot 10^4$
CO_2 emission factor	tons/kWh	$2.64 \cdot 10^{-4}$
CO_2 emissions per year	tons/year	46,200
Operating & maintenance costs	million EUR/year	0.5
Decommissioning costs	million EUR	1

* The capacity factor is the ratio of a power station actual generation to its maximum potential generation. This value represents the theoretical capacity factor of an oil-fired power station in good condition. In Italy there are some examples of fuel oil plants which have been running in full swing over the recent years: the Livorno Marzocco power plant, Tuscany, operating since 1965, in 2007 had a capacity factor of 79% (see http://enipedia.tudelft.nl/wiki/Livorno_Powerplant).

¶ The efficiency of a power station is a percentage measure given by the ratio between the electricity produced and the heat energy needed in order to produce it. According to IEA (2008), the average efficiency of oil-fired electricity production in Italy, over the 2001-2005 period, was 41%. For ease of calculation, 40% is taken as a proxy.

the return of the claim we are trying to give a value to. Being riskless, such a portfolio earns a risk-free rate of return. Both methods are in principle analytical ones, in which an explicit formula for the option value should be retrieved, by solving a partial integral differential equation (PIDE) subject to two key boundary conditions, the value-matching and the smooth-pasting ones; in practice, it is often not possible to do so, and instead of finding a closed-form solution, numerical methods are employed, as is the case in our model. As a computational method of choice, given that we model our two relevant state variables with different stochastic processes, and given the complexity of the VG one, we chose to implement a Least Squares Monte Carlo (LSMC) simulation rather than a simpler binomial tree for efficiency purposes.

The optimization procedure starts by defining the relevant state variables, choosing a stochastic process for each one of them, and calibrating such pro-

cesses on historical data. Using those fitted processes, Monte Carlo methods are then employed to simulate paths for the relevant state variables. We then match this simulation to a dynamic programming algorithm, in order to compare the expected outcome of investing in the PV plant (that is, exercising the option), with the one obtained by postponing the decision for an additional period. By taking the maximum between the immediate investment net present value (NPV) and the NPV obtained by delaying the decision, we find the optimal exercise decision at any point in time.

In case the firm decides to invest in the alternative energy plant, it will have to pay for the decommissioning of the oil-fired plant, whose cost is reported in Table 2.1. Given the negligible construction time of PV plants, we assumed the switching decision to have immediate effect. We further assumed the PV plant to have an economic lifetime of 25 years (average economic lifetime of PV plants according to IEA (2014a)).

Once defined the total electricity output produced in the entire lifetime of the solar plant, the investment required to build it is expressed by the levelised cost of electricity (LCOE) of PV technology, an indicator summarizing the various costs related to building and operating a power station. Taking into account the benefits given by the so-called "learning curves" over time, the LCOE is modeled as a decreasing exponential, as seen in Biondi and Moretto (2015):

$$\mathrm{LCOE}(t) = \mathrm{LCOE}(0)\, \mathrm{e}^{\alpha_C t} \tag{2.3.1}$$

where $\alpha_C < 0$ is the product between the negative learning curve coefficient and the average growth rate of the PV industry.

The real option, thus, has a strike price K equal to the sunk costs the firm incurs once it decides to invest:

$$K(t) = c + Q \cdot \mathrm{LCOE}(t),$$

where c represents the decommissioning cost of the high-carbon plant, and Q is the total electricity produced over the PV plant lifetime. On the other hand, exercising the option grants Φ, which represents the conditional expected value of the savings the company obtains by investing in the clean technology plant, discounted with a risk-free factor r, and summed up from the moment when the investment takes place, t, until the end of the model

horizon, T:

$$\begin{aligned}\Phi(D_t, P_t, t) = \mathbf{E}^{\mathbb{Q}} \Bigg[\int_t^T BD_s \, \mathrm{e}^{-r(s-t)} \, \mathrm{d}s \, + \int_t^T XP_s \, \mathrm{e}^{-r(s-t)} \, \mathrm{d}s + \\ + \int_t^T Op \, \mathrm{e}^{-r(s-t)} \, \mathrm{d}s \, \Big| \, \mathcal{F}_t \Bigg] + K(T) \, \frac{T_{pv} - (T-t)}{T_{pv}} \, \mathrm{e}^{-r(T-t)} = \\ = \int_t^T \mathbf{E}^{\mathbb{Q}} \left[BD_s \, \mathrm{e}^{-r(s-t)} \big| \, \mathcal{F}_t \right] \, \mathrm{d}s + \int_t^T \mathbf{E}^{\mathbb{Q}} \left[XP_s \, \mathrm{e}^{-r(s-t)} \big| \, \mathcal{F}_t \right] \, \mathrm{d}s + \\ + \int_t^T \mathbf{E}^{\mathbb{Q}} \left[Op \, \mathrm{e}^{-r(s-t)} \big| \, \mathcal{F}_t \right] \, \mathrm{d}s + K(T) \, \frac{T_{pv} - (T-t)}{T_{pv}} \, \mathrm{e}^{-r(T-t)}\end{aligned} \tag{2.3.2}$$

where D is the oil spot price, P is the carbon spot price, which are multiplied respectively by the fuel consumption coefficient of the oil-fired plant B, and by its yearly CO_2 emissions X, while Op represents the operating and maintenance costs of the high-carbon technology plant. The model horizon is set to coincide with the residual economic lifetime of the fossil fuel-powered plant (25 years). If the end of the model horizon does not also coincide with the end of the economic lifetime of the low-carbon plant (T_{pv}), in $t = T$, the existing plant is sold for its book value, and an additional positive cash flow is given.

The real option R to defer the investment is thus an American call option on the value of the project:

$$R(P_t, D_t, t) = \max_{\tau} \mathbf{E} \left[\mathrm{e}^{-r(\tau - t)} \left(\Phi(D_\tau, P_\tau, \tau) - K(\tau) \right) \right]$$

where the maximum is taken over all stopping times τ with $t < \tau < T$. To compute the value of the option, first we solved the expression for Φ. Since the solution of (2.3.2) depends on the choice of the relevant state variables dynamics, defined in the following section, we refer the reader to Section 2.3.3 for the closed-form solution of the expression in (2.3.2).

Once the payoff given by exercising the option is computed at each point in time, an efficient exercise rule is to assess the convenience of investing in the project as opposed to deferring the investment at every point in time when the decision has to be made. We followed the procedure outlined in Longstaff and Schwartz (2001), where the estimate of the continuation value,

that is the value given by deferring the investment decision to the following period, is computed through a least-squares Monte Carlo simulation. Following Brauneis et al. (2013), we defined a quadratic relationship between the value of continuing, $CV_{t,i}$, and the value our relevant simulated variables assume at each time the investment decision has to be made, where i indicates the different Monte Carlo simulated paths and $t \in [0, T]$:

$$CV_{t,i} = \alpha_t + \beta_1 D_{t,i} + \beta_2 P_{t,i} + \beta_3 (D_{t,i})^2 + \beta_4 (P_{t,i})^2 + \epsilon_{t,i}. \tag{2.3.3}$$

Through the least-squares analysis, we determined the regression coefficients providing the best fit. Using these estimated coefficients and working backwards, at each point in time the payoff given by exercising the option is compared to the continuation value.

Policy intervention: the carbon price floor

The procedure as outlined above represents the baseline scenario, without policy interventions. If instead we want to include a price stabilization mechanism in the model, we need to reconsider (2.3.2). In fact, in presence of a floor F on EUA prices, we need to consider $\max(P_s, F)$ in place of P_s in Equation (2.3.2). It can be noticed that

$$\max(P_s, F) = P_s + (F - P_s)^+ . \tag{2.3.4}$$

and that the new benefits equation Φ_F becomes

$$\begin{aligned}\Phi_F(D_t, P_t, t) = &\int_t^T \mathbf{E}^{\mathbb{Q}} \left[B D_s \, \mathrm{e}^{-r(s-t)} \middle| \mathcal{F}_t \right] \mathrm{d}s + \\ &+ X \int_t^T \mathrm{e}^{-r(s-t)} \, \mathbf{E}^{\mathbb{Q}} \left[P_s + (F - P_s)^+ \middle| \mathcal{F}_t \right] \mathrm{d}s + \\ &+ \int_t^T \mathbf{E}^{\mathbb{Q}} \left[Op \, \mathrm{e}^{-r(s-t)} \middle| \mathcal{F}_t \right] \mathrm{d}s + K(T) \, \frac{T_{pv} - (T-t)}{T_{pv}} \, \mathrm{e}^{-r(T-t)}\end{aligned} \tag{2.3.5}$$

Bounding carbon prices downwards, thus, is equivalent to having a put option with the floor F as strike price, and the solution to (2.3.5) is again the solution to (2.3.2), plus the integral on $[t, T]$ of the price of such a put option.

To compute the value of this option, we employed Fourier inversion as the

computational method of choice. The Fourier method is efficient in presence of a complex or unknown probability density function of the underlying asset, provided that its characteristic function is analytically tractable Pascucci (2011). This is the case for the VG process, which, as stated above, is the specification of choice for the carbon price. Starting from Carr and Madan (1999), other authors (e.g. Lee (2004)) have used and extended Fourier transform methods in option pricing. The main idea is to use the Fourier inversion formula on the payoff function of the option, and then, after changing the integration order by Fubini's theorem, one can insert in the pricing formula the characteristic function of the desired underlying process under the selected equivalent martingale measure (EMM) Q. Of course, a problem arises when the payoff of the option is non-integrable, since the classical Fourier transform

$$\Phi(u) = \int_{\mathbb{R}} \mathrm{e}^{iux} f(x)\,\mathrm{d}x$$

is only defined for $f \in L^1(\mathbb{R})$. This happens even for vanilla options like calls or puts, but the problem can be solved, as Carr and Madan (1999) show, by damping, or penalizing, the payoff function. While they operate on the function in order to make it decay as $\log F \to -\infty$, we follow Pascucci (2011) in order to make the payoff function decay as the underlying goes to $+\infty$. Let us then define the damped function as:

$$f_\gamma(x) = \mathrm{e}^{-\gamma x} f(x), \qquad \gamma \in \mathbb{R}.$$

In this way, we have that the damped payoff of the call is $f^C_\gamma(x) = \mathrm{e}^{-\gamma x}\,(\mathrm{e}^x - F)^+$, and the damped payoff of the put is $f^P_\alpha(x) = \mathrm{e}^{-\gamma x}\,(F - \mathrm{e}^x)^+$, and we can see that $f^C_\gamma \in L^1(\mathbb{R})$ for $\gamma > 1$ and $f^P_\gamma \in L^1(\mathbb{R})$ for $\gamma < 0$.
Following the procedure outlined above, we obtain the following formula for the put option price (Pascucci (2011)):

$$\mathrm{Price}(P_t, F, T) = \frac{\mathrm{e}^{-r(T-t)} P_t^{\gamma} F^{1-\gamma}}{\pi} \int_0^\infty \mathrm{e}^{-iu \log \frac{P_t}{F}} \frac{\phi_{X_T}(-(u+i\gamma))}{(iu-\gamma)(iu-\gamma+1)}\,\mathrm{d}u \tag{2.3.6}$$

where $\phi_{X_T}(u)$ is the characteristic function, under the selected EMM Q, of the underlying price process, which in our case, is a VG. This formula returns both the price of a call, when $\gamma > 1$, and that of a put, when $\gamma < 0$.

The LCOE of PV technology

As stated above, the LCOE is a synthetic indicator summarizing the unitary cost of electricity production related to a certain technology. In our case, it depends on a number of factors, including the price of PV modules, the capacity factor of the plant, and the installation, maintenance, insurance and decommissioning costs. Due to the uncertainty related to government incentives, we did not include them in our analysis. To estimate the current LCOE and the LCOE parameter α_C we mentioned above, we first need to estimate the magnitude of the costs outlined above and to compute the learning curve coefficient and the average growth rate of the PV industry, as α_C is the product of the two.

The learning curve coefficent. According to Fraunhofer ISE (2015), the learning rate LR of PV industry ranges between 0.19 and 0.23. We took the average 0.21 as a proxy. The economic meaning of such a value is that, each time the cumulated capacity doubles, the unitary cost decreases by 21%. Given that the progress ratio PR, that is the cost improvement at each doubling of cumulated capacity, is equal to $1 - LR$, we get that $PR = 0.79$. Since the learning curve coefficient is defined as $\frac{\log PR}{\log 2}$, it is equal to -0.34.

Growth rate of PV the industry. According to Fraunhofer ISE (2015), in a pessimistic scenario the 2015-2050 compound annual growth rate will be 5%, in the intermediate scenario it will be 7.5%, while, in the optimistic one, the growth rate will be 10%. We took 7.5% as a proxy. The LCOE parameter α_C is thus equal to -0.0255.

The current cost of PV technology. Since the plant will be built in Italy, we assume an average full load hours value of 1250 kWh/kW, which corresponds to a 14.3% capacity factor. As for the cost estimates, Fraunhofer ISE (2015) provides an estimate of the costs of a 1 MW PV utility in Germany, related to 2014. We use them to compute the LCOE relative to year 2014, and then update it to year 2017 with the exponential relationship mentioned above. The LCOE relative to 2014, resulting from these assumptions, is equal to 0.087 €/kWh. Thus, according to (2.3.1), the LCOE for 2017 is 0.081 €/kWh.

2.3.2 Price modeling

In what follows, we model the two relevant stochastic variables, carbon and oil spot prices, with two different specifications. The correlation between EUA and WTI crude oil prices is assumed to be equal to zero, given its very volatile nature over time, and following Chevallier (2012), who finds the time-varying correlation between these two variables is comprised in the range $[-0.05; 0.05]$.

Carbon price

EU carbon prices have followed a particular path over time. A huge drop in prices towards the end of 2007 marked the transition between the first and the second trading phase. In fact, the first phase was conceived as a sort of trial stage, used for "learning by doing": soon the market realized that the number of allowances was excessive and the price fell to zero in 2007. The second trading phase was then launched with an adjusted cap (and the possibility of banking permits was introduced), but the 2008 financial crisis deeply affected the price development, leading to declining and unstable prices. We are currently in the third carbon trading phase, but the price behavior is still marked by high price uncertainty. As Grüll and Kiesel (2012) show, the high price sensitivity of permits and their proneness to jumps are structural features of the EU ETS in its present configuration. For these reasons, a simple GBM model does not seem appropriate to describe carbon prices, and the data analysis supports this conjecture: the chi-squared goodness of fit test on log-returns gives an extremely low p-value ($7.76 \cdot 10^{-10}$) and the null hypothesis of normality is rejected at the 5% significance level. This is mainly due to the pronounced leptokurtic behavior of the log-return distribution, which causes the high peakedness about the mean and lack of shoulders. These characteristics suggest another stochastic process to model this variable, the Variance Gamma (VG) one, originally proposed by Madan et al. (1998). The VG process is obtained by subordinating (i.e. time-changing) a Brownian motion by a Gamma process T_t with i.i.d. increments, so that the final process has bounded variation and infinite activity. In this way, the carbon spot price P_t is modeled as:

$$P_t = P_0 \, \mathrm{e}^{\mu t + \theta_P T_t + \sigma_P B(T_t)} \tag{2.3.7}$$

where P_0 is the initial price, $\mu, \theta_P \in \mathbb{R}, \sigma_P \in \mathbb{R}^+$ and $T_t \sim \Gamma(\alpha t, \alpha)$ is a Gamma process.

As we can see in the bottom panels of Figure 2.1, the VG process graphically fits the data on spot carbon prices better than the GBM; the chi-squared goodness of fit test confirms this visual intuition, indicating that the test does not reject the null hypothesis at the 1% significance level, with a p-value equal to 0.44. The estimated carbon parameters are reported in Table 2.2.

Parameter	Estimated value
$\hat{\mu}$	$-5.09 \cdot 10^{-4}$
$\hat{\sigma_P}$	0.030
$\hat{\theta_P}$	$-3.59 \cdot 10^{-9}$
$\hat{\alpha}$	0.935

Table 2.2: Estimated parameters for carbon spot data fitted via MLE using a VG model.

Oil price

In commodity markets, a widely accepted assumption is that of mean reverting spot prices (see for example Lutz (2010)). Thus, we chose a Brennan-Schwartz (BS) process for the WTI crude oil spot price $D(t)$:

$$\mathrm{d}D(t) = k(\theta_D(t) - D(t))\,\mathrm{d}t + \sigma_D D(t)\,\mathrm{d}W(t) \tag{2.3.8}$$

where k is the speed of reversion toward the mean, θ_D is the long run mean price level, σ_D is the volatility of the process and $\mathrm{d}W(t)$ is the increment of a Wiener process. The estimated oil parameters are reported in Table 2.3.

Parameter	Estimated value
$\hat{k}$	0.0014
$\hat{\theta_D}$	445.64
$\hat{\sigma_D}$	0.025

Table 2.3: Estimated parameters for WTI crude oil spot data fitted via MLE using a BS model.

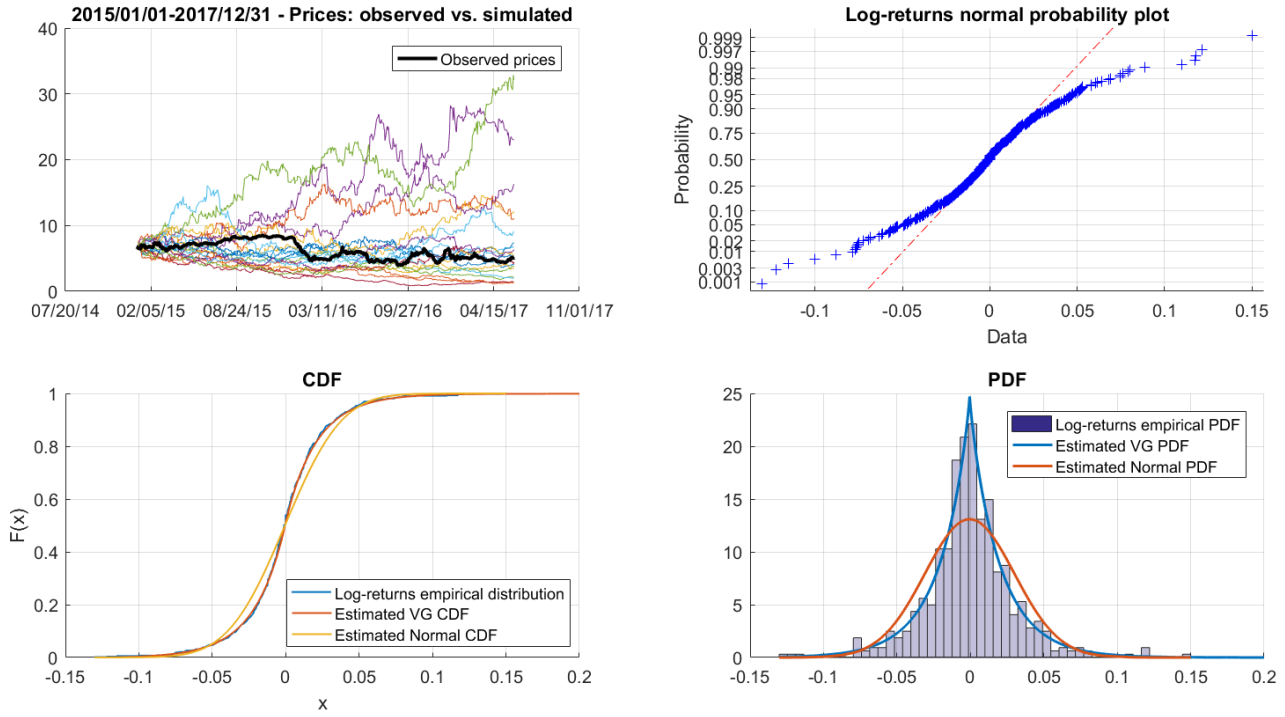

Figure 2.1: Variance-Gamma vs. Normal fit on EUA spot prices, listed at the European Energy Exchange (EEX).

2.3.3 The real option payoff - A closed-form solution

Baseline scenario

Given the price dynamics in the previous section, we can now provide the solution to (2.3.2) (we refer the reader to the Appendix A.2 for the detailed procedure):

$$\begin{aligned}\Phi(D_t, P_t, t) =& BD_t \frac{1 - \mathrm{e}^{-(T-t)(r+k)}}{r+k} + \frac{kB\,\mathrm{e}^{rt}}{r+k} \int_t^T \theta_D(u) \left[\mathrm{e}^{-ru} - \mathrm{e}^{-rT-k(T-u)}\right] \mathrm{d}u \\ &+ X\,P_t\,(T-t) + \frac{Op}{r}\left(1 - \mathrm{e}^{-r(T-t)}\right) \\ &+ K(T)\,\frac{T_{pv} - (T-t)}{T_{pv}}\,\mathrm{e}^{-r(T-t)}\end{aligned} \tag{2.3.9}$$

Regulatory intervention scenario

As Madan et al. (1998) show, the characteristic function for the VG process is

$$\varphi_{X_T}(u) = \mathbf{E}\left[\mathrm{e}^{iuX_T}\right] = \mathrm{e}^{i\mu Tu}\left(1 - i\theta_P \frac{u}{\alpha} + \frac{1}{2}\sigma_P^2 \frac{u^2}{\alpha}\right)^{-T\alpha} \tag{2.3.10}$$

As shown in Appendix A.2, as a necessary condition for (2.3.10) to be under the EMM Q, we need to have

$$\mu = r + \alpha \log\left(1 - \frac{\theta + \frac{1}{2}\sigma^2}{\alpha}\right). \tag{2.3.11}$$

Looking back at (2.3.5), and using (2.3.6) along with (2.3.10), we get that

the value of the put is:

$$
\begin{aligned}
&X \int_t^T \mathrm{e}^{-r(s-t)}\, \mathbf{E}^{\mathbb{Q}} \left[(F - P_s)^+ \middle|\, \mathcal{F}_t \right] \mathrm{d}s = \\
&= X \int_t^T \frac{\mathrm{e}^{-r(s-t)} P_t^{\gamma} F^{1-\gamma}}{\pi} \cdot \\
&\qquad \cdot \int_0^{+\infty} \frac{\mathrm{e}^{-iu \log \frac{P_t}{F} + \mu(s-t)(\gamma - iu)} \left(1 + i\theta_P \frac{u+i\gamma}{\alpha} + \frac{1}{2}\sigma_P^2 \frac{(u+i\gamma)^2}{\alpha} \right)^{-(s-t)\alpha}}{(iu-\gamma)(iu-\gamma+1)} \mathrm{d}u \; \mathrm{d}s = \\
&= X \frac{P_t^{\gamma} F^{1-\gamma}}{\pi} \int_0^{+\infty} \frac{\mathrm{e}^{-iu \log \frac{P_t}{F}}}{(iu-\gamma)(iu-\gamma+1)} \left[\frac{\mathrm{e}^{(T-t)\, m(u)} - 1}{m(u)} \right] \mathrm{d}u
\end{aligned}
\tag{2.3.12}
$$

where

$$
m(u) = -r - i\mu(u + i\gamma) - \alpha \log \left(1 + i\theta_P \frac{u+i\gamma}{\alpha} + \frac{1}{2}\sigma_P^2 \frac{(u+i\gamma)^2}{\alpha} \right),
$$

with μ satisfying (2.3.11). In this way,

$$
\begin{aligned}
\Phi_F(D_t, P_t, t) = &\Phi(D_t, P_t, t) + X \frac{P_t^{\gamma} F^{1-\gamma}}{\pi} \cdot \\
&\cdot \int_0^{+\infty} \frac{\mathrm{e}^{-iu \log \frac{P_t}{F}}}{(iu-\gamma)(iu-\gamma+1)} \left[\frac{\mathrm{e}^{(T-t)\, m(u)} - 1}{m(u)} \right] \mathrm{d}u
\end{aligned}
\tag{2.3.13}
$$

Choice of the damping parameter

Even if, theoretically, equation (2.3.6) is valid for any $\gamma < 0$, many authors have noticed that the integrand in the pricing formula may be oscillatory or highly peaked, depending on the choice of γ.

As a criterion for the selection of the damping parameter, we plot the integrand in (2.3.6) as a function of the different variables, and examine the graphs in order to detect oscillatory behaviors.

For example, as we can see in Figure 2.2, the more the maturity increases, the smaller γ needs to be. According to our graphical results, with the estimated VG parameters, an optimal choice for γ lies in the interval $[-1, 0)$. Specifically, we chose $\gamma = -0.8$.

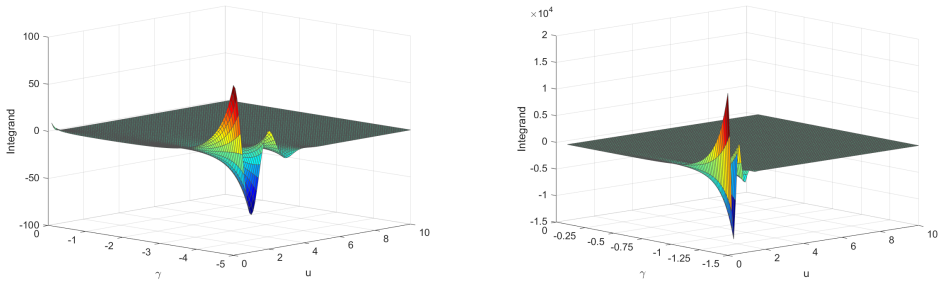

(a) T = 2, $\gamma \in [-5, 0]$ **(b)** T = 20, $\gamma \in [-1.5, 0]$

Figure 2.2: Integrand for the VG model with the estimated parameters.

2.4 Results

This section discusses the results obtained using our model. In what follows, we use an initial market price for oil of 54.00 $ per barrel (365.73 €/ton), and an initial carbon price of 5.05 €/ton of CO_2. We use a risk-free annual interest rate r equal to 2.5%. All other parameters are as stated in the previous sections. The results are shown in terms of expected value of the option (computed as the average of the values on all simulated paths) and of cumulative investment probability, defined as the sum of the number of paths in which the investment takes place before a certain year, over the total number of simulated paths. We run our model on Matlab, with 10,000 simulated paths.

2.4.1 Baseline scenario

Using the parameters stated above, and assuming no policy interventions in the carbon market, the probability to invest in the clean energy project before 10 years reaches 50%. Before the end of the model horizon, the optimal strategy consists in replacing the oil-fired power plant in 92% of the cases (Fig. 2.3a, dashed purple line).

This result, however, is quite sensitive to the choice of the discount rate r, as shown in Fig. 2.3. If r is higher than the one assumed in our model, the investment probability shifts downward and the expected option value declines. On the contrary, the lower the discount rate, the higher the probability of switching production method, with $r = 1\%$ suggesting almost immediate

investment.

As a second sensitivity test, we looked at the impact that different long term mean prices for oil θ_D could have on the optimal timing of the investment. We thus run our model with a set of different θ_D, corresponding to a reduction or increase of 3%, 6% or 9% with respect to the initial θ_D estimate. Figure 2.4 shows, as we would expect, that having higher long term mean values for oil prices results in earlier investment for a given probability value, and this is contextual to an increase in the expected option value. An increase in θ_D of 9% with respect to our estimate leads to a probability of 100% that it is optimal to exercise the option before the end of the model horizon. On the other hand, a decrease of 9% in the same initial value results in a decrease by 20% in the corresponding probability.

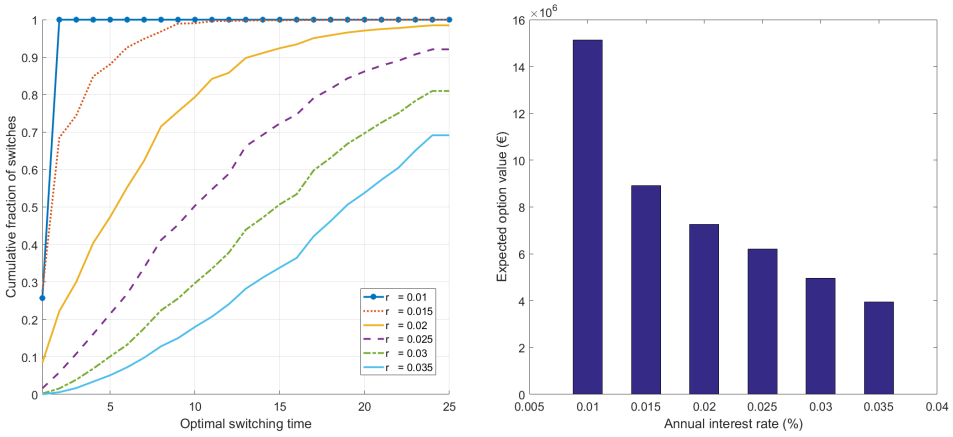

(a) Cumulative switches **(b)** Expected option value

Figure 2.3: Sensitivity analysis of the results using different annual risk-free interest rates r.

2.4.2 Regulatory intervention scenario

The impact of introducing a minimum price for EU emission allowances is shown in Fig. 2.5 and 2.6. In Fig. 2.5 and 2.6a, we show the results on the investment probability and on the expected option value, respectively, of having a carbon floor price equal to {10, 20, 30, 40} €/ ton of CO_2. As the floor gets higher, the number of simulation runs in which it is convenient to invest in the clean energy project increases for each point in time, and the

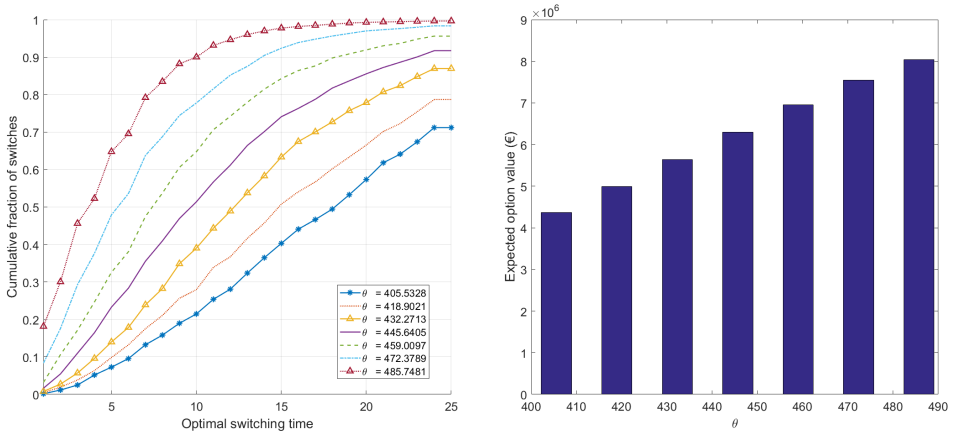

(a) Cumulative switches **(b)** Expected option value

Figure 2.4: Sensitivity analysis of the results using different long term means θ_D for oil.

option to replace the "dirty" technology with a "clean" one appreciates in value. Specifically, with a floor of 10 €, that is slightly above the current market price (as of February 2018), the probability that exercising the real option before 10 years is optimal shifts from about 50% to almost 80%. With a floor as high as 20 €/ton, in about 55% of the cases it is optimal to invest immediately in the project, and the probability rises to 100% if the floor is 30 €/ton.

Finally, we run again our model using two different risk-free interest rates r, and the results, reported in Fig. 2.7, confirm the positive effect of a floor on carbon prices.

2.5 Conclusions

In this chapter, we evaluated the impact of the EU ETS on renewable energy investments in the power generation sector, by extending the model in Brauneis et al. (2013).

As our case study is based in Italy, and given the country's consistent share of PV energy production over the total incremental renewable energy generation over the last years (as explained in the previous sections), we chose PV technology as the alternative production method of the electricity producer, currently running a fossil fuel-fired power plant. After having

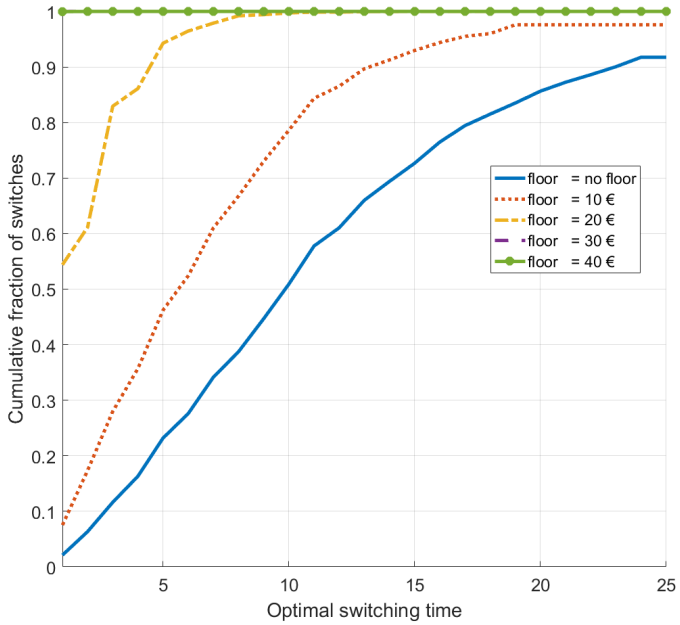

Figure 2.5: Investment probability evolution over the years with different carbon floor prices, r=2.5%.

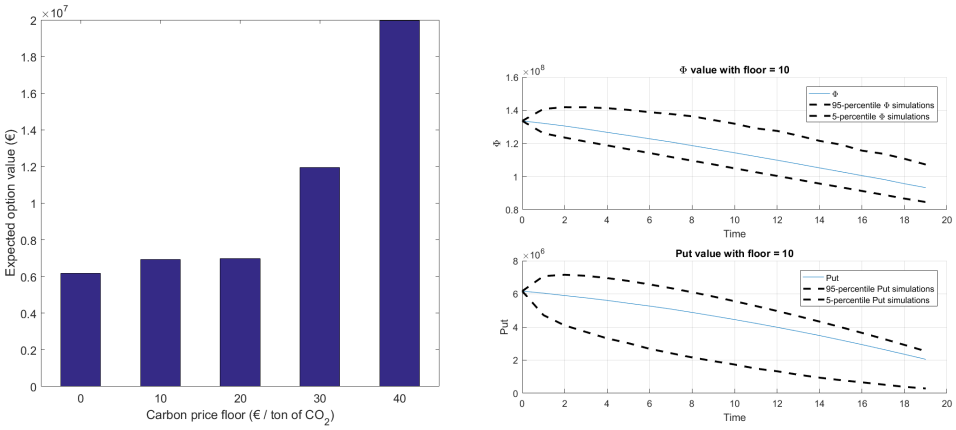

(a) Expected option value

(b) 5^{th} and 95^{th} percentiles for the benefits equation Φ and for the value of the put given in presence of a floor = 10.

Figure 2.6: Results in presence of a carbon floor price, r=2.5%.

analyzed the statistical features of carbon prices, we found a VG process was

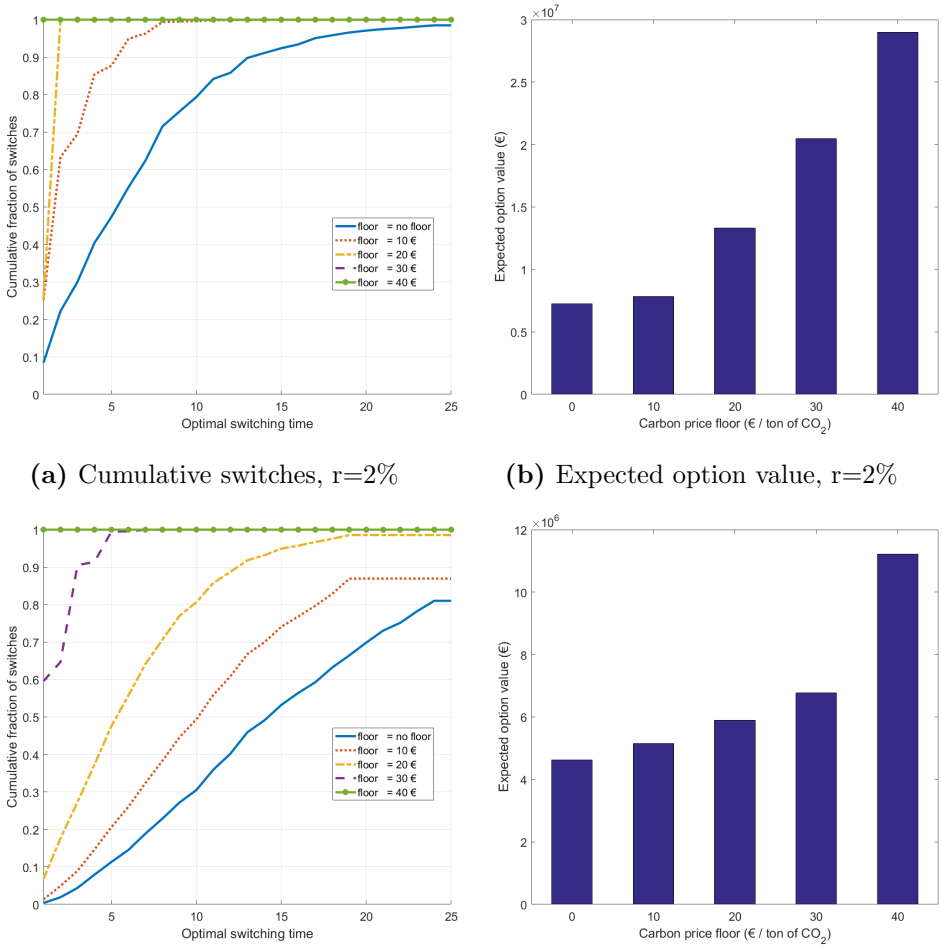

(a) Cumulative switches, r=2%

(b) Expected option value, r=2%

(c) Cumulative switches, r=3%

(d) Expected option value, r=3%

Figure 2.7: Sensitivity analysis of the results with a floor, using different annual risk-free interest rates r.

particularly suited for best fitting EUA price data. The other relevant state variable in our model, fossil fuel price, was modeled according to a mean-reverting stochastic process, as is usual practice for energy commodities: specifically, we chose a Brennan-Schwartz dynamics. Through a Monte Carlo simulation, we then generated a number of paths for each state variable. After defining the payoff function of the option to replace the current power plant with a PV one, we used a dynamic programming approach in order to assess the optimal switching time on each path. Specifically, we used LSMC as the computational method of choice. We also assessed the impact of a regulatory intervention in the EU ETS, in the form of a floor price on carbon

allowances. To do so, we computed the expected value of the investment project, by means of Fourier methods.

Our results show that a minimum CO_2 price of 30 €/ton of CO_2 would trigger immediate investment in the clean energy plant, and this result is quite robust to changes in the risk-free interest rate. On the other hand, without regulatory interventions, only in 50% of the simulated paths the optimal decision consists in exercising the option before 10 years.

Thus, according to the results of our model, a pure carbon trading system has a limited impact on renewable energy investments, and a policy intervention in the EU ETS seems advisable. Through a floor price, one of the goals of the EU ETS, namely boosting low-carbon investments in the power generation sector, could be achieved. Such a price management mechanism has already been implemented in the UK, as well as in three other emission trading programs, the northeastern US Regional Greenhouse Gas Initiative (RGGI), the California emission trading program and the Quebec one. The floor is implemented as a minimum bid in auctions, and, in all these three programs, it has been successful in enhancing environmental outcomes. The present work confirms the positive impact that such a policy intervention could have.

2.6 Appendix A

A.1 Technical characteristics of the oil-fired power plant

Given the capacity and the capacity factor values reported in Table 2.1 (10 MW and 80%, respectively), the yearly electricity output is computed:

$$\text{Electricity output} = 10,000\,\text{kW} \cdot 0.8 \cdot 365 \cdot 24\text{h} = 7.01 \cdot 10^7\,\text{kWh/year}.$$

The corresponding amount of energy needed to produce such an output is retrieved by simply dividing the electricity output by the efficiency rate of the plant (40%, as reported in Table 2.1), which results in $1.75{\cdot}10^8$ kWh/year. Given that the calorific value of crude oil is 42.5 MJ/kg, or 11,800 kWh/ton, the fuel consumption of the oil-fired plant is computed:

$$\text{Fuel consumption} = \frac{1.75 \cdot 10^8\,\text{kWh/year}}{11,800\,\text{kWh/ton}} = 1.48 \cdot 10^4\,\text{tons/year}.$$

As stated by the Intergovernmental Panel on Climate Change, the default CO_2 emission factor for crude oil is 73,300 kg/TJ IPCC (2006), or $2.64 \cdot 10^{-4}$ tons/kWh (since 1 kWh = 3.6 MJ). The yearly carbon emissions are thus given by:

CO_2 emissions $= 1.75{\cdot}10^8$ kWh/year $\cdot\, 2.64{\cdot}10^{-4}$ tons/kWh $= 46,200$ tons/year.

A.2 Solving the benefits equation

The oil spot price

The oil spot price follows a Brennan-Schwartz process, defined as

$$\mathrm{d}D(t) = k(\theta_D(t) - D(t))\,\mathrm{d}t + \sigma_D D(t)\,\mathrm{d}W(t) \tag{A.1}$$

To solve this stochastic differential equation (SDE), let us first consider the dynamics without the terms which do not depend on $D(t)$:

$$\mathrm{d}D_0(t) = -kD_0(t)\,\mathrm{d}t + \sigma_D D_0(t)\,\mathrm{d}B(t), \quad D_0(0) = d_0 > 0 \tag{A.2}$$

We can solve this SDE using Itō's formula:

$$D_0(t) = D_0(0)\,\mathrm{e}^{-\left(k+\frac{1}{2}\sigma_D^2\right)t+\sigma_D B(t)} \tag{A.3}$$

We now search for a solution to Equation (A.1), of the form $D(t) = D_0(t)Y(t)$. Applying Itō to $Y(t) = D(t)/D_0(t)$, we get:

$$\begin{aligned}
&\mathrm{d}Y(t) = \mathrm{d}\left(\frac{D(t)}{D_0(t)}\right) = \\
&= Y'_t + Y'_{D_1}\mathrm{d}D + Y'_{D_0}\mathrm{d}D_0 + \\
&\qquad + \frac{1}{2}\left(\frac{\delta^2 Y}{\delta D^2}(\mathrm{d}D)^2 + 2\frac{\delta^2 Y}{\delta D \delta D_0}\mathrm{d}D\mathrm{d}D_0 + \frac{\delta^2 Y}{\delta D_0^2}(\mathrm{d}D_0)^2\right) = \\
&= \frac{1}{D_0(t)}\mathrm{d}D(t) - \frac{D(t)}{D_0^2(t)}\mathrm{d}D_0(t) + \\
&\qquad + \frac{1}{2}\left(-\frac{2}{D_0^2(t)}\mathrm{d}D(t)\mathrm{d}D_0(t) + 2\frac{D(t)}{D_0^3(t)}\sigma_D^2 D_0^2(t)\mathrm{d}t\right) = \\
&= \frac{k\theta_D(t)}{D_0(t)}\mathrm{d}t
\end{aligned}$$

$$\Rightarrow \frac{D(t)}{D_0(t)} = \frac{D(0)}{D_0(0)} + \int_0^t \frac{k\theta_D(s)}{D_0(s)}\,\mathrm{d}s$$

So we have

$$D(t) = D_0(t)\left[\frac{D(0)}{D_0(0)} + \int_0^t \frac{k\theta_D(s)}{D_0(s)}\,\mathrm{d}s\right] \tag{A.4}$$

where $D_0(t)$ is given by eq. (A.3), and, more in general,

$$D(t) = D_0(t)\left[\frac{D(t_0)}{D_0(t_0)} + \int_{t_0}^t \frac{k\theta_D(s)}{D_0(s)}\,\mathrm{d}s\right] \tag{A.5}$$

with $s > t > 0$.

Solving $\Phi(D_t, P_t, t)$

We can now use equation (A.5) to solve (2.3.2), the equation for Φ.

• Let us begin by solving the first expected value block:

$$\begin{aligned}
&\int_t^T \mathbf{E}\left[BD_s\,\mathrm{e}^{-r(s-t)}\,|\,\mathcal{F}_t\right]\mathrm{d}s = \\
&\quad = B\int_t^T \mathrm{e}^{-r(s-t)}\,\mathbf{E}\left[\,D_s|\mathcal{F}_t\,\right]\mathrm{d}s = \\
&\quad = B\int_t^T \mathrm{e}^{-r(s-t)}\left\{D_1(t)\,\mathbf{E}\left[\mathrm{e}^{-\left(k+\frac{1}{2}\sigma_D^2\right)(s-t)+\sigma_D[B(s)-B(t)]}\,\middle|\,\mathcal{F}_t\right]\right. \\
&\qquad + \mathbf{E}\left[\mathrm{e}^{-\left(k+\frac{1}{2}\sigma_D^2\right)(s-t)+\sigma_D[B(s)-B(t)]}\right. \\
&\qquad \left.\left.\cdot\int_t^s \frac{k\,\theta_D(u)}{\mathrm{e}^{-\left(k+\frac{1}{2}\sigma_D^2\right)(u-t)+\sigma_D[B(u)-B(t)]}}\,\mathrm{d}u\,\middle|\,\mathcal{F}_t\right]\right\}\mathrm{d}s = \\
&\quad = B\int_t^T \mathrm{e}^{-r(s-t)}\left\{D_t\,\mathbf{E}\left[\mathrm{e}^{-\left(k+\frac{1}{2}\sigma_D^2\right)(s-t)+\sigma_D(B(s)-B(t))}\right]\right. \qquad \text{(A.6)} \\
&\qquad \left.+\int_t^s \mathbf{E}\left[k\,\theta_D(u)\,\mathrm{e}^{-\left(k+\frac{1}{2}\sigma_D^2\right)(s-u)+\sigma_D(B(s)-B(u))}\right]\mathrm{d}u\right\}\mathrm{d}s = \qquad \text{(A.7)} \\
&\quad = B\int_t^T \mathrm{e}^{-r(s-t)}\left\{D_t\,\mathrm{e}^{-k(s-t)}+\int_t^s k\,\theta_D(u)\,\mathrm{e}^{-k(s-u)}\,\mathrm{d}u\right\}\mathrm{d}s = \\
&\qquad\qquad\qquad\qquad\qquad\qquad\qquad\qquad\qquad\qquad\qquad\qquad\qquad\qquad \text{(A.8)} \\
&\quad = BD_t\frac{1-\mathrm{e}^{-(T-t)(r+k)}}{r+k}+kB\int_t^T \mathrm{e}^{-r(s-t)}\int_t^s \theta_D(u)\,\mathrm{e}^{-k(s-u)}\,\mathrm{d}u\,\mathrm{d}s = \\
&\quad = BD_t\frac{1-\mathrm{e}^{-(T-t)(r+k)}}{r+k}+\frac{kB\,\mathrm{e}^{rt}}{r+k}\int_t^T \theta_D(u)\left[\mathrm{e}^{-ru}-\mathrm{e}^{-rT-k(T-u)}\right]\mathrm{d}u \\
&\qquad\qquad\qquad\qquad\qquad\qquad\qquad\qquad\qquad\qquad\qquad\qquad\qquad\qquad \text{(A.9)}
\end{aligned}$$

where (A.6) and (A.7) follow from independence of $B(s)-B(t)$ on the filtration $\mathcal{F}_t$, while (A.8) is computed using the characteristic function of a Normal random variable. In case θ_D is constant, we get that (A.9) is equal to:

$$B\left[\frac{1-\mathrm{e}^{-(T-t)(r+k)}}{r+k}(D_t-\theta_D)+\frac{\theta_D}{r}\left(1-\mathrm{e}^{-r(T-t)}\right)\right].$$

As for the second expected value block, let us recall that

$$P_t = P_0\,\mathrm{e}^{\mu t+\theta_P T_t+\sigma_P B(T_t)}$$

where T_t has i.i.d. gamma increments, with $T_t \sim \Gamma(\alpha t, \alpha)$.
To price in a risk-neutral setting, we need to impose a restriction on the parameters, in order for the the discounted price to be a martingale. Specifically, for $t < s$, we need

$$\mathbf{E}\left[\mathrm{e}^{-rs} P_s \middle| \mathcal{F}_t\right] = \mathrm{e}^{-rt} P_t \,. \tag{A.10}$$

We have

$$\begin{aligned}
\mathbf{E}\left[\mathrm{e}^{-rs} P_s \middle| \mathcal{F}_t\right] &= \mathrm{e}^{-rs}\, P_0\, \mathbf{E}\left[\mathrm{e}^{\mu s + \theta_P T_s + \sigma_P B(T_s)} \middle| \mathcal{F}_t\right] = \\
&= \mathrm{e}^{-rs} P_0\, \mathbf{E}\left[\mathrm{e}^{\mu s + \theta_P (T_s - T_t + T_t) + \sigma_P (B(T_s) - B(T_t) + B(T_t))} \middle| \mathcal{F}_t\right] = \\
&= \mathrm{e}^{-rs-\mu t}\, P_t\, \mathbf{E}\left[\mathbf{E}\left[\mathrm{e}^{\mu s + \theta_P (T_s - T_t) + \sigma_P (B(T_s) - B(T_t))} \middle| \mathcal{F}_t^*\right] \middle| \mathcal{F}_t\right] = \qquad \text{(A.11)} \\
&= \mathrm{e}^{-rs+\mu(s-t)}\, P_t\, \mathbf{E}\left[\mathrm{e}^{\left(\theta_P + \frac{1}{2}\sigma_P^2\right)(T_s - T_t)} \middle| \mathcal{F}_t\right] = \qquad \text{(A.12)} \\
&= P_t\, \mathrm{e}^{-rs+\mu(s-t)} \left(1 - \frac{\theta_P + \frac{1}{2}\sigma_P^2}{\alpha}\right)^{-\alpha(s-t)} = \qquad \text{(A.13)} \\
&= \mathrm{e}^{-rt} P_t\, \mathrm{e}^{(\mu - r)(s-t)} \left(1 - \frac{\theta_P + \frac{1}{2}\sigma_P^2}{\alpha}\right)^{-\alpha(s-t)}
\end{aligned}$$

where (A.11) follows from the "tower", or repeated expectation, property. In fact, we define $\mathcal{F}_t$ as the information available up until time t, that is

$$\mathcal{F}_t = \sigma\left(\{B(u), u \le T_t\}, \{T_u, u \le t\}\right),$$

while $\mathcal{F}_t^*$ is defined as

$$\mathcal{F}_t^* = \sigma\left(\{B(u), u \le T_t\}, \{T_u, u \le T\}\right),$$

so that $\mathcal{F}_t \subset \mathcal{F}_t^*$. (A.12) follows again from the moment generating function of a Normal random variable and (A.13) follows from the moment generating function of the gamma density, with $\alpha > \theta_P + \frac{1}{2}\sigma_P^2$ which ensures the equation is finite.

Thus, for (A.10) to hold, we need to have

$$\mathrm{e}^{(\mu - r)(s-t)} \left(1 - \frac{\theta_P + \frac{1}{2}\sigma_P^2}{\alpha}\right)^{-\alpha(s-t)} = 1.$$

The necessary condition is then

$$\mu = r + \alpha \log\left(1 - \frac{\theta + \frac{1}{2}\sigma^2}{\alpha}\right) \tag{A.14}$$

and the second expected value block becomes

$$\int_t^T \mathbf{E}^{\mathbb{Q}}\left[X P_s \, \mathrm{e}^{-r(s-t)} \middle| \mathcal{F}_t\right] \mathrm{d}s = X \int_t^T \mathrm{e}^{rt} \, \mathrm{e}^{-rt} P_t \, \mathrm{d}s = \\ = X \, P_t \, (T-t) \, . \tag{A.15}$$

The solution to the third expected value block is trivial:

$$\int_t^T \mathbf{E}^{\mathbb{Q}}\left[Op \ \mathrm{e}^{-r(s-t)} \,\middle|\, \mathcal{F}_t\right] \mathrm{d}s = \frac{Op}{r}\left(1 - \mathrm{e}^{-r(T-t)}\right) \tag{A.16}$$

Putting together equations (A.9), (A.15) and (A.16), we have the solution for (2.3.2), given in (2.3.9).

Chapter 3

Pricing Reliability Options under different electricity price regimes *

Reliability Options are capacity remuneration mechanisms aimed at enhance security of supply in electricity systems. Can be framed as call options on power production sold by power producers to the System Operators. This chapter provides a comprehensive mathematical treatment of the Reliability Options. Their value is first derived by means of closed-form pricing formulas, which are obtained under several assumptions about the dynamics of the electricity prices and the strike prices. Then, the value of the Reliability Option is simulated under a real-market calibration, using data of the Italian Power market. Sensitivity analyses are performed to highlight the impact of power and strike price level and volatility, mean reversion speeds and correlation coefficient on the Reliability Options' evaluation.

*This paper is a joint work with Fulvio Fontini (Università degli Studi di Padova) and Tiziano Vargiolu (Università degli Studi di Padova). This paper has been submitted to an international journal.

3.1 Introduction

In several electricity markets worldwide there are capacity remuneration mechanisms that explicitly remunerate power capacity.[1] Among these, Reliability Options (RO) recognize the option nature of the investments in power capacity (or in load reduction) and create a market for such an option. ROs, firstly proposed in Vázquez et al. (2002), have been implemented in Colombia (Firm Energy Obligations (Cramton and Stoft (2007))), NE-ISO (Forward Capacity Market (FERC (2014))) and in Ireland (SEM (2015, 2016b,a))) and are about to be implemented in Italy (ARERA (2018); EC (2018); Mastropietro et al. (2017)). They are real options, namely, tools to commercialize through a financial product the possibility given by generation capacity (or load reduction) of providing security of supply by producing electricity (or reducing load). They give the holder, i.e., the System Operator (SO), which acquires them in a competitive setting, the right to call the generation capacity (or load) to produce power (or to reduce the load), and receive the positive difference between the electricity price that effectively occurs in the market and a pre-defined price level. Such a level, which corresponds to the strike price of the option, is set in order to represent the value of the power at that specific level for which load is not shed, i.e., it is the highest system marginal price compatible with load provision with no load shedding.

It is interesting to evaluate the RO as a financial asset. As any finance textbook shows (see e.g. Benth et al. (2008); Bjork (1998)), there are two ways to calculate the value of a financial product. The first one calls for defining its demand and supply, and searching for the equilibrium price under some market rules. The other one is the arbitrage approach, which asks for calculating the value of a replicating portfolio that yields the same return of the asset under all possible states of the world.

For the case of ROs, the equilibrium approach requires estimating their demand and supply. The demand of ROs is expressed by the SO. Even though the details of the RO demands depend on the specific rules in place in the different RO schemes, the procedure followed to derive such a demand is quite general and requires first to identify the targeted Security of Supply (SoS), then translate it into a desired level of installed capacity and finally introduce

[1] See Rodilla and Batlle (2013) and Cramton et al. (2013) for an introduction to capacity remuneration mechanisms

some security interval around that level and the corresponding premium and discount price that the SO is willing to pay to obtain it. The supply of RO is provided by eligible investors (that in some RO schemes might be further distinguished between existing capacity owners and future investors, depending on the different market rules), who participate in the RO market by first estimating their expected cost of investments and then strategically betting in the RO market. The arbitrage approach, on the contrary, requires identifying the stochastic property of the asset under evaluation as well as assuming that a continuous arbitrage between the financial derivative and the underlying asset is possible.

In a first-best world, with complete and perfectly competitive markets, both approaches lead to the same evaluation. However, in a second-best world, they rely on different assumptions. For instance, in the case of the RO, the evaluation following the equilibrium approach depends crucially on the estimation of the level of capacity needed to provide SoS and the TSO's willingness to pay for it, and on the strategic behavior of participants to the market mechanism allocating the RO. Such an estimate can turn out to be a difficult exercise. In fact, it is true that the amount of capacity that yields the targeted level of security of supply could be set administratively, or could be detected applying some simulation techniques; however, this does not guarantee that the demand is set at the efficient level, or that the estimate is correct, given the difficulties of measuring the willingness to pay for it. The same can be said about the strategic behavior of capacity providers, which might be influenced by several variables, including the auction market rules adopted to allocate ROs. The arbitrage approach, on the contrary, depends crucially on the assumption about the probability distribution of the underlying. In some cases, it can provide closed-form equations showing how the value depends on the different parameters of the distribution function of the underlying, in the style of the Black and Scholes formula (Benth et al. (2008); Bjork (1998)) evaluating European call options.

The latter is the framework of this analysis. We follow the arbitrage approach and estimate the value of the ROs under different possible assumptions about the dynamics of the stochastic processes on which they depend.

RO are complex options on power supply that can have different lengths and can be executed several times at different and possibly random strike

prices. Therefore, in order to evaluate ROs, it is necessary to provide a comprehensive mathematical treatment of all their aspects. This is the purpose of this chapter, which is, to the best of our knowledge, the first study undertaking this task. We first show semi-explicit formulae to evaluate the ROs, starting from the simplest possible assumption about electricity prices and the strike prices, and increasing the level of complexity of ROs, allowing for an underlying that can be a mean reverting process, for stochastic strike prices and for possibly negative electricity prices. We then simulate the RO values under different possible assumptions, and calibrate the RO parameters against real electricity market data, namely, the Italian Power Exchange ones. The availability of long hourly price time series and the forthcoming introduction of RO in the Italian market both justify the choice.

The chapter is structured as follows. Section 3.2 describes ROs and presents a pricing formula under realistic assumptions. Section 3.3 presents the pricing approaches, depending on the model that we can consider both for electricity prices as well as for the strike price of the RO. We start by defining the arbitrage-free boundaries of RO's evaluation. Then we move from the very simplistic model of geometric Brownian motion (GBM) with deterministic strike, to correlated GBMs for stochastic strike, and by increasing realism on the model, we arrive to the case when both electricity and strike prices are seasonal and mean-reverting. For all these models, we present semi-explicit pricing formulas. Finally, we provide some insights for the case of negative prices. In Section 3.4, we provide a simulation of the RO evaluation and perform a sensitivity analysis, using data of the Italian Power market for estimates and calibration. Section 3.5 concludes. Data of the estimates and proofs of propositions are in the Appendix.

3.2 Reliability options

ROs are sold in an auction, typically every year, to deliver electricity with a given lead time T_1, for a pre-defined $(T_2 - T_1)$-length period of delivery. The rules of the RO specify that the capacity provider, who sells the option, must commit to deliver the capacity to the buyer, which in general is the TSO. Such a commitment is made effective by prescribing that the seller must offer to the market an amount of electricity equal to the committed capacity and return any positive difference between the reference market price and the

strike price K.

Each RO contract scheme specifies what a market is. In a first approximation, the reference market can be a convex combination of different markets, such as the day-ahead or the balancing or the real-time ones. Some RO schemes, though, only have one reference market. For instance, in Ireland, the reference market is the day-ahead one, while in NE-ISO it is the real-time one.

Let P represent the day-ahead market price and $P^{(b)}$ the price in the balancing market (or in the real-time market). Then the reference market price R can be approximated as

$$R = \lambda P + (1 - \lambda)P^{(b)},$$

where $\lambda \in [0, 1]$ may depend on the country: $\lambda = 0$ for ISO New England; $\lambda = 1$ for Colombia and Ireland; $\lambda \in [0, 1]$ in the case of Italy (see Mastropietro et al. (2017) for a description of the forthcoming Italian market).

The strike price is, in general, determined by taking into account the variable costs of the reference peak technology, i.e. the dispatchable technology that would be included in the optimal generation mix with the lowest unitary investment cost. In actual RO markets, the strike price is communicated to potential sellers of ROs before the auction takes place. Thus, it can be treated as a deterministic parameter. However, it is also possible that the strike price changes overtime during the life span of the RO. This is a possibility envisaged, for instance, in the forthcoming Italian RO scheme. In such a scheme, the rule linking the strike price to a reference marginal technology is set before the auction, but the marginal cost of such a technology is calculated every given period (a month) during the life span of the RO.[2] This implies that the strike price can also be conceived as a stochastic process. We shall first derive the RO value starting with the simplest case, and then increase the level of complexity, to derive a general representation of the value of the RO.

[2]See Mastropietro et al. (2017) and Terna (2017a,b,c).

3.2.1 A simple mathematical model for Reliability Options

The mathematical modeling of the general RO is quite complex, as many auctions and prices are involved. We simplify it by defining a mathematical model for the case when the reference price is simply the day-ahead price P, i.e. $\lambda = 1$, as in the Colombian or in the Irish CRM schemes. In this way, only one state variable is needed for the reference market price R, and it is indeed P. We work on a filtered probability space $(\Omega, \mathcal{F}, \{\mathcal{F}_t\}_{t\geq 0}, \mathbb{Q})$ such that the probability measure $\mathbb{Q}$ is the risk-neutral pricing measure used by the market, and the day-ahead price $P = (P_t)_{t\geq 0}$ is a $\mathbb{Q}$-semimartingale. We set $t = 0$ as the auction time concerning capacity in the time period $[T_1, T_2]$.

Starting from these assumptions, we consider a simple case, namely that of a thermal plant, with total capacity $Q > 0$. This plant converts a fuel (oil, gas or coal) into electricity, whose spot price is P. Let $C = (C_t)_{t\geq 0}$ represent the costs associated to the power plant, i.e. fuel costs, emission costs, operational costs and others. The power plant sells the electricity at time $t \geq 0$ when it wins the day-ahead auction, i.e. when its bid b_t is less than or equal to P_t.

We adopt the usual simplifications, as continuous time instead of hourly granularity and no ramping penalties/constraints. The plant can decide its bid process $b = (b_t)_{t\geq 0}$ to maximize its revenues. Therefore the *value of the power plant* at $t = 0$, concerning the time period $[T_1, T_2]$, depends on its income over that time interval. This depends on the solution of the problem

$$V(T_1, T_2) = \sup_{b\in\mathcal{B}} \mathbf{E}^{\mathbb{Q}} \left[\int_{T_1}^{T_2} e^{-rt} Q \mathbb{1}_{b_t \leq P_t} (P_t - C_t) dt \middle| \mathcal{F}_0 \right],$$

with $\mathcal{B}$ being the set of adapted processes on $[T_1, T_2]$, r the instantaneous risk-free rate of return, and $\mathbf{E}^{\mathbb{Q}}$ the expectation with respect to $\mathbb{Q}$.

Obviously it will be optimal to have $\mathbb{1}_{b_t \leq P_t} = 1$ if and only if $P_t > C_t$, i.e. the optimal bidding process is $b_t = C_t$, for all $t \in [T_1, T_2]$ and the final payoff for a thermal plant is

$$V(T_1, T_2) = \mathbf{E}^{\mathbb{Q}} \left[Q \int_{T_1}^{T_2} e^{-rt} (P_t - C_t)^+ dt \middle| \mathcal{F}_0 \right].$$

On the other hand, when the thermal plant writes a RO with strike price $K = (K_t)_{t\geq 0}$, it must again place a bid, the bidding price b_t remains at its choice, and the plant must always pay back $(P_t - K_t)^+$. Therefore the payoff, in this case, takes the value:

$$V_{ro}(T_1, T_2) = \sup_{b\in\mathcal{B}} \mathbf{E}^{\mathbb{Q}} \left[\int_{T_1}^{T_2} e^{-rt} Q(\mathbb{1}_{b_t \leq P_t}(P_t - C_t) - (P_t - K_t)^+) \, dt \middle| \mathcal{F}_0 \right]$$

and $b_t = C_t$ for all $t \in [T_1, T_2]$ is again the optimal bidding strategy. Thus,

$$V_{ro}(T_1, T_2) = V(T_1, T_2) - \mathbf{E}^{\mathbb{Q}} \left[\int_{T_1}^{T_2} e^{-rt} Q(P_t - K_t)^+ \, dt \middle| \mathcal{F}_0 \right] .$$

In a risk-neutral world, the value $RO(T_1, T_2)$ of a RO written on the time interval $[T_1, T_2]$ should make the investor indifferent between having the original plant without the RO, and having it with the RO written on it plus the price of the option, i.e. $V(T_1, T_2) = V_{ro}(T_1, T_2) + RO(T_1, T_2)$. Therefore, the final result is

$$\begin{aligned} RO(T_1, T_2) &= V(T_1, T_2) - V_{ro}(T_1, T_2) \\ &= \mathbf{E}^{\mathbb{Q}} \left[\int_{T_1}^{T_2} e^{-rt} Q(P_t - K_t)^+ \, dt \middle| \mathcal{F}_0 \right] \end{aligned} \tag{3.2.1}$$

Thus, the value of a reliability option issued by a thermal plant is equivalent to the price of an insurance contract against price peaks. Interestingly enough, notice that the operating strategy of the power plants does not change. In electricity markets, it is well known that perfectly competitive markets without CRMs, the so called energy only markets, provide enough incentives to investment, and the same is true for optimally designed CRMs, since the latter simply anticipate ex ante the supermarginal profits that investors would gain in energy only markets. In other words, the amount of remuneration of capacity accruing from perfectly competitive markets for CRMs equals the expected discounted value of the supermarginal profits gained in electricity markets; in a world without market failures, the two levels coincide. This is confirmed in this framework: without market power, the value of operating the plant is independent on the form of remuneration of power production, i.e., on whether the revenues accrue ex-ante from the CRM or ex-post from selling electricity in the market.

3.3 Pricing of Reliability Options

3.3.1 Model-free no-arbitrage bounds

Equation (3.2.1) already allows to produce model-free no-arbitrage bounds on the price of the RO. In fact, starting from the put-call parity

$$(P_t - K_t)^+ = (K_t - P_t)^+ + P_t - K_t$$

we have that, since obviously $0 \leq (K_t - P_t)^+ \leq K_t$,

$$P_t - K_t \leq (P_t - K_t)^+ \leq P_t$$

By multiplying the inequalities for e^{-rt}, integrating and taking the expectation, we get

$$Q\mathbf{E}^{\mathbb{Q}}\left[\int_{T_1}^{T_2} e^{-rt}(P_t - K_t)\ dt \middle| \mathcal{F}_0\right] \leq RO(T_1, T_2) \leq Q\mathbf{E}^{\mathbb{Q}}\left[\int_{T_1}^{T_2} e^{-rt}P_t\ dt \middle| \mathcal{F}_0\right].$$

The right-hand side represents the forward price of delivering the quantity Q of electricity over the period $[T_1, T_2]$[3]. By introducing the quantity

$$F_P(0; T_1, T_2) := \mathbf{E}^{\mathbb{Q}}\left[\int_{T_1}^{T_2} e^{-rt}P_t\ dt \middle| \mathcal{F}_0\right]$$

for this (unitary) forward price, in the case when $K_t \equiv K$, i.e., with fixed strike, and recalling that we must have $RO(T_1, T_2) \geq 0$, after a simple integration we can rewrite the no-arbitrage relation above as

$$Q\left(F_P(0; T_1, T_2) - K\frac{e^{-rT_1} - e^{-rT_2}}{r}\right)^+ \leq RO(T_1, T_2) \leq QF_P(0; T_1, T_2)\,, \tag{3.3.1}$$

i.e. the value of a reliability option written on a total capacity Q for the period $[T_1, T_2]$ lies between the intrinsic value of Q call options on the forward $F_P(0; T_1, T_2)$ with a modified strike $K\frac{e^{-rT_1} - e^{-rT_2}}{r}$, and Q forwards $F_P(0; T_1, T_2)$.

Conversely, when K follows itself a stochastic process, by introducing an

[3] this is alternatively referred to as *flow forward* or *swap*, see e.g. Benth et al. (2008)

analogous quantity

$$F_K(0;T_1,T_2) := \mathbf{E}^{\mathbb{Q}}\left[\int_{T_1}^{T_2} e^{-rt}K_t\ dt\middle|\mathcal{F}_0\right],$$

we have

$$Q\left(F_P(0;T_1,T_2)-F_K(0;T_1,T_2)\right)^+ \leq RO(T_1,T_2) \leq QF_P(0;T_1,T_2)\,. \quad (3.3.2)$$

Thus, the upper bound is the same, while the lower bound is now the intrinsic value of Q exchange options on the forward $F_P(0;T_1,T_2)$ for the forward $F_K(0;T_1,T_2)$.

The advantage of these no-arbitrage bounds lies in the fact that, though no forward contract for the total period $[T_1,T_2]$ could possibly be traded on the markets, usually this period is a multiple of calendar years, whose contracts are traded. For example, in the Italian RO design, the period $[T_1,T_2]$ typically starts on January, 1 of year Y and lasts until December, 31 of year $Y+2$: thus, $F_P(0;T_1,T_2)$ ends up being just the sum of the three calendar products for the years Y, $Y+1$ and $Y+2$. In the case when the stochastic strike K is indexed with some marginal technology fixed in advance (e.g. combined cycle gas turbines), analogous forward contracts possibly exist for the corresponding fuel (gas in this case).

The no-arbitrage bounds above are model-free, in the sense that they should hold for any no-arbitrage model that we specify for the dynamics of P, and possibly of K. However, in order to evaluate the RO as a financial contract, it is necessary to specify the stochastic process modeling electricity prices. The electricity price shows peculiarities that make it difficult to model, as strong seasonality and mean-reversion. For this reason, several processes have been adopted to reproduce the price dynamics. In the rest of this section, we provide semi-explicit formulae to price ROs over the time period $[T_1,T_2]$ under different price dynamics, starting from the simplest one, namely a GBM.

3.3.2 Electricity spot price as a geometric Brownian motion

Let us start with the simplest assumption, i.e. that the price of electricity P evolves as a GBM, and the option's strike price K is a fixed deterministic value. We stress that the former is an assumption that we already know is unreasonable, in the sense that it cannot be assumed to provide a realistic representation of the dynamics of electricity prices. However, it is the simplest possible assumption that is used to derive explicit pricing formulas for call options. Thus, we treat it as a first simplified approach that helps us presenting the main features of the model. In this case, the price P, under the risk-neutral measure $\mathbb{Q}$, is assumed to be the solution of the following SDE:

$$dP_t = rP_t dt + \sigma P_t dB_t, \tag{3.3.3}$$

where B is a one-dimensional $\mathbb{Q}$-Brownian motion and r is the instantaneous risk-free rate of return.

The price of a RO in this case is equivalent to the time integral over the interval $[T_1, T_2]$ of a European call option with strike price K and maturity ranging in $[T_1, T_2]$.

In the following proposition we provide a semi-explicit formula to price the RO, under the assumptions above.

Proposition 3.3.1. *Let the reference market price P follow the dynamics* (3.3.3)*, then the price of a reliability option over the time interval $[T_1, T_2]$ with fixed strike price $K \geq 0$ is given by the following formula:*

$$RO(T_1, T_2) = \int_{T_1}^{T_2} Q \left[P_0 N(d_1(K, P_0, t)) - e^{-rt} K N(d_2(K, P_0, t)) \right] dt \,, \tag{3.3.4}$$

where N is the cumulative distribution function of a standard Gaussian ran-

dom variable and

$$d_1(K, P_0, t) = \frac{1}{\sigma\sqrt{t}}\left[\ln\left(\frac{P_0}{K}\right) + \left(r + \frac{\sigma^2}{2}\right)t\right],$$
$$d_2(K, P_0, t) = d_1(K, P_0, t) - \sigma\sqrt{t}\,.$$

Proposition 3.3.1 simply makes use of the Black and Scholes formula, since the $RO(T_1, T_2)$ value turns out to be the time integral of a family of call options with the same underlying and strike price, indexed by their maturity in $[T_1, T_2]$.[4] Thus, it provides a formula that can be applied to calculate the value of the RO, once that the parameters upon which the call depends on have been set, namely, the riskless interest rate, the starting price P_0 and the volatility of the electricity price.

3.3.3 Electricity price and strike price as correlated Geometric Brownian Motions

A first step towards increasing the level of complexity refers to modeling the strike price as a stochastic process. Recall that, in ROs, the strike price is the marginal cost of the marginal technology. Complex RO schemes can allow it to change over time, according to a predefined rule. For instance, it can be assumed that the strike price is given by the fuel cost of a predefined marginal technology, such as Combined Cycle Gas Turbines, thus linked to a reference fuel price. Alternatively, it can be established that the reference price changes at fixed regular dates according to a given indexing formula, for example monthly, and stays constant in each of these sub periods.[5] In any case, this requires to treat the strike price as a stochastic process. Thus, a first extension of the model defined in Section 3.3.2 is modeling K and P as two (possibly correlated) geometric Brownian motions. This means that the prices $(K_t, P_t)_{t\geq 0}$ follow a risk-neutral dynamics of the following type:

$$\begin{cases} dK_t = (r - q_k)K_t dt + \sigma_k K_t dB_t^1 \\ dP_t = (r - q_p)P_t dt + \sigma_p P_t dB_t^2\,, \end{cases} \tag{3.3.5}$$

[4] Interestingly enough, this result solves also a problem firstly posed in McDonald and Siegel (1985), in the framework of firms' evaluations.

[5] As mentioned, this is going to be the case of the future Italian RO scheme.

where (B^1, B^2) are correlated $\mathbb{Q}$-Brownian motions, with correlation $\rho \in [-1, 1]$. Notice that the correlation of the two stochastic processes depends on their nature and on the rules defining the strike price. For instance, if the variable strike price is set to be equal to the marginal cost of the marginal technology, and if the electricity market is perfectly competitive, it would be natural to assume a correlation coefficient equal to 1, being the system marginal price equal to the marginal cost of the marginal technology. If, on the contrary, the stochastic strike price equals some weighted average of different marginal costs at different hours, for instance at peak and off-peak hours, then the correlation coefficient would be positive but less than 1, since the electricity price P would be more volatile than the strike price K. Finally, it is also possible that the strike price is negatively correlated with the electricity price, depending on what the formula of the strike price is and on what reference basket it is linked to. However, this possibility is rather unlikely, for the reasons expressed above.

The following proposition provides the value of the RO with two GBMs:

Proposition 3.3.2. *Let the reference market price P and the RO strike price K follow the dynamics* (3.3.5)*. Then the price of a reliability option over the time interval $[T_1, T_2]$ is given by*

$$RO(T_1, T_2) = \int_{T_1}^{T_2} \left(P_0 e^{-q_p t} N(a_1(K_0, P_0, t)) - K_0 e^{-q_k t} N(a_2(K_0, P_0, t)) \right) dt \,, \tag{3.3.6}$$

where N is the cumulative distribution function of a standard normal random variable, and

$$\begin{aligned} a_1(K_0, P_0, t) =& \frac{\ln\left(\frac{P_0}{K_0}\right) + (q_p - q_k)t}{\sigma\sqrt{t}} + \frac{1}{2}\sigma\sqrt{t} \,, \\ a_2(K_0, P_0, t) =& a_1(K_0, P_0, t) - \sigma\sqrt{t} \,, \\ \sigma =& \sqrt{\sigma_k^2 + \sigma_p^2 - 2\rho\sigma_k\sigma_p} = \sqrt{(\sigma_k - \sigma_p)^2 + 2(1-\rho)\sigma_k\sigma_p} \,. \end{aligned}$$

Proposition 3.3.2 is similar to Proposition 3.3.1, except for the fact that here the Margrabe formula with dividends is used (see, for instance, Carmona and Durrleman (2003)), instead of the Black-Scholes one. In fact, here $RO(T_1, T_2)$ turns out to be the time integral of a family of options to ex-

change the (random) electricity price P with the (random) strike price K, again indexed by their maturity. As usual in the Margrabe formula, the relevant volatility here is σ, which can be interpreted as the volatility of the ratio P/K (i.e., the electricity price expressed in units of the strike price), which is decreasing with respect to the correlation ρ. In particular, for $\rho \to 1$ (i.e. when the strike price is much correlated with the electricity price), we have $\sigma \to |\sigma_k - \sigma_p|$. In this case, when $\sigma_k = \sigma_p$, the volatility vanishes, and the value of the option is given just by its intrinsic value. Instead, for $\rho \to -1$ (i.e. when the strike price is much negatively correlated with the electricity price), we have $\sigma \to \sigma_k + \sigma_p$, i.e., the volatility is maximized. However, we stress that this latter case is rather unlikely for the case of RO, as typically a stochastic strike price K is defined in terms of quantities related to electricity generation (as e.g. the marginal price of the marginal technology, or some related market index), so that we should expect a positive correlation.

3.3.4 Mean-reverting electricity price with seasonality

As mentioned, the GBM dynamics for electricity prices used in the previous sections is too simple and does not capture typical stylized facts of electricity prices, namely seasonality and mean-reversion. A natural extension concerns the pricing of ROs when the dynamics of the reference price shows the aforementioned stylized facts. In particular, we choose to model the log-spot price of electricity with a mean-reverting dynamics that encodes different seasonalities by means of a time-dependent function. Seasonality can be modeled in different ways, for example using dummy variables , or a linear combination of trigonometric functions (see for instance Benth et al. (2008) and references therein). Here we chose to model seasonality using different dummies, as in Eq. (4.3.2). For simplicity, we start by assuming that the strike price is deterministic. In the next section, we shall remove this assumption.

We define the function describing seasonality trends for all $t \geq 0$, as

$$\mu(t) = \sum_{i=1}^{11} \beta_i \, month_i + \sum_{i=1}^{3} \delta_i \, day_i + \sum_{i=1}^{23} \gamma_i \, hour_i + \alpha \,, \tag{3.3.7}$$

where $month_i$, day_i and $hour_i$ are dummies for month, day of week and hour, used to capture different types of seasonality. Specifically, we assume that *day* can take 4 values: 'Friday', 'Weekend', 'Monday', and 'other working

day'. This captures the differences between working days and weekend as well as possible first- or end-of-the-working-week effect.

Then we consider the day-ahead price P as

$$P_t = e^{\mu(t)} e^{X_t}\,, \tag{3.3.8}$$

where X_t, under the risk-neutral measure $\mathbb{Q}$, is the solution of the SDE

$$dX_t = -\lambda X_t dt + \sigma dW_t\,, \tag{3.3.9}$$

where W is a one dimensional $\mathbb{Q}$-Brownian motion, σ stands for the volatility and $\lambda > 0$ is the mean-reversion speed. We have the following:

Proposition 3.3.3. *Let the reference market price P follow the dynamics* (3.3.8)–(3.3.9)*. Then the price of a reliability option over the time interval $[T_1, T_2]$ with fixed strike price $K \geq 0$ is given by*

$$RO(T_1,T_2) = Q \int_{T_1}^{T_2} e^{-rt} \left[e^{\mu(t)+m_t+\frac{Var(t)}{2}} N(d_2(K,P_0,t)) - K N(d_1(K,P_0,t)) \right] dt\,, \tag{3.3.10}$$

where N is the CDF of a normal random variable, $P_0 = e^{\mu(0)+X_0}$ and

$$\begin{aligned} m_t &= X_0 e^{-\lambda t}\,, \\ Var(t) &= \frac{\sigma^2}{2\lambda}(1 - e^{-2\lambda t})\,, \\ d_1(K,P_0,t) &= \frac{1}{\sqrt{Var(t)}} \left(\mu(t) + m_t - \ln K\right)\,, \\ d_2(K,P_0,s) &= d_1(K,P_0,t) + \sqrt{Var(t)}\,. \end{aligned}$$

Remark 3.3.1. Equation (3.3.10) is a generalization of Equation (3.3.4): in fact, if we let $\mu(t) := (r - q_p - \frac{1}{2}\sigma^2)t$ and $\lambda \to 0$, then, at the limit, we obtain again the model of the previous section. In fact, we have that $m_t \equiv X_0$, $Var(t) \to \sigma^2 t$,

$$e^{-rt} e^{\mu(t)+m_t+\frac{Var(t)}{2}} \to e^{(r-q_p)t+X_0}\,,$$

and

$$d_1(K, P_0, t) \to \frac{1}{\sigma\sqrt{t}}\left(X_0 + (r - q_p)t - \frac{1}{2}\sigma^2 t - \ln K\right)$$
$$= \frac{1}{\sigma\sqrt{t}} \ln \frac{e^{X_0+(r-q_p)t}}{K} - \frac{1}{2}\sigma\sqrt{t}\,.$$

Thus, the evaluation formula in Equation (3.3.10) collapses into that of Equation (3.3.4).

3.3.5 Allowing for mean-reverting strike price with seasonality

As already pointed out at the end of Section 3.2, a stochastic K is used to model its possible dependence on variables linked to electricity generation. Thus, a natural extension of the model in Section 3.3.4 consists in providing also K with a mean-reverting dynamics including a seasonality term. The dynamics of the state variables become then

$$\begin{cases} P_t = & e^{\mu(t)}e^{X_t}, \\ K_t = & e^{\nu(t)}e^{Y_t}. \end{cases} \tag{3.3.11}$$

Here μ is given by (4.3.2) and ν is a seasonality function for K of the same form, while the processes X and Y are solution to the following:

$$\begin{cases} dX_t = & -\lambda_x X_t dt + \sigma_x dW_t^1, \\ dY_t = & -\lambda_y Y_t dt + \sigma_y dW_t^2, \end{cases} \tag{3.3.12}$$

where (W^1, W^2) are correlated $\mathbb{Q}$-Brownian motions, with correlation $\rho \in [-1, 1]$. One can prove that the price of the reliability option is given by the following expression:

$$RO(T_1, T_2) = Q \int_{T_1}^{T_2} e^{-rt}\mathbf{E}^{\mathbb{Q}}\left[(e^{\mu(t)}e^{X_t} - e^{\nu(t)}e^{Y_t})^+ \;\middle|\; \mathcal{F}_0\right] dt. \tag{3.3.13}$$

It is easy to see that the above formula is the time integral of a family of exchange options, indexed by their expiration date in $[T_1, T_2]$.

Proposition 3.3.4. *Let the reference market price P and the RO strike price K follow the dynamics* (3.3.11)*; then the price of a reliability option over the time interval $[T_1, T_2]$ is given by*

$$RO(T_1,T_2) = Q\int_{T_1}^{T_2} e^{-rt}\left[\mathbf{E}^{\mathbb{Q}}[P_t]N\left(d_2(K_0,P_0,t)\right) - \mathbf{E}^{\mathbb{Q}}[K_t]N\left(d_1(K_0,P_0,t)\right)\right]dt \tag{3.3.14}$$

where N is the CDF of a normal random variable, $P_0 = e^{\mu(0)+X_0}$, $K_0 = e^{\nu(0)+Y_0}$ and

$$\mathbf{E}^{\mathbb{Q}}[P_t] = e^{\mu(t)+e^{-\lambda_x t}X_0+\frac{1}{2}\sigma_x^2\frac{1-e^{-2\lambda_x t}}{2\lambda_x}}, \tag{3.3.15}$$

$$\mathbf{E}^{\mathbb{Q}}[K_t] = e^{\nu(t)+e^{-\lambda_y t}Y_0+\frac{1}{2}\sigma_y^2\frac{1-e^{-2\lambda_y t}}{2\lambda_y}}, \tag{3.3.16}$$

$$d_1(K_0,P_0,t) := \frac{1}{\sqrt{\overline{Var}(t)}}\left(\mu(t)-\nu(t)+\bar{m}_t\right), \tag{3.3.17}$$

$$d_2(K_0,P_0,t) := d_1(K_0,P_0,t) + \sqrt{\overline{Var}(t)}, \tag{3.3.18}$$

$$\bar{m}_t := e^{-\lambda_x t}X_0 - e^{-\lambda_y t}Y_0 + \rho\sigma_x\sigma_y\frac{1-e^{-(\lambda_x+\lambda_y)t}}{\lambda_x+\lambda_y} - \sigma_y^2\frac{1-e^{-2\lambda_y t}}{2\lambda_y}, \tag{3.3.19}$$

$$\overline{Var}(t) := \sigma_x^2\frac{1-e^{-2\lambda_x t}}{2\lambda_x} + \sigma_y^2\frac{1-e^{-2\lambda_y t}}{2\lambda_y} - 2\rho\sigma_x\sigma_y\frac{1-e^{-(\lambda_x+\lambda_y)t}}{\lambda_x+\lambda_y}. \tag{3.3.20}$$

This result is a similar to Proposition 3.3.3 in the same sense as Proposition 3.3.2 is similar to Proposition 3.3.1: in fact, here $RO(T_1,T_2)$ turns out to be again the time integral of a family of options to exchange the electricity price P with the strike price K. Here too, the relevant volatility is $\overline{Var}(t)$, which can again be interpreted as the volatility of the ratio P/K (i.e., the electricity price expressed in units of the strike price: this is made explicit in the proof in Appendix 3.6), which is again decreasing with respect to the correlation ρ. In particular, for $\rho \to 1$ (i.e. when the strike price is much correlated with the electricity price), and $\lambda_x = \lambda_y =: \lambda$ (i.e. when the two mean-reversion speeds are the same), we have $\overline{Var}(t) \to \frac{1-e^{-2\lambda t}}{2\lambda}(\sigma_x-\sigma_y)^2$. In this case, when $\sigma_x = \sigma_y$, the volatility vanishes, and the value of the option is given

just by its intrinsic value. Instead, in the unlikely case (see the discussion at the end of Section 3.3.3) when $\rho \to -1$ (i.e. when the strike price is much negatively correlated with the electricity price) and $\lambda_x = \lambda_y =: \lambda$, we have $\overline{Var}(t) \to \frac{1-e^{-2\lambda t}}{2\lambda}(\sigma_x + \sigma_y)^2$, i.e., the volatility is maximized.

3.3.6 Possible extension to negative day-ahead and strike prices

In principle, it is possible to allow for power prices to have negative values, since we know this is a possibility in energy prices, see Edoli et al. (2017) and references therein. An analogous extension can be also imagined for strike prices, especially when these are linked to power prices.

A possible approach to model negative prices is to set negative values $-P^*$ and $-K^*$, for certain $P^*, K^* \geq 0$, as price floors for P and K, respectively, and to consider for them a shifted dynamics of the type

$$\begin{cases} P_t = & \left(e^{\mu(t)}e^{X_t} - P^*\right), \\ K_t = & \left(e^{\nu(t)}e^{Y_t} - K^*\right). \end{cases} \tag{3.3.21}$$

where μ and ν are again seasonality functions for P and K and the processes X and Y are solutions of Equation (3.3.12), in analogy with the previous section.

By setting $C := P^* - K^*$, one can prove that the price of the reliability option is now given by the following expression:

$$RO(T_1, T_2) = Q \int_{T_1}^{T_2} e^{-rt} \mathbf{E}^{\mathbb{Q}} \left[(e^{\mu(t)}e^{X_t} - e^{\nu(t)}e^{Y_t} - C)^+ \,\middle|\, \mathcal{F}_0 \right] dt. \tag{3.3.22}$$

It is easy to see that the above formula is the time integral of a family of spread options with a fixed strike price C and indexed by their expiration date in $[T_1, T_2]$. Therefore, considering dynamics of type (3.3.21) relates the problem of pricing a Reliability Option to the problem of pricing a spread option (see Carmona and Durrleman (2003) for a survey of classical frameworks and methods for spread options). Unfortunately, a general closed formula for the pricing of spread options is not available. However, since the RO is in principle a product which is quite illiquid, one can use a numerical method to price it in this general case, for example Monte Carlo.

3.4 Simulation and sensitivity analysis

In this section we simulate the value of the RO under realistic assumptions on the value of the parameters. To do so, we fit the parameters of the electricity price dynamics to a real market, using data of the Italian market. For simplicity, we consider day-ahead prices only, and use the weighted average of Italian zonal prices, called PUN (*Prezzo Unico Nazionale*), ranging from January 1, 2016 to December 31, 2016.

As previously explained, we use dummies to capture monthly, daily and hourly seasonality, as defined in Eq. (4.3.2). We choose 'January', 'Friday' and 'hour 1' as reference groups, against which the comparisons are made. Figure 3.1 shows the calibrated seasonality function, plotted against the historical PUN data. Furthermore, we consider an annual risk-free rate $r = 0.01$, and, in the pricing models where the only stochastic variable is the electricity price, we consider $K = 40$ €/MWh. The pricing of the RO starts 4 years from now, and the option has a maturity of 3 years ($T_1 = 4$, $T_2 = 7$). This resembles the structure of the RO which is about to be implemented in the Italian market. The starting point X_0 is taken equal to 0.

Table 3.1 reports the estimated parameters for each different model, while Table B.1 shows the estimated seasonality parameters.

	GBM	1-OU	2-OU
$\hat{\sigma}$	5.4041	6.5932	6.5932
$\hat{\lambda}$	-	294.84	294.84

Table 3.1: Estimated yearly parameters $\hat{\sigma}$ and $\hat{\lambda}$ for each pricing model (electricity price following a Geometric Brownian motion (GBM), electricity price following a mean-reverting Ornstein-Uhlenbeck process (1-OU), correlated electricity and strike prices following mean-reverting Ornstein-Uhlenbeck processes (2-OU)).

As mentioned, real electricity prices do not follow GBMs. Therefore, in the simulation, we start from the model defined in Section 3.3.4.

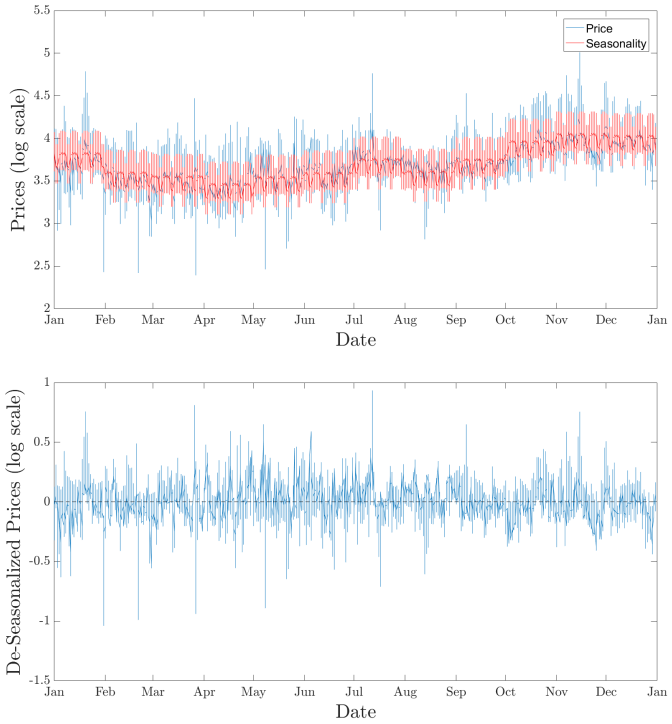

Figure 3.1: Seasonality function in (4.3.2) (solid red line, upper panel) calibrated on historical 2016 PUN electricity data (solid blue line, upper panel) and residuals (bottom panel).

3.4.1 Mean reverting electricity price with seasonality, fixed strike

We simulate the value of the RO using the Monte Carlo methodology. Specifically, we compute the RO value using 10,000 simulations of the price path of the underlying.

Figure 3.3 shows the comparative statics for different parameters σ and λ and strike price K. As expected, the higher the strike price, the lower the value of the reliability option for each value of σ (left panel). On the other hand, both the left and right panel show that, when σ increases, the RO value rises as well. Moreover, when λ is low, the relative increase in the RO value is high (right panel). This is consistent with the fact that a low λ allows fluctuations of the underlying that are far from the long term mean to be more persistent.

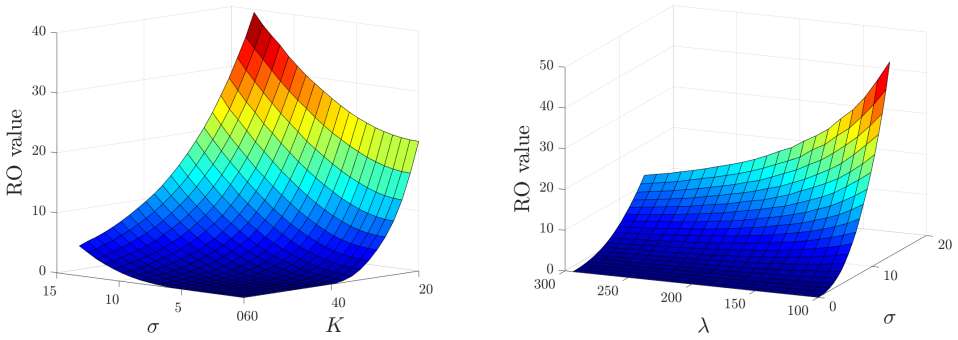

Figure 3.3: Sensitivity analysis of the results using a yearly σ in the range $(0; 2\hat{\sigma}]$ with a strike price K in the range $[20; 60]$ (left panel), and a yearly σ in the range $(0; 2\hat{\sigma}]$ with and a yearly λ in the range $(100; 2\hat{\lambda}]$ (right panel). The RO value is expressed in €/MWh.

3.4.2 Electricity spot price and RO strike price as correlated OU with seasonality

We simulate now the value of the RO using the model described in Section 3.3.5, again by means of a Monte Carlo method (again using 10,000 runs). We start from a given correlation coefficient, set at $\rho = 0.5$, and assume that λ_K and σ_K are equal to the ones estimated for the electricity price. Again, $X_0 = 0$. In line with the PUN mean price, which is equal to 42.77 €/MWh, K_0 is arbitrarily chosen equal to 40 €/MWh, so that, after de-seasonilizing (using the same estimated seasonality parameters of the PUN price), we obtain $Y_0 = -0.21$.

Figure 3.4 shows the results when we assume the strike price process to have the same parameters estimated for the electricity price P. The upper left panel shows that the initial level of the strike price K_0 has no influence on the value of the reliability option. This is due to the magnitude of the estimated λ_P, and thus of λ_K: a mean reversion speed as high as that estimated makes the strike price process return to its mean level in an amount of time negligible with respect to the maturity, meaning that the starting point of the process has no relevant impact on the RO value.

The upper right panel of Figure 3.4 instead shows how sensitive the RO value is to changes in the electricity price parameters λ_P and σ_P (and thus in turn in λ_K and σ_K). Similarly to what we have observed before, the higher

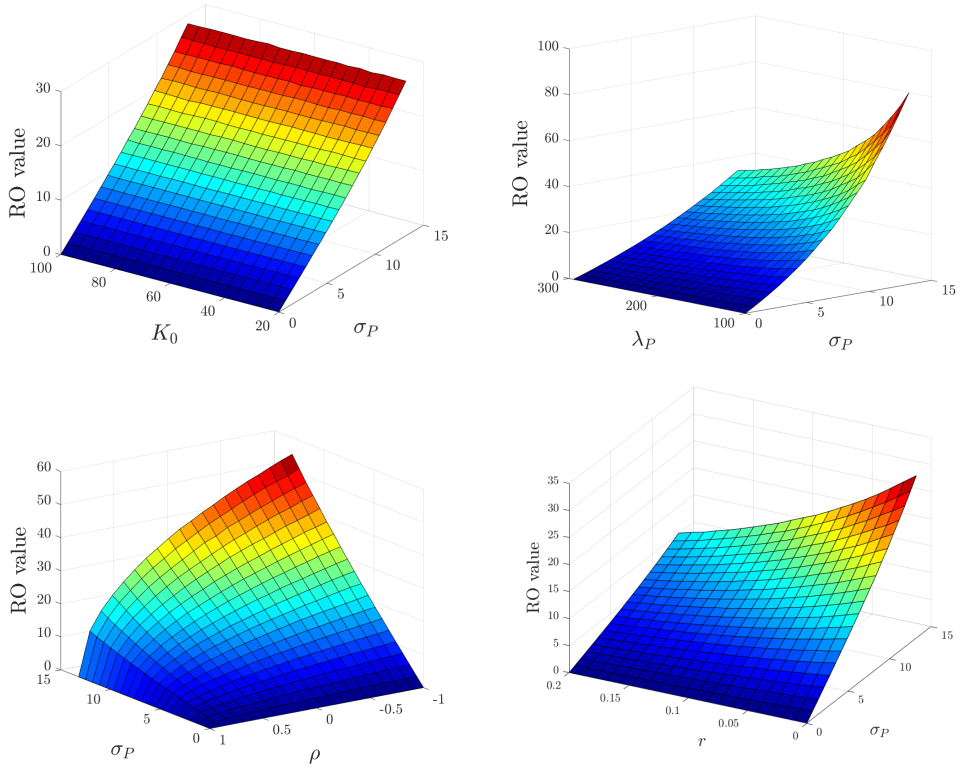

Figure 3.4: Sensitivity analysis of the results using a yearly σ_P in the range $(0; 2\hat{\sigma}_P]$ with an initial strike K_0 in the range $[20; 100]$ (upper left panel), with a yearly λ_P in the range $(100; 2\hat{\lambda}_P]$(upper right panel), with a correlation ρ in the range $[-1; 1]$ (left bottom panel) and with a yearly risk free rate r in the range $[0; 0.2]$ (right bottom panel).

the volatility of the underlying (and, in this case, of the strike price), the higher the RO value, and this relationship increases in proportionality as the speed of mean reversion lowers, since it takes more time to return to the mean, and thus volatility matters more.

The impact of the correlation factor ρ is instead investigated in the bottom left panel, where we assessed how different correlation factors in the range $[1; -1]$ affect the price of the reliability option. When the two assets are perfectly correlated ($\rho = 1$), the RO value is zero for all levels of σ_P. In fact, as we have seen in Section 3.2, the volatility is minimized and the RO can be interpreted as an integral of calls, with maturity ranging in the interval $[T_1, T_2]$, being exactly at the money at the time of expiration, and thus having zero value. Instead, as shown, when the two processes are un-

correlated, the level of risk increases, and it reaches its maximum when they are perfectly negatively correlated. In this case, the volatilities of the two Brownian motions sum up, increasing the overall volatility of the option payoff and minimizing the risk of having the call options at the money. Finally, the bottom right panel shows that the RO price is negatively correlated with the risk free rate r: a higher r decreases the option value as it lowers the discounted cash flows.

In the previous figures, the parameters for λ_P and λ_K, and σ_P and σ_K, were tied together, in the sense that λ_K and σ_K were always equal to, respectively, λ_P and σ_P.

Instead, we now investigate what happens keeping σ_K equal to σ_P as before, but changing λ_K independently from λ_P. Moreover, we also investigate the effects of a variation in σ_P different from that in σ_K. Figure 3.5 and 3.6 show the results.

The left panel of Figure 3.5 reports the results for a variation in λ_K (in the range $(0; 2\hat{\lambda}_P]$ and shown in $\log_{10}$ scale) independent from the value of λ_P. We can see how K_0 hardly affects the reliability option value, having an impact only when both σ_K and λ_K are sufficiently small. This confirms the result shown above, i.e. that the initial condition of the parameters matters only when it takes a sufficient amount of time for them (for the strike price, in this case) to return to their long term value. The right panel instead shows the sensitivity of the RO value to changes in the yearly λ_K (again in the range $(0; \hat{\lambda}_P]$) independent from the value of λ_P, and in the correlation factor ρ (in the range $[-1; 1]$) (in this graph, σ_K is always equal to σ_P and they are in turn equal to $\hat{\sigma}_P$, $\lambda_P = \hat{\lambda}_P$, and λ_K is shown in $\log_{10}$ scale.). Here we can see that the ρ value matters more when <u>both</u> $\lambda_K = \lambda_P$ and $\sigma_K = \sigma_P$. In fact, ρ affects (negatively) the RO value only when it tends to -1 and λ_K is closer to the value of λ_P (note that, in the figure, $\lambda_K \in (0; \hat{\lambda}_P]$, where $\hat{\lambda}_P$ corresponds to the value of 2.47 in $\log_{10}$ scale). This confirms the intuition that when the initial value of the electricity price and the strike price are close, and the two random variables follow the same dynamics, the RO has a limited or null value since it is likely that it will be always at the money. Conversely, if the two random variables are not perfectly correlated, or they follow different dynamics, it is unlikely that at every point in time P_t and K_t coincide, and this adds value to the RO.

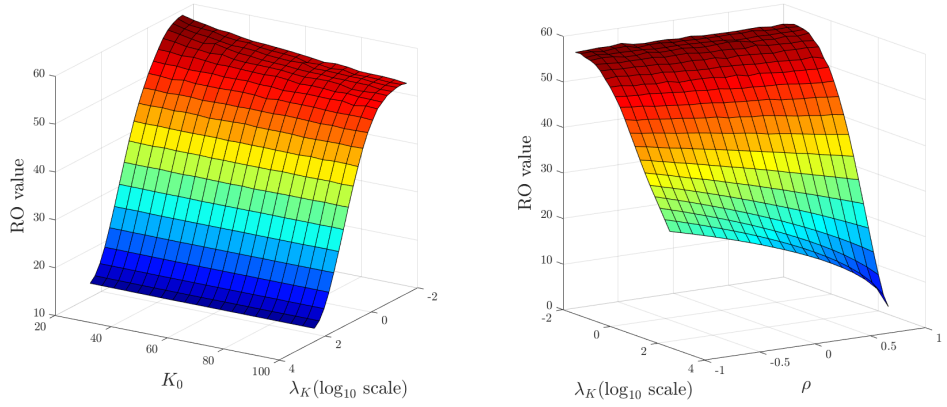

Figure 3.5: Sensitivity analysis of the results using a yearly λ_K in the range $(0; \hat{\lambda}_P]$ with an initial strike price K_0 in the range $[20; 100]$, both with a yearly σ_K equal to the yearly σ_P (upper left panel) and with and a scaled down yearly σ_K (upper right panel), and with a correlation ρ in the range $[-1; 1]$ (bottom panel) (here $\sigma_K = \sigma_P$). The RO value is expressed in €/MWh.

Finally, Figure 3.6 shows the effect of a disjoint variation in the two volatilities, with a yearly σ_P and σ_K in the range $(0; 2\hat{\sigma}_P]$, for different levels of ρ (in these graphs, λ_K is always equal to $\lambda_P = \hat{\lambda}_P$). When $\rho \leq 0$, we can see that the RO price is always increasing in the electricity price volatility σ_P and in the strike price's one σ_K. This is as expected, since the volatility adds value to the call options. Instead, when $\rho > 0$, the fact that the two processes move together can lower the aggregate risk, since the spread between the electricity price and the strike price decreases. This translates into a negative effect on the option value. The RO value is minimized when $\sigma_P = \sigma_K$. In Figure 3.6, panel $\rho = 0.5$, we can see that the option value is still positive; in the panel $\rho = 1$, the RO value becomes null for $\sigma_P = \sigma_K$, since, as we have seen, having two perfectly positively correlated identical processes means that the RO value simply corresponds to its intrinsic value. Thus, there is a non-monotone effect of the rise of volatility of one process, depending on the amount of volatility of the other process, and on the level of the correlation coefficient. The flex is maximum when the two processes are perfectly positively correlated.

3.5 Conclusions

In this chapter, we have studied the value of the RO from a financial perspective. The simplified mathematical model that we proposed is a starting point in the analysis of ROs. In particular, it does not consider the different market mechanisms through which they are sold, or the possible strategic behavior of power producers. However, even in this simplified framework, we obtained semi-explicit formulae for the value of the RO, increasing the level of realism and complexity of the model. We moved from simple integrals of call options written on GBMs to correlated mean reverting processes that capture the behavior of realistic electricity price time series, on the one hand, and complex rules for RO, on the other hand. Then, we simulated the value of the Reliability Option through a real-market calibration of the parameters. We saw that the value of the RO moves coherently with expectations of option theory: a rise in strike price lowers the RO value, which depends positively on the volatility of the electricity price, as well as on the volatility of the strike price itself. The mean reversion speed of the processes reduces the impact of the starting point, which was another expected result. However, when both the strike price and the electricity price are assumed to be stochastic processes, the value of the RO crucially depends on their correlation coefficient ρ. In particular, a positive correlation reduces the value of the RO. Moreover, there is a non-monotone impact of the volatility of one process, depending on the level of volatility of the other process and on a positive correlation. This is important when designing the rule of the RO. For instance, if the strike price is allowed to change with respect to a reference marginal cost, which is also believed to be the technology setting the system marginal price at the day ahead level, the two process clearly covariate positively. In this case, it is very likely that a RO scheme has a very limited value, for every possible starting value of the state variables P and K.

More in general, our results show that a careful estimate of the parameters is needed to calculate the value of the ROs. *Ceteris paribus*, the RO value will be lower the lower the volatility of the electricity price, the higher the strike price, the quicker the speed of mean reversion, the higher the correlation of the electricity price with the strike price, if the latter is allowed to change over time, and the closer the two volatilities to each other. These are all

factors that need to be taken into account when designing the market for ROs and calculating the equilibrium value.

Acknowledgments. The "Giorgio Levi-Cases" Interdepartmental Centre for Energy Economics and Technology, University of Padua, is gratefully acknowledged for its financial grant "Capacity markets and the evaluation of reliability options".

3.6 Appendix B

B.1 Seasonality parameters' estimates

	Estimate	S.E.	pValue		Estimate	S.E.	pValue
Intercept	3.79	0.01	0	$hour_6$	−0.13	0.01	0
$month_2$	−0.22	0.01	0	$hour_7$	−0.01	0.01	0.5
$month_3$	−0.27	0.01	0	$hour_8$	0.1	0.01	0
$month_4$	−0.36	0.01	0	$hour_9$	0.18	0.01	0
$month_5$	−0.28	0.01	0	$hour_{10}$	0.16	0.01	0
$month_6$	−0.23	0.01	0	$hour_{11}$	0.12	0.01	0
$month_7$	−0.07	0.01	0	$hour_{12}$	0.07	0.01	0
$month_8$	−0.21	0.01	0	$hour_{13}$	0	0.01	0.8
$month_9$	−0.07	0.01	0	$hour_{14}$	−0.05	0.01	0
$month_{10}$	0.14	0.01	0	$hour_{15}$	−0.02	0.01	0.13
$month_{11}$	0.23	0.01	0	$hour_{16}$	0.04	0.01	0
$month_{12}$	0.21	0.01	0	$hour_{17}$	0.09	0.01	0
Monday	−0.01	0.01	0.04	$hour_{18}$	0.15	0.01	0
Weekend	−0.14	0.01	0	$hour_{19}$	0.22	0.01	0
Working_day	0.02	0.01	0	$hour_{20}$	0.28	0.01	0
$hour_2$	−0.08	0.01	0	$hour_{21}$	0.27	0.01	0
$hour_3$	−0.15	0.01	0	$hour_{22}$	0.2	0.01	0
$hour_4$	−0.18	0.01	0	$hour_{23}$	0.12	0.01	0
$hour_5$	−0.18	0.01	0	$hour_{24}$	0.03	0.01	0.01

Table B.1: Linear regression estimates, standard errors and p-values obtained using the specification in (4.3.2). The base group categories for each dummy variable are $month_1$, $Friday$ and $hour_1$.

B.2 Proofs of pricing formulae

Proof of Proposition 3.3.1. Let us underline that we can write the following:

$$RO(T_1, T_2) = \int_\Omega \int_{T_1}^{T_2} f(s, \omega) ds \, d\mathbb{Q}(\omega | \mathcal{F}_0),$$

where $f(s, \omega) \colon = e^{-rs} Q (P_s(\omega) - K)^+$ is a non-negative measurable function from $[T_1, T_2] \times \Omega$ to $\mathbb{R}$. Then, if we set

$$A(K, P_0, s) \colon = e^{-rs} \mathbf{E}^{\mathbb{Q}} \left[(P_s - K)^+ \middle| \mathcal{F}_0 \right], \tag{B.1}$$

by Tonelli's theorem, we have immediately that

$$RO(T_1, T_2) = Q \int_{T_1}^{T_2} A(K, P_0, s) ds. \tag{B.2}$$

$A(K, P_0, s)$ is clearly the price of a European call option with strike price K and maturity s, thus equation (3.3.4) is obtained simply with Black and Scholes formula. □

Proof of Proposition 3.3.2. As in the proof of Proposition 3.3.1, if we write

$$A(K_0, P_0, s) \colon = e^{-rs} \mathbf{E}^{\mathbb{Q}} \left[(P_s - K_s)^+ \middle| \mathcal{F}_0 \right]; \tag{B.3}$$

then, by Tonelli's theorem, we have

$$RO(T_1, T_2) = Q \int_{T_1}^{T_2} A(K_0, P_0, s) ds.$$

Here $A(K, P_0, s)$ is clearly the price of an exchange option between the electricity price P and the strike price K, with maturity s, thus Equation (3.3.6) is obtained simply with the Margrabe formula with dividends (see Carmona and Durrleman (2003)).

□

Proof of Proposition 3.3.3. As in the previous proofs, writing $A(K, P_0, s) \colon =$

$e^{-rs}\mathbf{E}^{\mathbb{Q}}\left[(P_s-K)^+\middle|\mathcal{F}_0\right]$ and applying Tonelli's theorem give

$$RO(T_1,T_2)=Q\int_{T_1}^{T_2}A(K,P_0,s)ds.$$

We plan to evaluate $A(K,P_0,s)$ by exploiting the fact that the factor X, described by the dynamics (3.3.9), is a Gaussian process. Indeed, it is easy to show that almost surely, for all $t>0$, it holds

$$X_t=X_0e^{-\lambda t}+\int_0^t e^{-k\lambda(t-s)}\sigma dW_s=m_t+\sqrt{Var(t)}Z$$

with $Z\sim N(0,1)$ and

$$\begin{aligned}\mathbf{E}^{\mathbb{Q}}\left[X_t\middle|\mathcal{F}_0\right]=&X_0e^{-\lambda t}=:m_t,\\ \mathbf{Var}^{\mathbb{Q}}\left[X_t\middle|\mathcal{F}_0\right]=&\sigma^2\frac{1-e^{-2\lambda t}}{2\lambda}=:Var(t).\end{aligned}$$

Thus we have that

$$\mathbb{Q}\{P_s>K\}=\mathbb{Q}\{e^{\mu(s)+X_s}>K\}=\mathbb{Q}\{Z<d_1(K,P_0,s)\}$$

where $Z\sim N(0,1)$ under $\mathbb{Q}$. As above, we compute

$$\begin{aligned}&\mathbf{E}^{\mathbb{Q}}\left[(P_s-K)^+\middle|\mathcal{F}_0\right]=\mathbf{E}^{\mathbb{Q}}\left[P_s\mathbb{1}_{\{Z<d_1(K,P_0,s)\}}\right]-K\mathbb{Q}\{Z<d_1(K,P_0,s)\}=\\ &=\int_{-\infty}^{d_1(K,P_0,s)}e^{\mu(s)+m_s+\sqrt{Var(s)}x}\frac{1}{\sqrt{2\pi}}e^{-\frac{1}{2}x^2}\,dx-KN(d_1(K,P_0,s))=\\ &=e^{\mu(s)+m_s+\frac{1}{2}Var(s)}\int_{-\infty}^{d_1(K,P_0,s)}\frac{1}{\sqrt{2\pi}}e^{-\frac{1}{2}(x-\sqrt{Var(s)})^2}\,dx-KN(d_1(K,P_0,s))=\\ &=e^{\mu(s)+m_s+\frac{1}{2}Var(s)}\int_{-\infty}^{d_1(K,P_0,s)+\sqrt{Var(s)}}\frac{1}{\sqrt{2\pi}}e^{-\frac{1}{2}y^2}\,dy-KN(d_1(K,P_0,s))\end{aligned}$$

and Equation (3.3.10) follows. □

Proof of Proposition 3.3.4. As before, we write

$$A(P_0,K_0,s):=e^{-rs}\mathbf{E}^{\mathbb{Q}}\left[(e^{\mu(s)}e^{X_s}-e^{\nu(s)}e^{Y_s})^+\,\middle|\,\mathcal{F}_0\right],$$

we use by Tonelli's theorem and we obtain

$$RO(T_1, T_2) = Q \int_{T_1}^{T_2} A(K, P_0, K_0, s) ds.$$

We start by noticing that, under the pricing measure $\mathbb{Q}$, we have $(X_s, Y_s) \sim N(M(s), \Sigma(s))$, with

$$M(s) := \begin{pmatrix} e^{-\lambda_x s} X_0 \\ e^{-\lambda_y s} Y_0 \end{pmatrix}, \qquad \Sigma(s) := \begin{pmatrix} \sigma_x^2 \frac{1-e^{-2\lambda_x s}}{2\lambda_x} & \rho\sigma_x\sigma_y \frac{1-e^{-(\lambda_x+\lambda_y)s}}{\lambda_x+\lambda_y} \\ \rho\sigma_x\sigma_y \frac{1-e^{-(\lambda_x+\lambda_y)s}}{\lambda_x+\lambda_y} & \sigma_y^2 \frac{1-e^{-2\lambda_y s}}{2\lambda_y} \end{pmatrix}$$

From this, Equations (3.3.15) and (3.3.16) follow trivially. We now rewrite $A(P_0, K_0, s)$ as

$$\begin{aligned} A(K, P_0, K_0, s) &= e^{-rs} \mathbf{E}^{\mathbb{Q}} \left[K_s \left(\frac{P_s}{K_s} - 1 \right)^+ \middle| \mathcal{F}_0 \right] \\ &= e^{-rs} \mathbf{E}^{\mathbb{Q}_K} \left[\left(\frac{P_s}{K_s} - 1 \right)^+ \middle| \mathcal{F}_0 \right] \mathbf{E}^{\mathbb{Q}}[K_s] \end{aligned}$$

where we introduced the new probability measure $\mathbb{Q}_K$, defined via its density as

$$\frac{d\mathbb{Q}_K}{d\mathbb{Q}} := \frac{K_s}{\mathbf{E}^{\mathbb{Q}}[K_s]} = \frac{e^{Y_s}}{\mathbf{E}^{\mathbb{Q}}[e^{Y_s}]}.$$

With some algebra, one can verify that, under this new probability measure $\mathbb{Q}_K$, we have $(X_s, Y_s) \sim N(\tilde{M}(s), \Sigma(s))$, with

$$\tilde{M}(s) := M(s) + \begin{pmatrix} \rho\sigma_x\sigma_y \frac{1-e^{-(\lambda_x+\lambda_y)s}}{\lambda_x+\lambda_y} \\ \sigma_y^2 \frac{1-e^{-2\lambda_y s}}{2\lambda_y} \end{pmatrix},$$

Thus, $X_s - Y_s \sim N(\bar{m}_s, \overline{Var}(s))$, with $\bar{m}_s$ and $\overline{Var}(s)$ given by Equations (3.3.19) and (3.3.20), respectively. We then have that

$$\mathbb{Q}_K\left\{\frac{P_s}{K_s}>1\right\}=\mathbb{Q}_K\{e^{\mu(s)-\nu(s)+X_s-Y_s}>1\}=\mathbb{Q}_K\{Z<d_1(K_0,P_0,s)\},$$

where $Z\sim N(0,1)$ under $\mathbb{Q}_K$. Now, similarly to the proof of Proposition 3.3.3, we can now compute

$$\begin{aligned}
&\mathbf{E}^{\mathbb{Q}}\left[(P_s-K_s)^+\middle|\mathcal{F}_0\right]=\mathbf{E}^{\mathbb{Q}}[K_s]\mathbf{E}^{\mathbb{Q}_K}\left[\left(\frac{P_s}{K_s}-1\right)^+\middle|\mathcal{F}_0\right]=\\
&=\mathbf{E}^{\mathbb{Q}}[K_s]\left(\mathbf{E}^{\mathbb{Q}_{\mathbb{K}}}\left[\frac{P_s}{K_s}\mathbb{1}_{\{Z<d_1(K_0,P_0,s)\}}\right]-\mathbb{Q}_{\mathbb{K}}\{Z<d_1(K_0,P_0,s)\}\right)=\\
&=\mathbf{E}^{\mathbb{Q}}[K_s]\left(\int_{-\infty}^{d_1(K,P_0,s)}e^{\mu(s)-\nu_s+\bar{m}_s+\sqrt{\overline{Var}(s)}x}\frac{1}{\sqrt{2\pi}}e^{-\frac{1}{2}x^2}\,\mathrm{d}x-N(d_1(K,P_0,s))\right)=\\
&=\mathbf{E}^{\mathbb{Q}}[K_s]\left(e^{\mu(s)-\nu_s+\bar{m}_s+\frac{1}{2}\overline{Var}(s)}\int_{-\infty}^{d_1(K_0,P_0,s)}\frac{1}{\sqrt{2\pi}}e^{-\frac{1}{2}(x-\sqrt{\overline{Var}(s)})^2}\,\mathrm{d}x-\right.\\
&\left.-N(d_1(K_0,P_0,s))\right)=\\
&=\mathbf{E}^{\mathbb{Q}}[K_s]\left(e^{\mu(s)-\nu(s)+\bar{m}_s+\frac{1}{2}\overline{Var}(s)}\int_{-\infty}^{d_1(K,P_0,s)+\sqrt{\overline{Var}(s)}}\frac{1}{\sqrt{2\pi}}e^{-\frac{1}{2}y^2}\,\mathrm{d}y-\right.\\
&\left.-N(d_1(K,P_0,s))\right).
\end{aligned}$$

By using Equation (3.3.16) for $\mathbf{E}^{\mathbb{Q}}[K_s]$,

after some simplifications we arrive at the final result

$$\begin{aligned}
\mathbf{E}^{\mathbb{Q}}\left[(P_s-K_s)^+\middle|\mathcal{F}_0\right]=&e^{\mu(s)+e^{-\lambda_x s}X_0+\frac{1}{2}\sigma_x^2\frac{1-e^{-2\lambda_x s}}{2\lambda_x}}N\left(d_1(K,P_0,s)+\sqrt{\overline{Var}(s)}\right)-\\
&-e^{\nu(s)+e^{-\lambda_y s}Y_0+\frac{1}{2}\sigma_y^2\frac{1-e^{-2\lambda_y s}}{2\lambda_y}}N(d_1(K,P_0,s))
\end{aligned}$$

and Equation (3.3.14) follows.

□

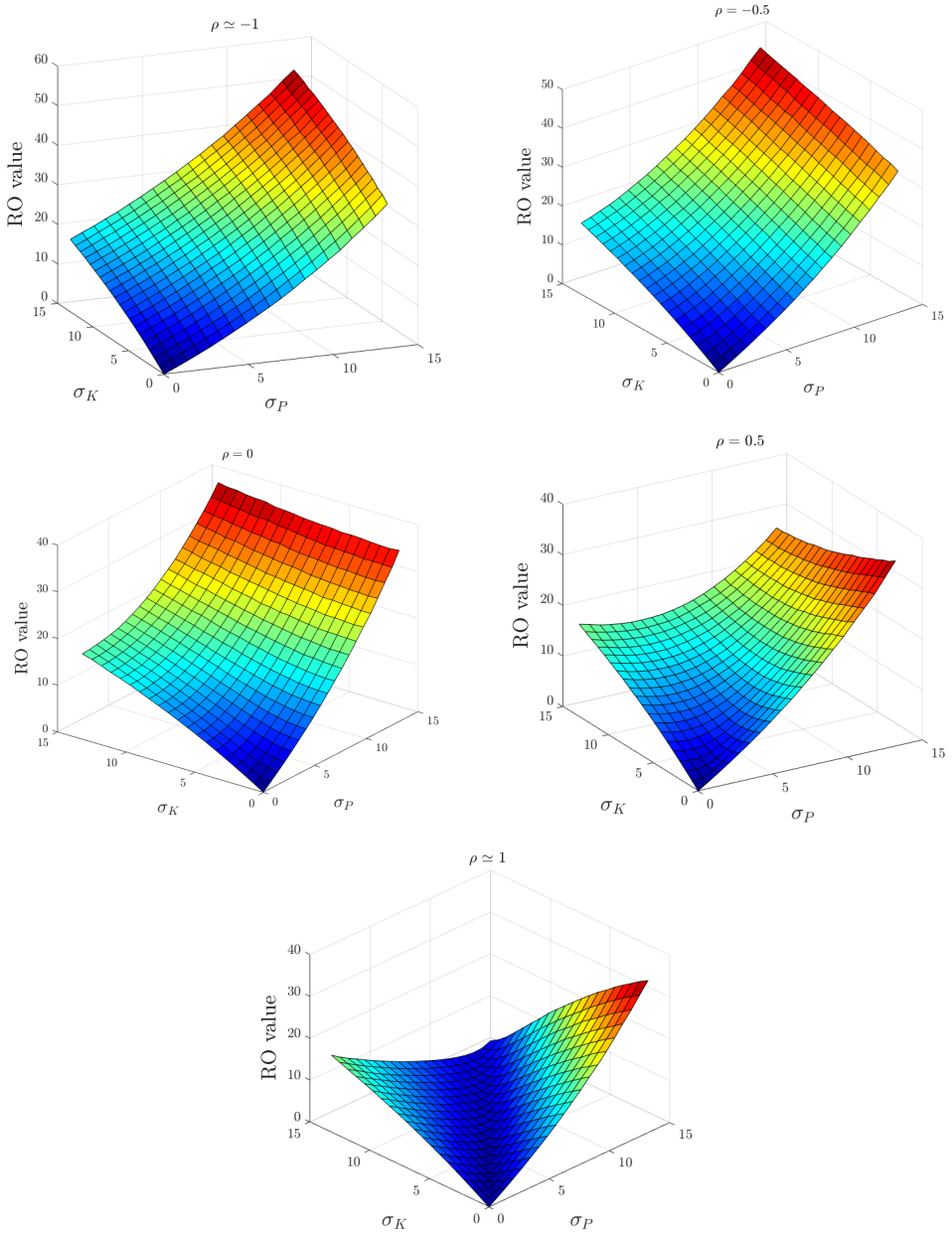

Figure 3.6: Sensitivity analysis of the RO value to a disjoint variation in the two volatilities, with a yearly σ_P and σ_K in the range $(0; 2\hat{\sigma}_P]$ (here $\lambda_K = \lambda_P$). In the different panels, we can see how a variation in the correlation coefficient ρ affects the RO value: when the two processes are independent or negatively correlated, higher σ_P and σ_K result in a higher option value. However, when the correlation is positive (middle right and bottom panels), the higher the correlation, and the more the two volatilities are similar, the lower the value of the option. The RO value is expressed in €/MWh.

Chapter 4

Optimal cross-border electricity trading *

We show that electricity flows between interconnected locations have a direct and indirect effect on electricity prices in the different locations. The direct effect refers to how prices between two locations are affected when power is flowing between these two locations only. The indirect effect refers to how the flows between two locations affect the price of power in other locations that are part of the interconnected electricity network. Based on this result we propose a model of the joint dynamics of electricity prices where flows of electricity affect, directly and indirectly, prices in all locations, and model a common co-integration factor of prices. We solve the optimal control problem of an agent who uses the interconnector to take positions in a subset of locations that are part of the interconnected network. We reduce the Hamilton-Jacobi-Equation satisfied by the value function of the investor to a system of Riccati equations, which we solve analytically, and obtain the optimal electricity trading strategy in closed-form. We show that including cross-border effects in the trading strategy specification significantly improves the performance of the strategy, that takes advantages of price differentials in interconnected locations. For example, for contracts with delivery at 3 p.m., we show that over a time horizon of one year, the optimal strategy delivers a profit that is approximately

*This paper is a joint work with Álvaro Cartea (University of Oxford), Tiziano Vargiolu (Università degli Studi di Padova) and Georgi Slavov (Marex Spectron Ltd). This paper was awarded the best paper general prize at the Commodity and Energy Markets 2018 Annual Meeting.

4% more than the profit of a naive strategy, which is based on the spread between locations (i.e., does not take into account cross-border effects).

4.1 Introduction

The recent market coupling initiatives in the European Union are aimed at integrating the European wholesale electricity markets, thus increasing security of supply while reducing price volatility across Europe. At the core of the market coupling process, there is the construction of new interconnecting facilities, namely bi-directional transmission lines connecting the grids of two countries. The aim of this Chapter is to develop an optimal trading strategy for an agent who uses the interconnectors to take simultaneous positions in electricity contracts in all locations.

The first part is devoted to an econometric analysis of the electricity price determinants, and the results of this analysis are employed in the second part of the work, where we derive the optimal trading strategy by posing and solving a stochastic control problem.

In our setup, we consider permanent and temporary impacts of cross-border electricity flows on the electricity price, and we assume these impacts to be linear in the agent's speed of trading. The econometric analysis is instrumental in determining the magnitude of these impacts.

Our trading strategy makes then use of these market impacts, as well as of the information provided by the co-movement of the electricity prices in three interconnected countries object of our study. This is done by considering the joint dynamics of the three price processes, driven by intertwined co-integration factors, and profiting from the structural dependence in the electricity prices' dynamics. We then pose an optimal control problem, and solve the resulting dynamic programming equation, deriving a closed-form solution up to a 10-ODEs system.

Our work builds on two streams of literature. The first one is related to pairs trading. In this respect, one of the earliest contributions employing co-integration in a stochastic control problem is that of Mudchanatongsuk et al. (2008), who model the log-price spread of a pair of stocks as a mean-reverting process, and use this in a stochastic control framework based on

trading in the spread. Tourin and Yan (2013) employ a similar co-integration model and find a closed-form solution for a dynamic trading strategy based on a portfolio composed of a money bank account and two stocks. Extending their work, Leung and Li (2015) and Lei and Xu (2015) formulate an optimal entry-exit strategy on a pair of co-integrated assets. Benth et al. (2017) develop a cross-commodity model with co-integrated dynamics in a Heath-Jarrow-Morton framework. Finally, another extension to Tourin and Yan (2013) is given by Cartea and Jaimungal (2016a) and Lintilhac and Tourin (2017), who generalize their dynamic model for an arbitrary number of assets. These last two works are those closest to ours, although our study differs in the nature of assets traded, in the specification of the asset's dynamics, and in the definition of the co-integration factor.

Our model is also related to a second stream of literature, relative to the modeling of power prices. Relevant works are those of Cartea and Figueroa (2005), Roncoroni (2002), Geman and Roncoroni (2006), Benth et al. (2007) and Weron (2007) (see also Benth et al. (2012) for a critical comparison of the first four models).

The remainder of the chapter is organized as follows: Section 4.2 presents the intra-day data collected for the analysis. In Section 4.3, using econometric tools, we show the direct and indirect effects of the cross-border flows of electricity on the electricity price in the countries object of our study; moreover, we describe the stochastic process employed for modeling the electricity price, and estimate the relative parameters. Section 4.4 derives the optimal trading strategy for an agent taking positions in electricity contracts in all markets considered in the study. Section 4.5 showcases the empirical performance of the strategy, while Section 4.6 concludes.

4.2 Data

Electricity is a commodity that can be traded in different markets, and the three main ones are the day-ahead market, the intra-day one and the forward one. The main difference among these three markets is that, in each one of them, one can trade contracts on electricity with a specific range of delivery times.

As mentioned earlier in Chapter 1, the two spot markets, i.e. the day-

ahead and the intra-day ones, also differ in their level of interconnectedness: the day-ahead market is an integrated market, and prices are coupled, while the intra-day market is not as integrated, and agents can decide to go and buy electricity in another country, so that there are arbitrage opportunities.

The aim of this Chapter is to build on this opportunity and to develop an optimal trading strategy for an agent who uses the interconnectors to take simultaneous positions in electricity contracts in a set of locations in the intra-day market.

One of the biggest exchanges where electricity can be traded is EPEX Spot, the European power exchange for spot trading. Thus, we use tick data relative to all hours and 15-minute period contracts traded on EPEX Spot Intraday Continuous, for the period 01/01/2016 - 31/12/2017, corresponding to 7,306,380 transactions (see Table 4.1 for a sample of the dataset).

Delivery	Time Stamp	Market Area Buy	Market Area Sell	Volume (MWh)	Price (€/MWh)
05/03/2017 h 21	2017-03-05 10:00:00	FR	AT	12	35.70
05/03/2017 h 21	2017-03-05 10:02:00	FR	AT	1	35.70
05/03/2017 h 21	2017-03-05 10:04:00	CH	DE	1	39.00
05/03/2017 h 21	2017-03-05 10:04:00	CH	AT	1	39.00
05/03/2017 h 21	2017-03-05 10:06:00	CH	DE	1	38.80
05/03/2017 h 21	2017-03-05 10:08:00	DE	DE	1	38.80
05/03/2017 h 21	2017-03-05 10:08:00	DE	AT	19	39.00
05/03/2017 h 21	2017-03-05 10:14:00	DE	CH	6	35.90
05/03/2017 h 21	2017-03-05 10:35:00	NL	AT	20	38.90
05/03/2017 h 21	2017-03-05 10:35:00	NL	DE	25	39.00
05/03/2017 h 21	2017-03-05 11:05:00	FR	DE	5	37.10
05/03/2017 h 21	2017-03-05 11:05:00	DE	DE	6	37.00
05/03/2017 h 21	2017-03-05 11:17:00	NL	FR	1	38.00
05/03/2017 h 21	2017-03-05 11:48:00	DE	DE	18	38.90
05/03/2017 h 21	2017-03-05 12:02:00	DE	AT	11	38.30
05/03/2017 h 21	2017-03-05 12:02:00	DE	AT	2	38.20
05/03/2017 h 21	2017-03-05 12:02:00	DE	AT	10	38.10

Table 4.1: Sample of the dataset. Each row represents a different trade on the intra-day spot market, and provides information about (from left to right) the hour and day of delivery, about the time of execution of the transaction, about the originating market area and the delivery market area, about the volume and the price of the transaction.

In our model, we treated each country as if it was a distinct markets, so that the agent can buy or sell electricity in all directions in any of these markets.

The possibility of trading across the interconnected locations is limited by the available transfer capacity (ATC) (Table 4.2), resulting from the subtrac-

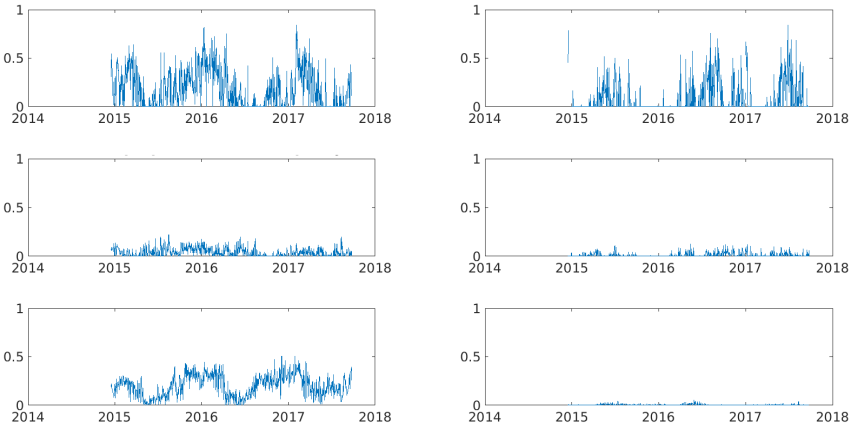

Figure 4.1: Physical flow of electricity (relative to contracts with delivery at 3 p.m.) for each trading direction (starting from the top left panel: France to Switzerland, Switzerland to France, France to Germany, Germany to France, Germany to Switzerland and Switzerland to Germany) over the corresponding ATC.

tion from nominal capacity (NTC) of the committed volume under long term contracts, and after taking into account the transmission reliability margin. The volumes in Table 4.1 are the so-called commercial flows; however, to check the level of actual usage of the ATC, we need data about the so-called physical flows, which are provided by ENTSO-E on their Transparency Platform. In fact, the physical flows are the actual flows of electricity transiting across the national borders into another country's grid. As we can see in Figure 4.1, the proportion of used ATC varies a lot throughout the year, highlighting a seasonal pattern.

From	To	Available Transfer Capacity (MW)
France	Switzerland	3,200
France	Germany	3,000
Germany	France	3,050
Germany	Switzerland	800
Switzerland	France	2,200
Switzerland	Germany	4,000

Table 4.2: Available transfer capacity (ATC) for each trading direction.

The descriptive statistics relative to the volumes of electricity traded every-

day in the intra-day market across the interconnected locations are reported in Table 4.3. For exemplificatory purposes, we decided to report statistics for contracts with delivery at 3 p.m. and 3 a.m., respectively a peak and an off-peak hour. As we can see from the table, and as is also clear from Figure 4.1, on average, the greatest load of electricity flows from France to Switzerland, and there is a high volatility in volumes of electricity across all the interconnected countries.

		Mean	Std. Dev.	Max	Min	Skewness	Kurtosis	# of obs.
FR-CH	3 p.m.	16.10	9.72	100	0.1	0.52	6.66	5,061
	3 a.m.	14.18	10.08	50	0.1	0.33	2.64	1,177
CH-FR	3 p.m.	14.55	9.88	100	0.1	0.59	4.98	3,465
	3 a.m.	14.15	11.05	101	0.1	1.28	9.4	1,141
FR-DE	3 p.m.	10.84	9.69	148.4	0.1	1.76	15.24	6,382
	3 a.m.	10.17	9.43	100	0.1	1.78	11.91	5,571
DE-FR	3 p.m.	11.91	10.98	342	0.1	6.03	144.13	7,879
	3 a.m.	10.81	10.25	300	0.1	5.32	122.03	5,600
CH-DE	3 p.m.	9.79	8.32	50	0.1	0.79	2.74	4,364
	3 a.m.	8.74	8.49	98	0.1	1.52	8.25	3,322
DE-CH	3 p.m.	10.69	8.71	100	0.1	0.99	5.32	5,749
	3 a.m.	8.26	8.01	76	0.1	1.34	5.66	3,114

Table 4.3: Descriptive statistics of intra-day volumes between interconnected countries for contracts with delivery during a peak (3 p.m.) and an off-peak (3 a.m.) hour. The values of mean, standard deviation, maximum and minimum are expressed in MWh.

Table 4.4 instead shows the descriptive statistics for intra-day prices (Panel A) and price spreads (Panel B), for the same specific peak and off-peak hours. Specifically, the statistics depicted in Panel A are found using all tick data for each specific hour of delivery, while Panel B is built using a sub-sample of the dataset: we divide the data in intervals of 60 minutes each, and consider the "closing price" of each interval, that is the price of the last transaction over those 60 minutes. In such a way, we can compare the prices of two different countries hour by hour, and consider the difference between them (price spread). Looking at Panel B, from a mean price point of view, we can see that it would be profitable (leaving aside the transaction costs) to

Panel A: Intra-day Prices						
	France		Switzerland		Germany	
	3 p.m.	3 a.m.	3 p.m.	3 a.m.	3 p.m.	3 a.m.
Mean	39.99	27.74	40.5	28.15	29.97	23.91
Std. Dev.	20.29	12.16	24.22	11.92	20.01	10.35
Max	295.00	120.00	185.00	139.80	209.00	200.00
Min	−18.00	−10.00	−150.00	−18.90	−320.00	−85.00
Skewness	1.56	1.26	1.24	1.65	−0.68	−1.25
Kurtosis	8.01	6.57	9.71	8.95	27.41	9.58
ADF	0.01%	0.01%	0.01%	0.01%	0.01%	0.01%
Jarque-Bera	0.01%	0.01%	0.01%	0.01%	0.01%	0.01%
# of obs.	39,717	19,280	23,532	10,475	364,273	192,447
Panel B: Intra-day Price Spread						
	France - Switzerland		Switzerland - Germany		Germany - France	
	3 p.m.	3 a.m.	3 p.m.	3 a.m.	3 p.m.	3 a.m.
Mean	3.63	1.22	−2.77	−4.29	−0.86	3.07
Std. Dev.	16.56	13.61	20.98	16.33	19.62	15.22
Max	295.00	120.00	252.01	139.80	130.00	60.00
Min	−87.90	−139.80	−175.00	−60.00	−252.01	−86.00
Skewness	2.68	0.22	0.04	0.44	−0.73	−0.07
Kurtosis	26.48	15.03	11.35	6.86	14.2	5.55
ADF	0.01%	0.01%	0.01%	0.01%	0.01%	0.01%
Jarque-Bera	0.01%	0.01%	0.01%	0.01%	0.01%	0.01%
# of obs.	7,158	5,215	7,158	5,215	7,158	5,215

Table 4.4: Descriptive statistics of intra-day prices and price spreads for a peak (3 p.m.) and off-peak (3 a.m.) hour. The values for mean, standard deviation, maximum and minimum are expressed in €/MWh. We report the p-values of the Augmented Dickey-Fuller (ADF) test statistic, which indicate that the null hypothesis of unit root is rejected in favor of the mean reverting alternative in all cases. We also report the p-values for the Jarque-Bera test, which reject, in all cases, the null hypothesis of normality.

send electricity from Switzerland to France, from Switzerland to Germany, and from Germany to France when trading contracts with delivery at 3 p.m., from France to Germany when trading contracts with delivery at 3 a.m.. If we have a look at the results for the Augmented Dickey-Fuller (ADF) test on prices and spreads, we can see that the unit root hypothesis is rejected in all

cases, with a p-value equal or lower than 0.01%, favoring the mean reverting alternative. The Jarque-Bera test, again with p-values lower than 0.01% in all cases, suggests that both prices and spreads are far from being normally distributed. The same results, both for the ADF test and the Jarque-Bera one, hold for all single peak and off-peak hours.

4.3 Econometric Analysis

Using data for all intraday contracts traded on EPEX, we first look for patterns in the dynamics of prices and flows of electricity across the different countries, and choose a sub-set of locations where to base our trading strategy. Specifically, the locations we choose are Germany, Switzerland and France, because all of them are interconnected with each other, and thus the agent can buy or sell electricity in all directions in each of these three markets. We want to understand how the volumes of electricity traded can affect the electricity price over time, so to calibrate the agent's trading strategy accordingly.

We run the multivariate robust OLS (ordinary least squares) regression in (4.3.1), where the dependent variables are the price increments over 1 hour of trading, and the explanatory variables are the total volumes per trading hour, traded in all possible directions. The price increment is computed over 1 hour because the market is not a particularly liquid one, so that the effects of the different trades are evident over a somewhat appreciable amount of time.

$$\begin{aligned}\Delta \boldsymbol{P}_t = {} & \boldsymbol{\beta}_1 \mathrm{Vol}_{t-1}^{SF} + \boldsymbol{\beta}_2 \mathrm{Vol}_{t-1}^{FS} + \boldsymbol{\beta}_3 \mathrm{Vol}_{t-1}^{GS} + \boldsymbol{\beta}_4 \mathrm{Vol}_{t-1}^{SG} + \boldsymbol{\beta}_5 \mathrm{Vol}_{t-1}^{GF} + \boldsymbol{\beta}_6 \mathrm{Vol}_{t-1}^{FG} \\ & + \boldsymbol{\beta}_7 \mathrm{Vol}_{t-1}^{OF} + \boldsymbol{\beta}_8 \mathrm{Vol}_{t-1}^{FO} + \boldsymbol{\beta}_9 \mathrm{Vol}_{t-1}^{OS} + \boldsymbol{\beta}_{10} \mathrm{Vol}_{t-1}^{SO} + \boldsymbol{\beta}_{11} \mathrm{Vol}_{t-1}^{OG} + \boldsymbol{\beta}_{12} \mathrm{Vol}_{t-1}^{GO} + \boldsymbol{\varepsilon}_t \,,\end{aligned} \tag{4.3.1}$$

with

$$\boldsymbol{P}_t = \begin{pmatrix} P_t^F \\ P_t^S \\ P_t^G \end{pmatrix} \,,$$

where F stands for "France", S for "Switzerland", G for "Germany", and O for "other country", so that P_t^F is the French price of electricity at time t, P_t^S is the Swiss one, and P_t^G is the German one; Vol_t^{FS} represents the sum of all volumes of the transactions hour by hour where the market area Buy

is France and the market area Sell is Switzerland, and so on. Finally, $\boldsymbol{\varepsilon}_t$ is a vector of normally distributed error terms.

Then, we also run (4.3.1) using a stepwise algorithm. In a stepwise regression, the choice of the predictive variables is carried out by an algorithm. In fact, the algorithm adds or removes terms of the multilinear model based on their statistical significance, so that the final choice of regressors has the maximum explanatory power.

We expect that, when the agent buys a certain amount of electricity in France to sell it in Switzerland, the French price will be negatively affected (in the sense that it will increase), while the Swiss one will proportionally decrease. When buying electricity, the agent is reducing the electricity supply, so that the price will increase. On the other hand, selling electricity will increase the supply, and prices will drop. The estimated coefficients of (4.3.1) confirm this intuition, both with the multivariate regression and with the stepwise one (see, for example, Table 4.5). We observe that, when the dependent variable is ΔP_t^F, most of the times β_1 is negative, while β_2 is positive, β_5 is negative, while β_6 is positive, β_7 is negative, while β_8 is positive (when significant). If the dependent variable is instead ΔP_t^S, most of the times β_1 is positive, while β_2 is negative, β_3 is negative, while β_4 is positive, β_9 is negative, while β_{10} is positive (when significant). Coherently, when the dependent variable is ΔP_t^G, most of the times β_3 is positive, while β_4 is negative, β_5 is positive, and so is β_{12}, while β_6 is negative, and so is β_{11} (when significant) (see Appendix C.1 for the complete results both for the multivariate and the stepwise regressions).

Moreover, the coefficients referring to the same country pair are statistically different one from the other when taken in absolute value ($\beta_1 \neq -\beta_2$, for example).

These results show that flows of electricity between two locations affect the prices of the two locations that receive/send electricity and also affect the prices of other locations which are not directly receiving electricity. That is, the price increment relative to a specific country is not only affected by the trades between that country and another, but is also affected by electricity trades happening somewhere else in the system. We label these effects "cross-border permanent impacts". When constructing our optimal trading strategy, we take into account the presence of these price impacts,

	ΔP_t^F	ΔP_t^S	ΔP_t^G
Vol_t^{SF}	0	0	0
Vol_t^{FS}	0.0032^{***}	-0.0007^{***}	0
Vol_t^{GS}	0	0	0.0064^{***}
Vol_t^{SG}	0	0	0
Vol_t^{GF}	0	0.0009^{***}	0
Vol_t^{FG}	0	-0.0007^{***}	-0.0060^{***}
Vol_t^{OF}	0	0	-0.0013^{***}
Vol_t^{FO}	0.0022^{***}	0	-0.0038^{***}
Vol_t^{OS}	0	0	0
Vol_t^{SO}	0	0	0
Vol_t^{OG}	0	0	-0.0068^{***}
Vol_t^{GO}	0	0	0.0052^{***}

Table 4.5: OLS robust estimates, obtained using the stepwise algorithm, for contracts with delivery at 3 p.m.. Dependent variables: ΔP_t^F, ΔP_t^S, ΔP_t^G. $^{***} = p < 0.01, ^{**} = p < 0.05, ^{*} = p < 0.1$.

because the agent's trades are going to permanently affect the price in a way proportional to the quantity traded.

The β coefficients in (4.3.1) give an indication of the magnitude and sign of the permanent price impacts that trading activity in each direction has on the price of electricity in each country of the interconnected network.

In our setup, we assume these impacts to be linear in the agent's speed of trading.

4.3.1 Co-integrated electricity prices

As mentioned in the previous chapter, the behavior of electricity prices displays pecularities that make its statistical features different from those of other financial assets. When high demand brings on stream less efficient power generation sources, the electricity price exhibits spikes and jumps, and, depending on different electricity usage throughout the year, it also displays a marked seasonal component.

For this reason, before using the price data, we need to de-seasonalize them. We model the seasonal component $f(t)$ using sinusoidal functions with different periodicities (in this case, annual, semi-annual and weekly

with different centers) (see for example Lucia and Schwartz (2002), Seifert and Uhrig-Homburg (2007) and Pilipovic (1998)). We thus get

$$f(t) = b_1 \sin(2\pi t) + b_2 \cos(2\pi t) + b_3 \sin(4\pi t) + b_4 \cos(4\pi t) + b_5 \sin(104\pi t) + b_6 \cos(104\pi t) + b_7 \,. \tag{4.3.2}$$

The seasonality parameters are calibrated using OLS, and Figure 4.2 reports the results of the calibration for intra-day contracts with delivery at 3 p.m..

In our set up, because the three countries are interconnected and, as shown in the previous section, there is presence of cross-border effects, we model the prices as co-integrated. Co-integration was first defined in Engle and Granger (1987) as the property according to which a combination of two non-stationary processes can be stationary, and has since then found several applications, from macroeconomic analysis to fund management and portfolio selection. The core of the idea is to take advantage of the co-movement among the co-integrated stochastic variables in a dynamic specification framework.

In our model, the drift of the stochastic process we use to model electricity prices is composed of an idiosyncratic component, which only affects the single country, and a systemic one, which is a proxy for all the common drivers of the electricity price in all countries, and which is what causes them to co-move. This common component is the co-integration factor. In this respect, our specification is similar to that of Cartea and Jaimungal (2016a), but differs from their one in the nature of the assets traded (electricity prices versus IT stocks), in the definition of the co-integration factor, in that we add a jump component to the dynamics, and most importantly, in that we consider the permanent impacts that cross-border trading has on the electricity price, as found in the previous section. Our electricity price dynamics is thus defined as:

$$\mathrm{d}P_t^k = \left(\theta_k + \sum_{i=1}^{n} \delta_{ki}\alpha_t^i\right)\mathrm{d}t + \sum_{i=1}^{n} \sigma_{ki}\mathrm{d}W_t^i + J(\psi_k, \xi_k)\mathrm{d}\Pi(\lambda_k)\,, \tag{4.3.3}$$

where $(P_t^k)_{t>0}$ is the de-seasonalized price of electricity in country k at time t (from now on, we will simply refer to the de-seasonalized electricity price as 'electricity price'), θ_k is the idiosyncratic component of the drift, δ_{ki} are country-specific constants, W_t^i are standard Brownian motions independent

(a) Historical closing prices with seasonality - hour 3 p.m.

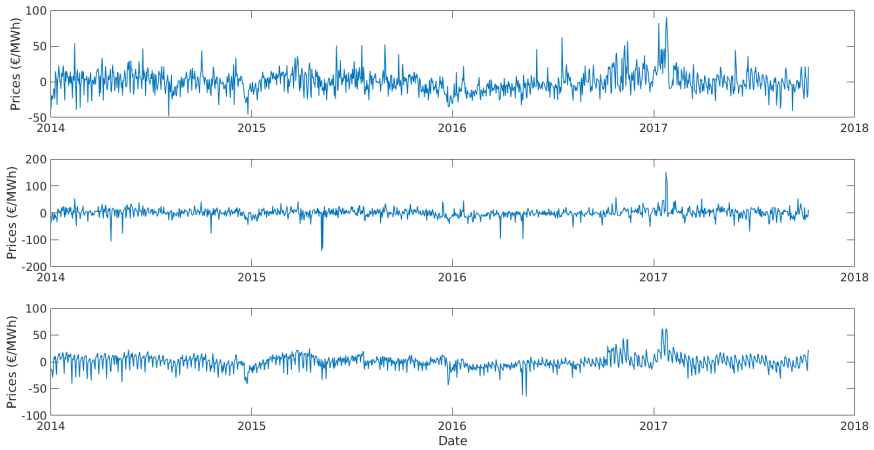

(b) Residuals - hour 3 p.m.

Figure 4.2: Historical (4.2a) and de-seasonalized (4.2b) electricity price for contracts with delivery at 3 p.m. for each country in the sample. The three sub-figures in each panel show the prices for, from top to bottom, France, Switzerland and Germany. The red solid line in 4.2a represents the calibrated seasonality function $f(t)$. Prices are expressed in €/MWh.

of each other, and σ_{ki} are the elements of the Cholesky decomposition of the instantaneous variance-covariance matrix of electricity prices. Jumps arrive as a Poisson process Π with intensity λ_k and have a normally distributed

jump size with mean ψ_k and standard deviation ξ_k. Moreover,

$$\alpha_t^i = \sum_{j=1}^{n} a_{ij} P_t^j \tag{4.3.4}$$

is the co-integration factor for country i, where a_{ij} are constants. We can thus see that the price of electricity in each country also depends on the electricity price in the other ones.

Eq. (4.3.3) can be rewritten in matrix notation as

$$\mathrm{d}\mathbf{P}_t = (\boldsymbol{\theta} - \boldsymbol{\Phi}\,\mathbf{P}_t)\,\mathrm{d}t + \boldsymbol{\sigma}\,\mathrm{d}\mathbf{W}_t + J(\boldsymbol{\psi}, \boldsymbol{\xi})\mathrm{d}\boldsymbol{\Pi}(\boldsymbol{\lambda})\,. \tag{4.3.5}$$

Here $\boldsymbol{\Phi}$ is a $n \times n$ matrix and $\boldsymbol{\Phi} = -\boldsymbol{\Delta} \cdot \mathbf{A}$, where

$$\boldsymbol{\Delta} = \begin{pmatrix} \delta_{11} & \cdots & \delta_{1n} \\ \vdots & \ddots & \vdots \\ \delta_{n1} & \cdots & \delta_{nn} \end{pmatrix} \quad \text{and} \quad \mathbf{A} = \begin{pmatrix} a_{11} & \cdots & a_{1n} \\ \vdots & \ddots & \vdots \\ a_{n1} & \cdots & a_{nn} \end{pmatrix} .$$

Since we defined a different co-integration factor for each of the three countries, $\boldsymbol{\Phi}$ contains exactly three positive eigenvalues, and this ensures that the three price processes display mean reverting behavior. For reasons that will be clear later on in what follows, we impose the restriction that $\boldsymbol{\Phi}$ has to be a symmetric matrix.

The parameters in (4.3.5) can be estimated through Maximum Likelihood Estimation (MLE). In order to do this, we first need to find the multivariate density function of the price process. Thus, we perform an Euler discretization on (4.3.5). To discretize the jump component, we assume that, within a small time interval $\mathrm{d}t$, the increment of the Poisson process behaves like a Bernoulli random variable. This means that, over the interval $\mathrm{d}t$, we can have at most one jump. Thus, in presence of jumps, we get

$$\boldsymbol{P}_{t+1} = \boldsymbol{\theta} + (\mathbb{1}_n - \boldsymbol{\Phi})\,\boldsymbol{P}_t + \boldsymbol{\sigma}\,\varepsilon_t + (\boldsymbol{\psi} + \boldsymbol{\xi}\,\varepsilon_{Jt})\,\boldsymbol{Y}_\lambda\,, \tag{4.3.6}$$

where $\mathbb{1}_n$ is a $n \times n$ identity matrix, $(\varepsilon_t)_t$ and $(\varepsilon_{Jt})_t$ are i.i.d. sequences of

standard normal random variables, also independent of each other, and

$$\boldsymbol{Y}_{\lambda} = \begin{pmatrix} Y_1^{\lambda_1} & 0 & \cdots & 0 \\ 0 & Y_2^{\lambda_2} & \ddots & \vdots \\ \vdots & \ddots & \ddots & 0 \\ 0 & \cdots & 0 & Y_n^{\lambda_n} \end{pmatrix},$$

with $Y_k^{\lambda_k} \sim \text{Bern}(\lambda_k)$ independent of $Y_i^{\lambda_i}$ $\forall\, k \neq i$, $k = 1, ..., n$. We thus get that the multivariate conditional density function is

$$f\left(\boldsymbol{P}_{t+1}|\boldsymbol{P}_t\right) = \sum_{\mathrm{e}\in E} \left[\prod_{i=1}^{n} \lambda_i^{\mathrm{e}_i}\left(1-\lambda_i^{1-\mathrm{e}_i}\right)\right] \left(2\pi\right)^{-\frac{n}{2}} \left|\boldsymbol{\Omega}+\boldsymbol{\xi}_{\mathrm{e}}\right|^{-\frac{1}{2}} \cdot e^{-\frac{1}{2}[\boldsymbol{P}_{t+1}-\boldsymbol{\psi}_{\mathrm{e}}+\boldsymbol{\theta}+(\mathbb{1}_n-\boldsymbol{\Phi})\boldsymbol{P}_t]^{\intercal}(\boldsymbol{\Omega}+\boldsymbol{\xi}_{\mathrm{e}})^{-1}[\boldsymbol{P}_{t+1}-\boldsymbol{\psi}_{\mathrm{e}}+\boldsymbol{\theta}+(\mathbb{1}_n-\boldsymbol{\Phi})\boldsymbol{P}_t]}, \tag{4.3.7}$$

where $\boldsymbol{\Omega} = \boldsymbol{\sigma}\boldsymbol{\sigma}^{\intercal}$, and $|\,\boldsymbol{\Omega}+\boldsymbol{\xi}_{\mathrm{e}}\,|$ is the determinant of $\boldsymbol{\Omega}+\boldsymbol{\xi}_{\mathrm{e}}$. Let $E = \{0,1\}^n$, then, $\forall\, \mathrm{e} \in E$, $\boldsymbol{\xi}_{\mathrm{e}}$ is the $n \times n$ diagonal matrix with elements $(\xi_{\mathrm{e}})_{ii} = \xi_{ii}^2 \cdot \mathrm{e}_i$ and $(\xi_{\mathrm{e}})_{ij} = 0$ $\forall\, i \neq j$. Similarly, $\boldsymbol{\psi}_{\mathrm{e}}$ is a vector with n elements $(\psi_{\mathrm{e}})_i = \psi_i \cdot \mathrm{e}_i$.

A numerical maximization of the log-likelihood function returns the estimates reported in Table 4.6. Figure 4.3 shows simulated in-sample and out-of-sample paths for the (non-deseasonalized) price process, both for a peak (3 p.m.) and an off-peak (3 a.m.) hour.

4.4 Optimal trading strategy

In this section, we show how to build up on the previous section's findings in order to set up an optimal trading strategy. To do this, the agent's trading should not only be based on the price spreads observed over time among the three interconnected countries, but also on the market impacts of electricity flowing across the neighbouring locations.

4.4.1 Cross-border trading impacts on the electricity price

We assume two different types of impact: permanent and temporary ones. According to the previous section's findings, the agents' trading activity has

(a) Historical and simulated prices - hour 3 p.m.

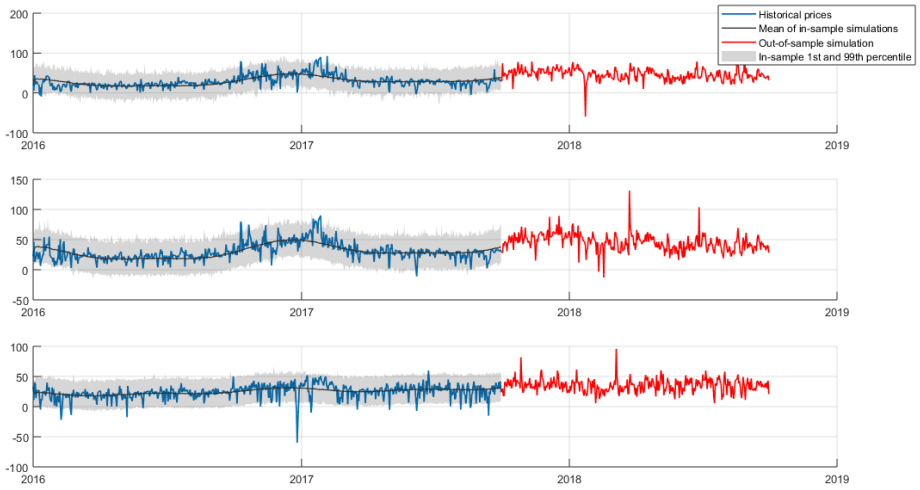

(b) Historical and simulated prices - hour 3 a.m.

Figure 4.3: Historical and simulated electricity price paths for contracts with delivery at a peak – 3 p.m. (4.3a), and an off-peak – 3 a.m. (4.3b), hour, for France (top panels), Switzerland (middle panels) and Germany (bottom panels). The blue solid line represents the historical price path, while the red one represents a single out-of-sample price simulation. The gray area represents the 1^{st} and 99^{th} percentiles of all in-sample simulations, while the black solid line is their mean. Prices are expressed in €/MWh.

		France	Switzerland	Germany
Φ	France	0.78 $(2.62 \cdot 10^{-146})$	-0.14 $(3.49 \cdot 10^{-8})$	-0.06 (0.03)
	Switzerland	-0.14 $(3.49 \cdot 10^{-8})$	0.76 $(2.85 \cdot 10^{-58})$	-0.04 (0.06)
	Germany	-0.06 (0.03)	-0.04 (0.06)	0.86 $(6.99 \cdot 10^{-27})$
σ	France	11.95 $(1.91 \cdot 10^{-64})$	0 (-)	0 (-)
	Switzerland	10.28 $(7.95 \cdot 10^{-74})$	4.60 $(2.06 \cdot 10^{-9})$	0 (-)
	Germany	7.12 $(1.79 \cdot 10^{-15})$	2.26 (0.07)	10.04 $(9.54 \cdot 10^{-7})$
θ		-1.26 (0.03)	-0.14 (0.79)	0.70 (0.39)
ψ		-7.07 (0)	2.60 $(6.53 \cdot 10^{-87})$	25.00 (0)
$\mathrm{diag}(\xi)$		68.31 (0)	57.79 (0)	99.84 (0)
λ		0.03 (0.76	0.02 (0.84)	0.03 (0.79)

Table 4.6: Daily parameters of the multivariate price process in (4.3.5), estimated via MLE against price data relative to contracts with delivery at 3 p.m.. P-values are in parentheses.

a permanent impact on the price of electricity contracts. This is due to the fact that buying (or selling) these contracts increases the demand (or supply) of electricity in each country, thus causing upward (or downward) pressure on prices. (For a further discussion on permanent price impacts, see Alfonsi et al. (2010), Cartea and Jaimungal (2016b) and Cartea et al. (2016)).

We denote by $\boldsymbol{\nu} = (\boldsymbol{\nu}_t)_{\{0 \leq t \leq T\}}$ the vector of the agent's speed of trading for each trading direction. Since we are treating the three countries as distinct markets, we consider trading in opposite directions across each country couple as two separate positions. Moreover, the choice of keeping 6 controls, rather than 3, is also motivated by the results of Section

4.3. These show that the impact of trading in a specific direction is statistically different, in absolute value, from the impact of trading in the opposite direction. We thus get a vector of six elements, one for each trading direction: France-Switzerland, Switzerland-Germany, Germany-France, Switzerland-France, Germany-Switzerland and France-Germany.

The permanent impact function on power prices is thus defined as:

$$g_k(\nu_t) = \beta_k^a \nu_t^{ij} + \beta_k^b \nu_t^{ji} + \beta_k^c \nu_t^{iz} + \beta_k^d \nu_t^{zi} + \beta_k^e \nu_t^{jz} + \beta_k^f \nu_t^{zj}\,, \tag{4.4.1}$$

with $i, j, z \in \{\text{France}, \text{Switzerland}, \text{Germany}\}$ and $i \neq j \neq z$. Of course, with no trading activity, we get $g_k(0) = 0$. The permanent impact β is different for each country k, and the electricity price in each specific country is affected by the flow of electricity in each trading direction in different ways (this is why β is indexed by superscript). When the speed of trading ν_{ij} is positive, the agent, over a small time step Δt, is buying in country i a quantity of electricity $\nu_{ij}\Delta t$, and selling the same quantity in country j. On the contrary, when ν_{ij} is negative, the agent is buying contracts for $\nu_{ij}\Delta t$ MWh of electricity in country j to sell them in country i. Equivalently, in matrix notation,

$$\mathbf{g}(\boldsymbol{\nu}_t) = \boldsymbol{H}\boldsymbol{\nu}_t\,, \tag{4.4.2}$$

and, in our set-up, we define the vector of optimal controls as

$$\boldsymbol{\nu}^\intercal = \begin{pmatrix} \nu_t^{SF} & \nu_t^{FS} & \nu_t^{GS} & \nu_t^{SG} & \nu_t^{GF} & \nu_t^{FG} \end{pmatrix},$$

while $\boldsymbol{H}$ is the 3×6 matrix of permanent impacts β. Specifically, the entries $H_{1,\cdot}$ represent the permanent impacts of all trades on the price of electricity in France, $H_{2,\cdot}$ represent those on the price of electricity in Switzerland, and $H_{3,\cdot}$ those on that of Germany. It is noteworthy to underline that these β coefficients are the coefficients estimated in regression (4.3.1). Because of the greater explanatory power of the regressors, we use the estimates obtained by means of the stepwise algorithm, rather than those of the multivariate regression. Since, as the results of the regression in (4.3.1) indicate, the flows of electricity between two locations have a direct effect on the price electricity of those two locations, but also an indirect effect on the electricity price in all other locations, we include these impacts in the price dynamics (4.3.5),

which becomes:

$$\mathrm{d}\mathbf{P}_t = (\boldsymbol{\theta} - \boldsymbol{\Phi}\,\mathbf{P}_t + \mathbf{g}(\boldsymbol{\nu}_t))\,\mathrm{d}t + \boldsymbol{\sigma}\,\mathrm{d}\mathbf{W}_t + J(\boldsymbol{\psi},\boldsymbol{\xi})\mathrm{d}\boldsymbol{\Pi}(\boldsymbol{\lambda})\,. \tag{4.4.3}$$

The temporary impact is instead referred to the price the agent gets contextually to the market clearing. In fact, when her orders are executed, the price she gets is a little worse than the quoted one, the one she saw before her trading action. We define the 1×3 vector of temporary impacts on power prices as $\boldsymbol{\omega}$, whose elements are country-specific parameters, so that the (non-deseasonalized) price with temporary market impact is as follows:

$$\widehat{P}_t^k = \begin{cases} \widetilde{P}_t^k + \omega_k \nu_t^{kj} & \text{when buying in } k \text{ and selling in } j \\ \widetilde{P}_t^k - \omega_k \nu_t^{jk} & \text{when selling in } k \text{ and buying in } j \end{cases}, \quad j \neq k \,\wedge\, \omega_k \geq 0, \tag{4.4.4}$$

where $\{k, j\} \in \{\text{France}, \text{Switzerland}, \text{Germany}\}$. The execution price of electricity in country k at time t is denoted by $\widehat{P}_t^k$, while $\widetilde{P}_t^k$ denotes the (non-deseasonalized) quoted one, so that $\widetilde{P}_t^k = P_t^k + f^k(t)$, with $f^k(t)$ equal to the seasonal component of country k, in the form of Equation (4.3.2). In such a way, if, for example, $\nu_t^{FS} > 0$ ($\nu_t^{FS} < 0$), it means that, at time t, the agent will buy (sell) electricity contracts in France (and sell (buy) them in Switzerland), and the price $\widehat{P}_t^F$ that she will pay (get) will be slightly higher (lower) than the quoted price $\widetilde{P}_t^F$ she observed immediately before her trade. Similarly, when $\nu_t^{SF} > 0$, the agent will sell electricity contracts in France (and buy them in Switzerland), and the price $\widehat{P}_t^F$ that she will get will be slightly lower than the quoted price $\widetilde{P}_t^F$. The temporary impact is partly due to the fact that the agent is "walking the book" and partly to the fact that the trading activity implies transaction costs.

4.4.2 Optimal cross-border trading strategy

The agent aims at maximizing, over a trading horizon T, her marginal cash flows, here denoted by X. Her cash process at each time t is given by the sum of all price spreads between each country couple, times the relative speed of

trading. We thus get:

$$\begin{aligned} X(t, \mathbf{P}_t, \boldsymbol{\nu}_t) = &\left(\widehat{P}_t^S - \widehat{P}_t^F\right) \nu_t^{FS} + \left(\widehat{P}_t^F - \widehat{P}_t^S\right) \nu_t^{SF} + \left(\widehat{P}_t^G - \widehat{P}_t^S\right) \nu_t^{SG} \\ &+ \left(\widehat{P}_t^S - \widehat{P}_t^G\right) \nu_t^{GS} + \left(\widehat{P}_t^F - \widehat{P}_t^G\right) \nu_t^{GF} + \left(\widehat{P}_t^G - \widehat{P}_t^F\right) \nu_t^{FG} . \end{aligned} \tag{4.4.5}$$

Substituting (4.4.4) into (4.4.5), we get

$$\begin{aligned} X(t, \mathbf{P}_t, \boldsymbol{\nu}_t) = &\left(P_t^F - P_t^S\right) \left(\nu_t^{SF} - \nu_t^{FS}\right) - (\omega_F + \omega_S) \left(\nu_t^{2\,SF} + \nu_t^{2\,FS}\right) \\ &+ \left(P_t^S - P_t^G\right) \left(\nu_t^{GS} - \nu_t^{SG}\right) - (\omega_S + \omega_G) \left(\nu_t^{2\,GS} + \nu_t^{2\,SG}\right) \\ &+ \left(P_t^G - P_t^F\right) \left(\nu_t^{FG} - \nu_t^{GF}\right) - (\omega_F + \omega_G) \left(\nu_t^{2\,GF} + \nu_t^{2\,FG}\right) \\ &+ \left(f^F(t) - f^S(t)\right) \nu_t^{SF} + \left(f^S(t) - f^F(t)\right) \nu_t^{FS} \\ &+ \left(f^S(t) - f^G(t)\right) \nu_t^{GS} + \left(f^G(t) - f^S(t)\right) \nu_t^{SG} \\ &+ \left(f^F(t) - f^G(t)\right) \nu_t^{GF} + \left(f^G(t) - f^F(t)\right) \nu_t^{FG} . \end{aligned} \tag{4.4.6}$$

In matrix notation, this is equal to

$$X(t, P, \nu) = \boldsymbol{\nu}^\intercal \boldsymbol{B}^\intercal \boldsymbol{P} - \boldsymbol{\nu}^\intercal \boldsymbol{\Upsilon} \boldsymbol{\nu} + \boldsymbol{\nu}^\intercal \boldsymbol{f(t)} , \tag{4.4.7}$$

where

$$\boldsymbol{P}^\intercal = \begin{pmatrix} P^F & P^S & P^G \end{pmatrix} ,$$

$$\boldsymbol{B} = \begin{pmatrix} 1 & -1 & 0 & 0 & 1 & -1 \\ -1 & 1 & 1 & -1 & 0 & 0 \\ 0 & 0 & -1 & 1 & -1 & 1 \end{pmatrix} ,$$

$$\boldsymbol{f(t)} = \begin{pmatrix} f_F(t) - f_S(t) \\ f_S(t) - f_F(t) \\ f_S(t) - f_G(t) \\ f_G(t) - f_S(t) \\ f_F(t) - f_G(t) \\ f_G(t) - f_F(t) \end{pmatrix} ,$$

and

$$\boldsymbol{\Upsilon} = \begin{pmatrix} \omega_F + \omega_S & 0 & \cdots & & & 0 \\ 0 & \omega_F + \omega_S & 0 & \cdots & & \vdots \\ \vdots & 0 & \omega_S + \omega_G & 0 & \cdots & \\ & & 0 & \omega_S + \omega_G & 0 & \\ & & & 0 & \omega_F + \omega_G & 0 \\ 0 & \cdots & & & 0 & \omega_F + \omega_G \end{pmatrix} .$$

Thus, her value function is

$$V(t, \mathbf{P}) = \sup_{\boldsymbol{\nu} \in \mathcal{A}} \mathbb{E}_{t,\mathbf{P}} \left[\int_t^T X(u, \mathbf{P}_u, \boldsymbol{\nu}_u) \, \mathrm{d}u \;\middle|\; \mathbf{P}_t = \mathbf{P} \right] , \tag{4.4.8}$$

where the set of admissible strategies $\mathcal{A}$ is defined as

$$\mathcal{A} = \left\{ \left(\boldsymbol{\nu}_t = (\boldsymbol{\nu}_t^{ij})^{i,j \in \{F,G,S\}, i \neq j} \right)_{t \in [0,T]} \text{ progr. meas. and s.t. } \mathbb{E}\left[\int_0^T \|\boldsymbol{\nu}_t\|^2 \mathrm{d}u \right] < +\infty \right\} .$$

Moreover, $\mathbb{E}_{t,\mathbf{P}}$ denotes the expectation computed when the process $\{\mathbf{P}_u^{\boldsymbol{\nu};t,\mathbf{P}}, u \in [t,T]\}$ is the solution of Equation (4.4.3) with initial condition $\mathbf{P}_t = \mathbf{P}$ and control $\boldsymbol{\nu}$.

The dynamic programming principle suggests that (4.4.8) is the unique solution to the following Hamilton-Jacobi-Bellman (HJB) equation

$$\partial_t V(t, \mathbf{P}) + \sup_{\boldsymbol{\nu} \in \mathcal{A}} \left[\mathcal{L}^{\nu} V(t, \mathbf{P}) + X(t, \mathbf{P}, \boldsymbol{\nu}_t) \right] = 0 , \tag{4.4.9}$$

where the infinitesimal generator $\mathcal{L}^{\nu}$ acts as follows

$$\begin{aligned} \mathcal{L}^{\nu} V(t, \boldsymbol{P}) = {} & \left(\boldsymbol{\theta} - \boldsymbol{\Phi} \, \mathbf{P}_t + \boldsymbol{\nu}_t^{\intercal} \boldsymbol{H}^{\intercal} \right) V_P(t, \boldsymbol{P}) + \frac{1}{2} \mathrm{Tr} \left[\boldsymbol{\Omega} \, \mathcal{H} \right] \\ & + \sum_{k=1}^{n} \lambda_k \int_{-\infty}^{+\infty} \Delta_k(y) V(t, \mathbf{P}) \frac{1}{\sqrt{2\pi}\xi_k} \mathrm{e}^{\frac{-(y-\psi_k)^2}{2\xi_k^2}} \, \mathrm{d}y , \end{aligned}$$

where $V_P(t, \boldsymbol{P})$ is the vector with elements $\frac{\partial V}{\partial P_i}$, $\mathrm{Tr}[\cdot]$ denotes the trace operator and $\mathcal{H}$ is the Hessian of V, namely a matrix with elements $\mathcal{H}_{i,j} = \frac{\partial^2 V}{\partial P_i \partial P_j}$. The operator $\Delta_k(y)V(t, \mathbf{P})$, due to the jump part, acts as follows (cf. Cartea

et al. (2015) and Øksendal and Sulem (2007)):

$$\Delta_k(y)V(t,\mathbf{P}) = V(t,\mathbf{P}+y\mathbb{1}_k) - V(t,\mathbf{P}) \quad \forall\, k \in \{1,...,n\}\ ,$$

where the indicator function $\mathbb{1}_k$ is defined as

$$\mathbb{1}_1 = (1,0,\cdots,0)^\intercal\ , \qquad \mathbb{1}_2 = (0,1,\cdots,0)^\intercal\ ,\ \cdots\ ,\ \mathbb{1}_n = (0,0,\cdots,1)^\intercal\ .$$

Proposition 4.4.1. *Given* (4.4.9)*, the optimal speed of trading in feedback control form is defined as*

$$\boldsymbol{\nu}_t^* = \frac{1}{2}\,\boldsymbol{\Upsilon}^{-1}\left(\boldsymbol{H}^\intercal V_P(t,\boldsymbol{P}) + \boldsymbol{B}^\intercal \boldsymbol{P}_t + \boldsymbol{f(t)}\right)\ . \tag{4.4.10}$$

and the HJB reduces to the following partial integro-differential equation (PIDE):

$$\begin{aligned} 0 &= \partial_t V(t,\mathbf{P}) + \mathcal{L}V(t,\mathbf{P}) \\ &+ \frac{1}{4}\left[\boldsymbol{H}^\intercal V_P(t,\boldsymbol{P}) + \boldsymbol{B}^\intercal \boldsymbol{P}_t + \boldsymbol{f(t)}\right]^\intercal \boldsymbol{\Upsilon}^{-1}\left[\boldsymbol{H}^\intercal V_P(t,\boldsymbol{P}) + \boldsymbol{B}^\intercal \boldsymbol{P}_t + \boldsymbol{f(t)}\right]\ , \end{aligned} \tag{4.4.11}$$

with

$$\begin{aligned} \mathcal{L}V(t,\boldsymbol{P}) = (\boldsymbol{\theta} - \boldsymbol{\Phi}\,\mathbf{P}_t)\,V_P(t,\boldsymbol{P}) + \frac{1}{2}\mathrm{Tr}\left[\boldsymbol{\Omega}\,\mathcal{H}\right] \\ + \sum_{k=1}^{n}\lambda_k \int_{-\infty}^{+\infty} \Delta_k(y)V(t,\mathbf{P})\frac{1}{\sqrt{2\pi}\xi_k}\mathrm{e}^{\frac{-(y-\psi_k)^2}{2\xi_k^2}}\,\mathrm{d}y\ . \end{aligned}$$

Proof. See Appendix C.2. □

We remark here that the second term in brackets in (4.4.10) can be seen as a myopic trading strategy, simply based on the electricity price spread. The first term is instead the added value given by acknowledging the permanent impacts on prices. Finally, the third term is simply the seasonality spread between each country couple. In what follows, we are going to label *naïve strategy* the simple strategy based on the price spread, namely

$$\boldsymbol{\nu}_t^{\mathrm{n}} = \frac{1}{2}\,\boldsymbol{\Upsilon}^{-1}\left(\boldsymbol{B}^\intercal \boldsymbol{P}_t + \boldsymbol{f(t)}\right)\ . \tag{4.4.12}$$

This is going to be the benchmark against which to compare the performance of the optimal trading strategy $\boldsymbol{\nu}^*$.

Now, in order to solve (4.4.11), we need to guess a solution. We expect the value function to be a quadratic combination of prices. Thus, we propose the following ansatz:

Proposition 4.4.2 (Solving the HJB.)**.** *The PIDE in* (4.4.11) *admits a solution of the form*

$$V(t,\mathbf{P}) = A(t) + \boldsymbol{D}^\intercal(t)\mathbf{P} + \mathbf{P}^\intercal \boldsymbol{E}(t)\mathbf{P}\,, \tag{4.4.13}$$

where $A(t)$, a scalar, and

$$D(t) = \begin{pmatrix} D_1(t) \\ D_2(t) \\ D_3(t) \end{pmatrix}\,,\; E(t) = \begin{pmatrix} E_{11}(t) & E_{12}(t) & E_{13}(t) \\ E_{12}(t) & E_{22}(t) & E_{23}(t) \\ E_{13}(t) & E_{23}(t) & E_{33}(t) \end{pmatrix}$$

are the solution of the a 10-ODEs system: specifically, E solves a matrix Riccati equation, D solves a linear differential equation and A solves an integrable equation. Moreover, $E(t) = Y(t)X(t)^{-1}$, with

$$\begin{pmatrix} X(t) \\ Y(t) \end{pmatrix} = \exp\left[(T-t)\begin{pmatrix} -\frac{1}{2}\boldsymbol{H}\boldsymbol{\Upsilon}^{-1}\boldsymbol{B}^\intercal + \boldsymbol{\Phi} & -\boldsymbol{H}\boldsymbol{\Upsilon}^{-1}\boldsymbol{H}^\intercal \\ \frac{1}{4}\boldsymbol{B}\boldsymbol{\Upsilon}^{-1}\boldsymbol{B}^\intercal & \left(\frac{1}{2}\boldsymbol{H}\boldsymbol{\Upsilon}^{-1}\boldsymbol{B}^\intercal - \boldsymbol{\Phi}\right)^\intercal \end{pmatrix}\right]\begin{pmatrix} X(T) \\ Y(T) \end{pmatrix}\,, \tag{4.4.14}$$

and

$$\begin{pmatrix} X(T) \\ Y(T) \end{pmatrix} = \begin{pmatrix} I \\ E(T) \end{pmatrix}\,. \tag{4.4.15}$$

The solution of $D(t)$ is instead given by

$$\begin{aligned} D(t) = X^\intercal(t)^{-1}D(T) + \int_0^t \left[X(t)^{-1}\right]^\intercal X^\intercal(s)\,\Big[&2\boldsymbol{E}(s)(\boldsymbol{\theta} + \boldsymbol{\lambda}\circ\boldsymbol{\psi}) \\ &+ \boldsymbol{E}(s)\boldsymbol{H}\boldsymbol{\Upsilon}^{-1}\boldsymbol{f}(s) + \frac{1}{2}\boldsymbol{B}\boldsymbol{\Upsilon}^{-1}\boldsymbol{f}(s)\Big]\,\mathrm{d}s\,, \end{aligned} \tag{4.4.16}$$

where $\circ$ denotes the Hadamard product between two vectors, i.e. $(\boldsymbol{\lambda}\circ\boldsymbol{\psi})_i =$

$\lambda_i \psi_i \, \forall \, i$. *Finally,*

$$A(t) = A(T) + \int_t^T \frac{1}{4} \left(\boldsymbol{D}^\intercal(s)\boldsymbol{H} + \boldsymbol{f}^\intercal(s)\right) \boldsymbol{\Upsilon}^{-1} \left(\boldsymbol{H}^\intercal \boldsymbol{D}(s) + \boldsymbol{f}(s)\right) + \mathrm{Tr}\left[\boldsymbol{\Omega}\, \boldsymbol{E}(s)\right] + \boldsymbol{D}^\intercal(s)\left(\boldsymbol{\theta} + \boldsymbol{\lambda} \circ \boldsymbol{\psi}\right) + \boldsymbol{\psi}^\intercal diag(\boldsymbol{E}(s))\left(\boldsymbol{\lambda} \circ \boldsymbol{\psi}\right) + \boldsymbol{\xi}^\intercal diag(\boldsymbol{E}(s))\left(\boldsymbol{\lambda} \circ \boldsymbol{\xi}\right) \mathrm{d}s \,. \tag{4.4.17}$$

where $diag(\boldsymbol{E}(t))$ *is a matrix with the elements on the main diagonal equal to those on the main diagonal of* $\boldsymbol{E}(t)$*, and with all other elements equal to zero, such that*

$$diag(\boldsymbol{E}(t)) = \begin{pmatrix} E_{11}(t) & 0 & 0 \\ 0 & E_{22}(t) & 0 \\ 0 & 0 & E_{33}(t) \end{pmatrix} .$$

Moreover, the optimal controls are given by

$$\boldsymbol{\nu}_t^* = \boldsymbol{\Upsilon}^{-1} \left(\frac{1}{2} \boldsymbol{H}^\intercal \boldsymbol{D}(t) + \boldsymbol{H}^\intercal \boldsymbol{E}(t) \boldsymbol{P}_t + \frac{1}{2} \boldsymbol{B}^\intercal \boldsymbol{P}_t + \frac{1}{2} \boldsymbol{f(t)} \right) . \tag{4.4.18}$$

Proof. See Appendix C.2. □

We are now ready to close the gap between the original optimal control problem of the agent in Equation (4.4.8) and the HJB equation (4.4.9). First of all we need a technical lemma.

Lemma 4.4.1. *For all* $\nu \in \mathcal{A}$*, for all* $t \in [0, T]$ *and for all initial conditions* $\mathbf{P} \in \mathbb{R}^3$*, the process* $\mathbf{P}^{\boldsymbol{\nu};t,\mathbf{P}}$ *is such that*

$$\mathbb{E}_{t,\mathbf{P}} \left[\sup_{t \le u \le T} \| \mathbf{P}_u^{\boldsymbol{\nu};t,\mathbf{P}} \|^2 \right] < +\infty \,.$$

Proof. First of all, we have that, for $u \in [t, T]$, Equation (4.4.3) has the unique solution

$$\begin{aligned} \mathbf{P}_u^{\boldsymbol{\nu};t,\mathbf{P}} &= e^{-(u-t)\Phi} \mathbf{P}_t + \int_t^u e^{-(v-t)\Phi} (\boldsymbol{\theta} + H\boldsymbol{\nu}_v) \, \mathrm{d}v + \int_t^u e^{-(v-t)\Phi} (\boldsymbol{\sigma} \, \mathrm{d}\mathbf{W}_t + J(\boldsymbol{\psi}, \boldsymbol{\xi}) \mathrm{d}\boldsymbol{\Pi}(\boldsymbol{\lambda})) \\ &= \mathbf{P}_u^{0;t,\mathbf{P}} + \int_t^u e^{-(v-t)\Phi} H \boldsymbol{\nu}_v \, \mathrm{d}v \,. \end{aligned}$$

Thus,

$$\mathbb{E}_{t,\mathbf{P}}\left[\sup_{t\le u\le T}\|\mathbf{P}_u^{\boldsymbol{\nu};t,\mathbf{P}}\|^2\right] \le 2\mathbb{E}_{t,\mathbf{P}}\left[\sup_{t\le u\le T}\|\mathbf{P}_u^{0;t,\mathbf{P}}\|^2\right] + 2\mathbb{E}_{t,\mathbf{P}}\left[\sup_{t\le u\le T}\left\|\int_t^u e^{-(v-t)\Phi}H\boldsymbol{\nu}_v\,\mathrm{d}v\right\|^2\right].$$

Since the process $\mathbf{P}^{0;t,\mathbf{P}}$ is solution of Equation (4.4.3) with zero control, which satisfies the assumptions of Protter (2003, Theorem V.67), the first term in the right-hand side is finite. For the second term, we have

$$\mathbb{E}_{t,\mathbf{P}}\left[\sup_{t\le u\le T}\left\|\int_t^u e^{-(v-t)\Phi}H\boldsymbol{\nu}_v\,\mathrm{d}v\right\|^2\right] \le \mathbb{E}_{t,\mathbf{P}}\left[\int_t^T\|e^{-(v-t)\Phi}H\|^2\|\boldsymbol{\nu}_v\|^2\,\mathrm{d}v\right] \le \sup_{t\le v\le T}\|e^{-(v-t)\Phi}H\|^2\mathbb{E}_{t,\mathbf{P}}\left[\int_t^T\|\boldsymbol{\nu}_v\|^2\,\mathrm{d}v\right],$$

which is finite, as $[t,T]\ni v\to e^{-(v-t)\Phi}H$ is continuous and bounded and $\boldsymbol{\nu}$ is admissible. □

Theorem 4.4.1 (Verification Theorem)**.** *Assume that, for a certain $t\in[0,T]$, the matrix-valued function $t\to\boldsymbol{E}(t)$ defined in Equation* (4.4.14) *is the unique solution of Equation* (C.8) *on $[t,T]$. Then the function V in Equation* (4.4.13)*, solution of the HJB equation* (4.4.9)*, coincides with the value function* (4.4.8)*. Moreover, the process $\boldsymbol{\nu}^*$ defined in Equation* (4.4.10) *is the optimal control for the problem* (4.4.8)*.*

Proof. The proof is basically a check on the more general result in Fleming and Soner (1993, Theorem III.8.1). In fact, we already know that V is a classical (i.e., $C^{1,2}$) solution of the HJB equation (4.4.9). Thus, it follows that $V(t,\mathbf{P})\ge\mathbb{E}_{t,\mathbf{P}}\left[\int_t^T X(u,\mathbf{P}_u,\boldsymbol{\nu}_u)\,\mathrm{d}u\right]\ \forall\,\nu\in\mathcal{A}$, provided that the Dynkyn formula

$$\mathbb{E}_{t,\mathbf{P}}[V(T,\mathbf{P}_T)] = V(t,\mathbf{P}) + \mathbb{E}_{t,\mathbf{P}}\left[\int_t^T\mathcal{L}^\nu V(u,\boldsymbol{P}_u)\,\mathrm{d}u\right] \tag{4.4.19}$$

holds. To prove this, first of all we notice that the integral to the right-hand

side is well defined. In fact, since V is bilinear in $\mathbf{P}$, we have that

$$|\mathcal{L}^\nu V(u,\mathbf{P})| \leq C(1+\|\mathbf{P}\|^2+\|\mathbf{P}\|\cdot\|\boldsymbol{\nu}\|)$$

for a suitable C. This implies that

$$\begin{aligned}\mathbb{E}_{t,\mathbf{P}}\left[\int_t^T |\mathcal{L}^\nu V(u,\boldsymbol{P}_u)|\mathrm{d}u\right] &\leq \mathbb{E}_{t,\mathbf{P}}\left[\int_t^T C\left(1+\|\mathbf{P}_u\|^2+\|\mathbf{P}_u\|\cdot\|\boldsymbol{\nu}_u\|\right)\mathrm{d}u\right] \leq \\ &\leq C(T-t)+C\mathbb{E}_{t,\mathbf{P}}\left[\int_t^T \|\mathbf{P}_u^{\boldsymbol{\nu};t,\mathbf{P}}\|^2\mathrm{d}u\right] \\ &\quad + C\mathbb{E}_{t,\mathbf{P}}\left[\int_t^T \|\mathbf{P}_u^{\boldsymbol{\nu};t,\mathbf{P}}\|^2\mathrm{d}u\right]\cdot\mathbb{E}_{t,\mathbf{P}}\left[\int_t^T \|\boldsymbol{\nu}_u\|^2\mathrm{d}u\right],\end{aligned}$$

where the third term comes from the Cauchy-Schwarz inequality. Thus, it turns out that the sum above is finite from the fact that

$$\mathbb{E}_{t,\mathbf{P}}\left[\int_t^T \|\mathbf{P}_u^{\boldsymbol{\nu};t,\mathbf{P}}\|^2\mathrm{d}u\right] \leq (T-t)\mathbb{E}_{t,\mathbf{P}}\left[\sup_{u\in[t,T]}\|\mathbf{P}_u^{\boldsymbol{\nu};t,\mathbf{P}}\|^2\right] < +\infty\,, \tag{4.4.20}$$

by Lemma 4.4.1, and from $\boldsymbol{\nu}\in\mathcal{A}$.

To prove the Dynkyn formula, we notice that the Itō formula applied to $V(t,\mathbf{P}_t^{\boldsymbol{\nu}})$ gives

$$V(T,\mathbf{P}_T^{\boldsymbol{\nu}}) = V(t,\mathbf{P})+\int_t^T \mathcal{L}^\nu V(u,\boldsymbol{P}_u^{\boldsymbol{\nu}})\mathrm{d}u + I_T^1 + I_T^2\,, \tag{4.4.21}$$

where

$$\begin{aligned}I_u^1 &:= \int_t^u (D(v)+2E(v)P_v^{\boldsymbol{\nu}})^\intercal\sigma\ \mathrm{d}W_v\,,\\ I_u^2 &:= \int_t^u (D(v)+2E(v)P_{v-}^{\boldsymbol{\nu}})^\intercal J(\boldsymbol{\psi},\boldsymbol{\xi})\ \mathrm{d}\boldsymbol{\Pi}(\boldsymbol{\lambda})\,.\end{aligned}$$

By the Itō isometry, $(I^1_u)_{u\in[t,T]}$ is a martingale. In fact,

$$\begin{aligned}
&\mathbb{E}_{t,\mathbf{P}}\left[\int_t^T \|(D(v)+2E(v)P^{\boldsymbol{\nu}}_v)^\intercal\sigma\|^2\mathrm{d}v\right]\leq\\
&\leq\|\sigma\|^2\mathbb{E}_{t,\mathbf{P}}\left[\int_t^T(\|D(v)\|^2+2\|E(v)P^{\boldsymbol{\nu}}_v)\|^2)\mathrm{d}v\right]\leq\\
&\leq\|\sigma\|^2(T-t)\sup_{v\in[t,T]}\|D(v)\|^2+2\|\sigma\|^2\sup_{v\in[t,T]}\|E(v)\|^2\mathbb{E}_{t,\mathbf{P}}\left[\int_t^T\|P^{\boldsymbol{\nu}}_v\|^2\mathrm{d}v\right],
\end{aligned}$$

where the sup are finite, as D and E are continuous on $[t,T]$, and the latter term is finite by Equation (4.4.20); thus, I^1 is a martingale. For I^2, we invoke Protter (2003, Theorem V.66), for which, for all $u\in[t,T]$, we must check the finiteness of

$$\begin{aligned}
&\mathbb{E}_{t,\mathbf{P}}\left[\left\|\int_t^u J(\boldsymbol{\psi},\boldsymbol{\xi})\;d\boldsymbol{\Pi}(\boldsymbol{\lambda})\right\|^2\right]=\sum_{k=1}^3\mathbb{E}_{t,\mathbf{P}}\left[\left(\sum_{\ell=1}^{\Pi^k_u}J^k_\ell\right)^2\right]=\\
&=\sum_{k=1}^3\mathbb{E}_{t,\mathbf{P}}\left[\mathbb{E}_{t,\mathbf{P}}\left[\left(\sum_{\ell=1}^{\Pi^k_u}J^k_\ell\right)^2\middle|\,\Pi^k_u\right]\right]=\sum_{k=1}^3\mathbb{E}_{t,\mathbf{P}}\left[\sum_{\ell,m=1}^{\Pi^k_u}\mathbb{E}_{t,\mathbf{P}}\left[J^k_\ell J^k_m\right]\right]=\\
&=\sum_{k=1}^3\mathbb{E}_{t,\mathbf{P}}\left[\Pi^k_u(\psi_k^2+\xi_k^2)\right]=\sum_{k=1}^3\lambda_k(u-t)(\psi_k^2+\xi_k^2)<+\infty\,.
\end{aligned}$$

Since $v\to(D(v)+2E(v)P^{\boldsymbol{\nu}}_{v-})^\intercal$ is left-continuous, thus predictable, by Protter (2003, Theorem V.66) there exists a $K>0$ such that

$$\mathbb{E}_{t,\mathbf{P}}\left[\sup_{u\in[t,T]}|I^2_u|^2\right]\leq K\int_t^T\mathbb{E}_{t,\mathbf{P}}[\|D(u)+2E(u)P^{\boldsymbol{\nu}}_{u-}\|^2]\mathrm{d}u\,,$$

where the right-hand side is finite, in analogy with what we did with I^1. This means that also I^2 is a martingale: then, taking the expectation of Equation (4.4.21) gives the Dynkyn formula (4.4.19). As announced, this implies that $V(t,\mathbf{P})\geq\mathbb{E}_{t,\mathbf{P}}\left[\int_t^T X(u,\mathbf{P}_u,\boldsymbol{\nu}_u)\,\mathrm{d}u\right]\;\forall\;\nu\in\mathcal{A}$.

To prove the second part, we already have that $\boldsymbol{\nu}^*(t,\mathbf{P})$ defined in Equation (4.4.10) is a maximizer of the HJB equation (4.4.9). Thus, we only need to check that the process $(\boldsymbol{\nu}^*(t,\mathbf{P}_t))_t\in\mathcal{A}$. Given that it is progressively

measurable by construction, we only need to check its square integrability:

$$\begin{aligned}
&\mathbb{E}_{t,\mathbf{P}}\left[\int_t^T \|\boldsymbol{\nu}^*(u,\mathbf{P}_u)\|^2 \mathrm{d}u\right] = \\
&= \frac{1}{4}\|\boldsymbol{\Upsilon}\|^{-2}\mathbb{E}_{t,\mathbf{P}}\left[\int_t^T \|\boldsymbol{H}^\intercal(D(u)+2E(u)\mathbf{P}_u)+\boldsymbol{B}^\intercal\mathbf{P}_u+f^\intercal(u)\|^2\,\mathrm{d}u\right] \leq \\
&\leq C\mathbb{E}_{t,\mathbf{P}}\left[\int_t^T (1+\|\mathbf{P}_u\|^2)\mathrm{d}u\right],
\end{aligned}$$

for a suitable C. This is because D, E and f are continuous functions of time $u \in [t,T]$. Again, by Lemma 4.4.1 and arguments analogous to those used before, we can conclude that $\mathbb{E}_{t,\mathbf{P}}\left[\int_t^T \|\boldsymbol{\nu}^*(u,\mathbf{P}_u)\|^2\, du\right] < +\infty$ and $(\boldsymbol{\nu}^*(t,\mathbf{P}_t))_t \in \mathcal{A}$, which implies the second part of the verification theorem. □

4.5 Empirical performance

To showcase the strategy's performance, we first run 10,000 simulations of the multivariate price process using the parameters estimated above, for each day and for a trading horizon of 1 year. We use the solution (4.4.14) to the matrix Riccati equation in Appendix C.2, along with (4.4.16) and (4.4.17), to compute the six optimal controls for each run. Finally, the agent's cash process X is computed by taking the mean over the 10,000 runs.

The mean of all 10,000 paths for each optimal control is depicted for each day in Figure 4.4, both when trading a peak hour (3 p.m.) and an off-peak one (3 a.m.). The figure showcases a comparison between the controls paired by country pair (left panels) and a comparison between each control and the relative naïve strategy (right panels). We note here that the optimal controls for each country pair assume values that are quite similar in absolute value for each given day, although not exactly one the opposite of the other.

Figure 4.5 instead shows the cumulative cash process obtained when trading a peak (Figure 4.5a, upper panel) and an off-peak (Figure 4.5b, upper panel) hour, both using the optimal trading strategy (dashed blue lines), or the naïve one (dashed red line), as well as the difference between the two (blue area). Moreover, the bottom panels of Figure 4.5a and 4.5b depict the cumulative cash process broken down with respect to the three bilateral

transmission lines.

Overall, Figure 4.5 shows how, at $t = T$, the optimal trading strategy outperforms the naïve one, and this holds for all hourly contracts, as we can see in Figure 4.8. Specifically, the marginal gains with respect to the strategy purely based on the price spread are in the range of € 50,000 to € 4,351,000 after 1 year of trading. Trading in contracts with delivery at 7 p.m., 9 a.m. and 7 a.m. returns the highest yield at $T = 365$, with profits respectively about 24%, 16% and 16% higher than those obtaied with the naïve strategy. On the other hand, trading in contracts with delivery at 2 p.m., 12 p.m. and 11 a.m. gives the least considerable improvement, with a performance of respectively 0.6%, 0.9% and 1.5% more with respect to the naïve strategy.

$t = 0$	$t = 1$	$t = 2$	$t = 3$	$t = 4$	$t = 6$	$t = 8$
0	$-1,893.34$	$-3,511.36$	$-3,203.81$	-947.37	$7,886.19$	$2,3780.21$
$t = 10$	$t = 15$	$t = 20$	$t = 100$	$t = 200$	$t = 300$	$t = 365$
$43,224.3$	$94,291.27$	$140,853.19$	$623,671.06$	$1,158,672.06$	$2,123,017.42$	$4,351,132.31$

Table 4.7: Additional gains (in €) obtained when trading hour 7 p.m. using the optimal trading strategy over the naïve one. The incremental profits are shown for different times t (expressed in days), until the end of the trading horizon, $T = 365$.

It is also interesting to observe the evolution of the cumulative cash flows over the trading period. As we mentioned, trading hour 7 p.m. leads to the best marginal gains at $t = T$. Table 4.7 shows the value of the integral of the cash flows at different points in time t. It is worth noticing how, at the beginning of the trading period, the optimal strategy actually fell below the gains obtained using the naïve strategy. This means that, at the beginning of the trading period, it is optimal to actually go against the sensible trading direction. It can be conjectured that this serves to the purpose of widening the price spread even more, in order to profit from this later on, *de facto* acting as a speculative trading strategy.

However, it is worth stressing that these results strongly depend on the choice of the temporary impact parameters. These are the only parameters we cannot estimate. The results presented above were obtained using a temporary impact vector $\boldsymbol{\omega} = \begin{bmatrix} 0.01 & 0.01 & 0.01 \end{bmatrix}$. This choice is motivated by the conjecture that these parameters are mainly due to transaction costs, and they represent a sort of fee applied to each transaction ν_t. Nevertheless, to assess their actual impact on the overall performance of the strategy, we

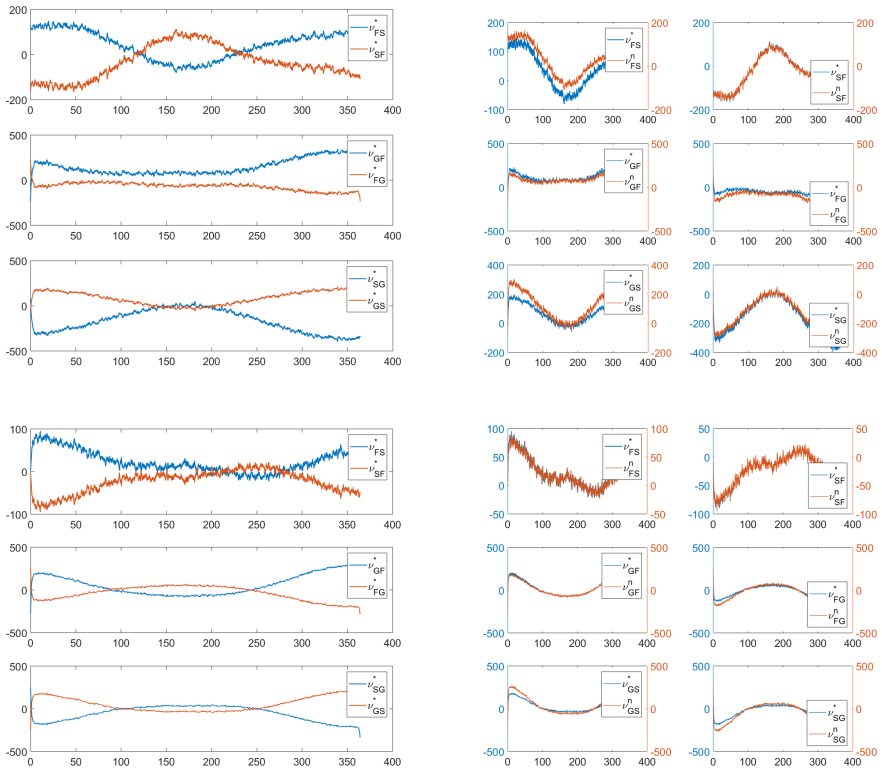

Figure 4.4: Optimal controls ν^* paired by country pair (left panels) and compared with the relative naïve strategy (right panels), with a trading horizon $T = 365$ days. Upper panels show the results when trading a peak hour (3 p.m.), and bottom panels depict those when trading an off-peak hour (3 a.m.).

conduct a sensitivity analysis. Figures 4.6 and 4.7 show the results.

Specifically, Figure 4.6 shows how the marginal gains at $t = T$ of the optimal strategy over the naïve one change depending on the different magnitudes of $\boldsymbol{\omega}$ and on different model horizons. In particular, we let $\boldsymbol{\omega} = \boldsymbol{\omega_0} \cdot (\text{K factor})$, where $\boldsymbol{\omega_0} = [0.02 \quad 0.02 \quad 0.02]$, and K factor $\in [0.1; 10]$. In such a way, we can observe how the marginal performance (in $\log_{10}$ scale) of the optimal trading strategy (that is, $\log_{10}(V^*(T) - V^{\mathrm{n}}(T))$) changes when the temporary impact factors ω_k vary by two orders of magnitude, from -1 to -3. Moreover, on the y-axis, we can also see how the performance depends on the model horizon T, with $T \in [30; 365]$. The results show that the marginal performance is increasing in T, and, obviously, decreasing in the temporary impacts. Moreover, it is always positive, showing that the optimal trad-

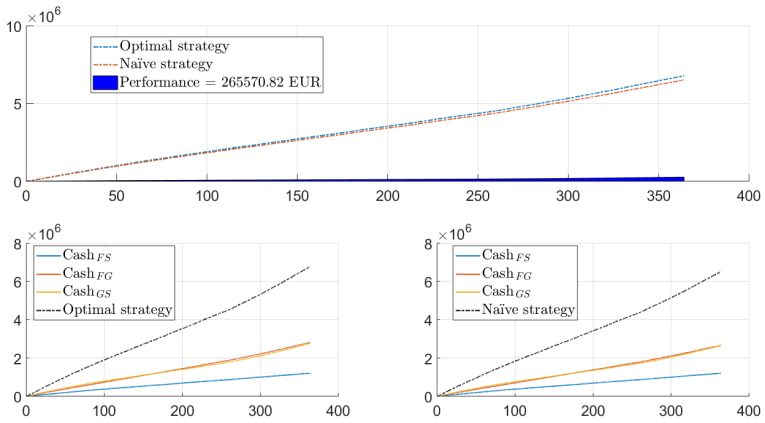

(a) $T = 365$ days, $\boldsymbol{\omega} = \begin{bmatrix} 0.01 & 0.01 & 0.01 \end{bmatrix}$. Trading hour 3 p.m.

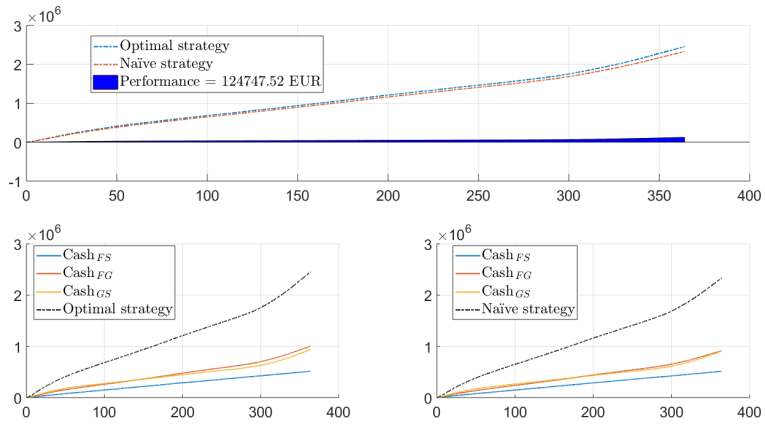

(b) $T = 365$ days, $\boldsymbol{\omega} = \begin{bmatrix} 0.01 & 0.01 & 0.01 \end{bmatrix}$. Trading hour 3 a.m.

Figure 4.5: Cumulative cash flows obtained when trading in contracts with delivery at 3 p.m. (4.5a), and in contracts with delivery at 3 a.m. (4.5b). The blue dashed lines in (4.5a) and (4.5b), upper panels, represent the cumulative cash flows obtained using the optimal trading strategy, while the red dashed lines in (4.5a) and (4.5b), upper panels, those obtained using the naïve trading strategy. The solid yellow, red and blue lines depict the profits resulting from trading in contracts between Germany-Switzerland, Germany-France and France-Switzerland, respectively, using the optimal strategy (left bottom panels of (4.5a) and (4.5b)), or the naïve one (right bottom panels of (4.5a) and (4.5b)).

ing strategy always outperforms the benchmark, for all trading horizons and temporary impact vectors considered. Finally, the heat maps in Figure 4.7 show similar results, depicting $V^*(T)$ and $V^{\mathrm{n}}(T)$ on separate graphs.

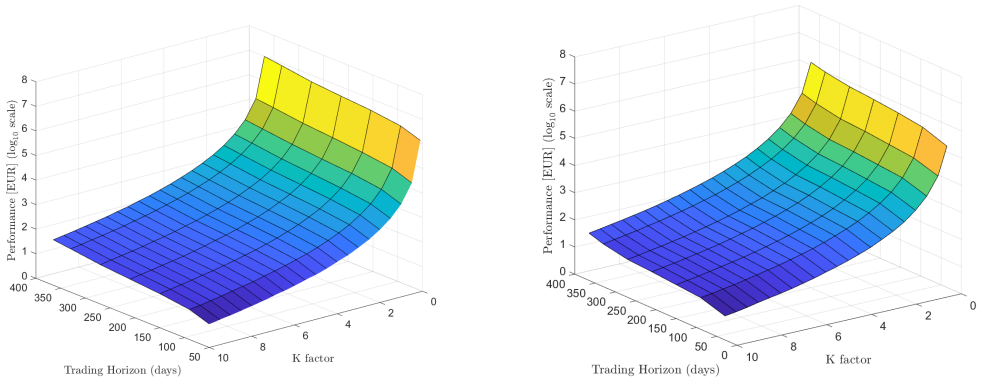

Figure 4.6: Analysis of sensitivity to the trading horizon T and to the vector of temporary impacts $\boldsymbol{\omega}$. The marginal gains (in €, expressed in $\log_{10}$ scale) of the optimal trading strategy over the naïve one at $t = T$ (i.e., $\log_{10}(V^*(T) - V^{\mathrm{n}}(T))$) are depicted when trading hour 3 p.m. (left panel) and hour 3 a.m. (right panel). $T \in [30; 365]$, while $\boldsymbol{\omega} = \boldsymbol{\omega_0}\cdot$(K factor), where $\boldsymbol{\omega_0} = \begin{bmatrix}0.02 & 0.02 & 0.02\end{bmatrix}$, and K factor $\in [0.1; 10]$.

4.6 Conclusions

Using econometric tools, we have shown statistical evidence of cross-effects on the price of electricity in neighbouring countries, due to electricity flows across interconnected locations. We built on this result to set up an optimal trading strategy, based not only on the price spreads observed over time among the selected interconnected countries, but also on the market impacts caused by the flows of electricity among them. Using the aforementioned econometric analysis findings, we modeled the joint dynamics of electricity prices as including both temporary and permanent impacts of electricity trades, as well as driven by a common co-integration factor. Finally, using optimal control techniques and the dynamic programming principle, we defined the optimal trading strategy for an agent trading in intra-day electricity contracts.

The results of the empirical analysis evidence a considerable improvement of our strategy over a naïve strategy purely based on the price spread, and the main sources of profits of our strategy derive from considering the co-movement of electricity prices through co-integration, and the direct and indirect impacts of the cross-border electricity flows on the electricity price.

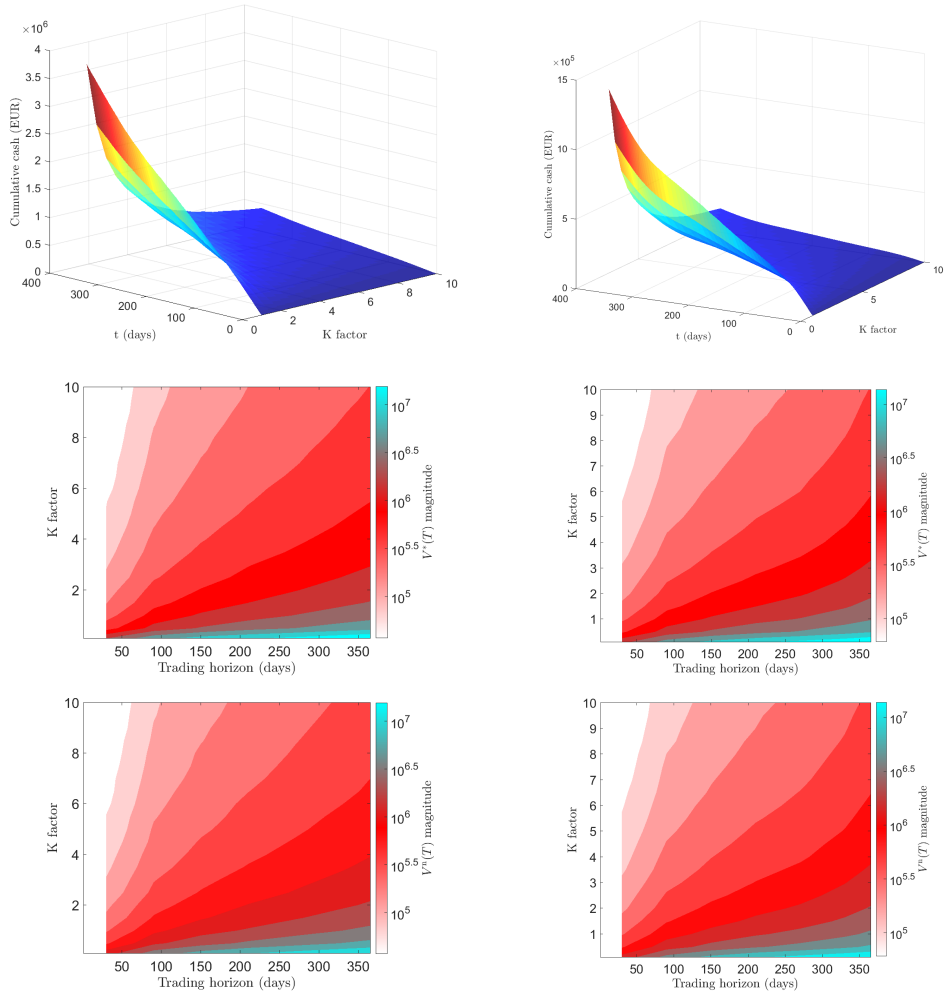

Figure 4.7: Analysis of sensitivity for trading in contracts with delivery at 3 p.m. (left panels) and at 3 a.m. (right panels). The upper panels depict the cumulative cash flows obtained with the optimal trading strategy over 1 year of trading when varying $\boldsymbol{\omega}$, with $\boldsymbol{\omega} = \boldsymbol{\omega_0} \cdot (\text{K factor})$, where $\boldsymbol{\omega_0} = \begin{bmatrix} 0.02 & 0.02 & 0.02 \end{bmatrix}$, and K factor $\in [1; 10]$. The remaining panels are heat maps depicting the level of the value function at time T, obtained when trading with the optimal trading strategy (middle panels), or with the naïve one (bottom panels), depending on the model horizon $T \in [30; 365]$, and on the K factor $\in [0.1; 10]$.

Finally, it is worth noticing that there are a number of directions of future research to improve our model. Firstly, as Kiesel and Paraschiv (2016) suggest, intraday prices adjust to the forecasting errors in renewables, thus a possible extension to this work would be to improve the regression specification (4.3.1), used to estimate the direct and indirect price impacts, with

additional explanatory variables. Secondly, the literature on price impacts is scarce as for electricity markets, but it is rich as for stock markets. This stream of literature (for instance, Engle and Dufour (2000) and Hasbrouck (1991)) makes use of order book data to provide an estimate of price impacts of trades. If we were to obtain such data relatively to the intra-day electricity market, we could build from those works to improve the estimation procedure. Finally, in this chapter we only analyzed how interconnecting countries affects the level of electricity prices. A possible extension would be to also analyze how cross-border trades affect the price volatility. It is reasonable to think that adding interconnector capacity lowers price volatility. Including this effect in the model could further improve it.

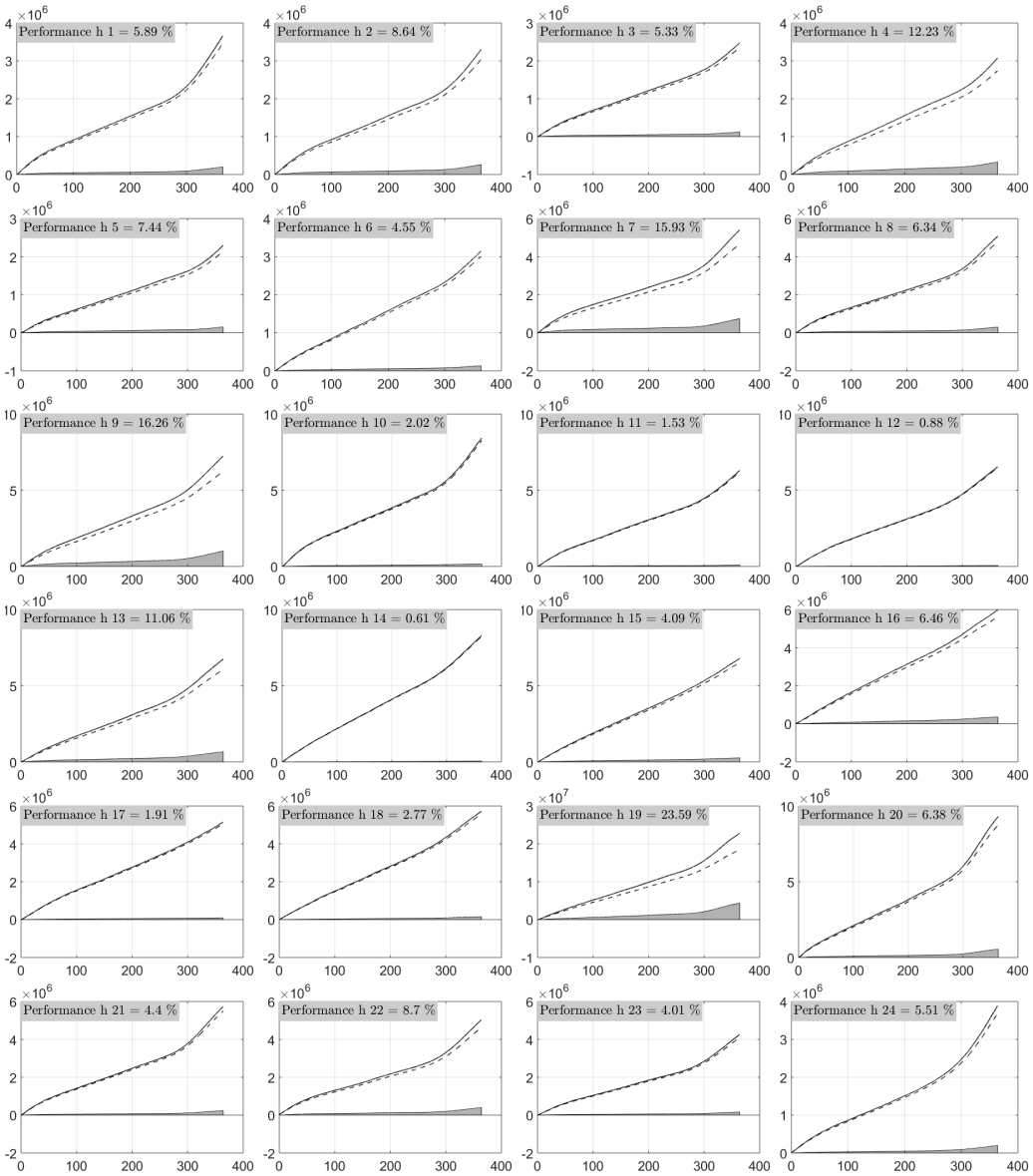

Figure 4.8: Cumulative cash flows (in €) obtained using the optimal strategy (solid black line) and the naïve one (dashed black line) for all hourly contracts, over 365 days of trading. The gray boxed area shows the percentage improvement at $T = 365$ days of the optimal strategy over the naïve one. $\boldsymbol{\omega} = \begin{bmatrix} 0.01 & 0.01 & 0.01 \end{bmatrix}$.

4.7 Appendix C

C.1 Econometric analysis results

	01:00	02:00	03:00	04:00	05:00	06:00
(1)	0.0020^{***}	0.0012	-0.0016^{***}	0.0001	-0.0006	-0.0003
(2)	0.0006	-0.0002	-0.0006	-0.0006	-0.0013^{*}	0.0004
(3)	-0.0017^{***}	-0.0005	-0.0002	-0.0011^{*}	-0.0001	0.0001
(4)	0.0139^{***}	0.008^{***}	0.0052^{***}	0.0044^{***}	0.009^{***}	-0.0005
(5)	-0.0004	-0.0002	0.0004	0.0002	0.0004	0.0008
(6)	-0.0047^{***}	-0.0018^{*}	0.0007	0.0001	-0.002	-0.0027^{**}
	07:00	08:00	09:00	10:00	11:00	12:00
(1)	0.0006	-0.0001	-0.001^{**}	-0.0009^{*}	-0.0003	-0.0021^{***}
(2)	0.0005	0.0001	-0.001^{***}	0.0018^{***}	-0.0002	-0.0005
(3)	-0.0008	-0.0008	-0.0004	0.0001	-0.0003	-0.0007
(4)	-0.0003	0.007^{***}	0.0049^{***}	-0.002^{***}	0.0028^{***}	0.0036^{***}
(5)	-0.0014	-0.0008	0.00	-0.0007^{*}	0.0003	0.0023^{***}
(6)	0.0009	-0.0001	0.0005	-0.004^{***}	-0.0017^{***}	0.0001
	13:00	14:00	15:00	16:00	17:00	18:00
(1)	-0.0030^{***}	-0.0009^{*}	0.0022^{***}	0.0025^{***}	0.0026^{***}	0.0013^{***}
(2)	0.0011^{***}	0.0006^{**}	0.0006	0.0007^{**}	0.0012^{***}	0.0006^{**}
(3)	-0.0003	-0.0012^{**}	-0.0013^{***}	0.0007	-0.0004	0.0018^{***}
(4)	0.0032^{***}	0.007^{***}	0.0048^{***}	0.0018^{***}	0.0023^{***}	0.0087^{***}
(5)	0.0014^{**}	0.002^{***}	-0.0009	-0.0010^{*}	0.0010^{**}	-0.0001
(6)	-0.002^{***}	-0.0026^{***}	-0.0015^{**}	-0.0008	-0.0045^{***}	-0.0012^{**}
	19:00	20:00	21:00	22:00	23:00	24:00
(1)	-0.0013^{***}	-0.0025^{***}	-0.0003	-0.0005	-0.0015^{***}	-0.0014^{**}
(2)	-0.0008^{***}	0.0021^{***}	0.0002	0.0001	0.002^{***}	0.0013^{***}
(3)	-0.0025^{***}	-0.0014^{***}	-0.0006	0.0002	0.0004	-0.0001
(4)	0.0087^{***}	0.0059^{***}	0.0047^{***}	0.0026^{***}	0.0035^{***}	0.0021^{***}
(5)	-0.0023^{***}	0.0011^{***}	0.0005	0.0002	-0.0005	0.0017^{***}
(6)	-0.0124^{***}	-0.01^{***}	-0.0035^{***}	-0.0018^{***}	-0.0065^{***}	-0.0047^{***}

Table C.1: Mutivariate OLS robust estimates. Dependent variable: ΔP_t^F. Explanatory variables: Vol_{t-1}^{GF} (1), Vol_{t-1}^{GS} (2), Vol_{t-1}^{FG} (3), Vol_{t-1}^{FS} (4), Vol_{t-1}^{SG} (5), Vol_{t-1}^{SF} (6). $^{***} = p < 0.01, ^{**} = p < 0.05, ^{*} = p < 0.1$.

Table C.2: Mutivariate OLS robust estimates. Dependent variable: ΔP_t^F. Explanatory variables: Vol_{t-1}^{GO} (7), Vol_{t-1}^{OG} (8), Vol_{t-1}^{FO} (9), Vol_{t-1}^{OF} (10), Vol_{t-1}^{SO} (11), Vol_{t-1}^{OS} (12).

	01:00	02:00	03:00	04:00	05:00	06:00	07:00	08:00
(7)	-0.0011^{**}	-0.0004	0.0007^{*}	0.00	-0.0005	-0.0002	-0.0002	0.0010^{***}
(8)	0.0018^{***}	0.0012^{**}	0.0002	0.00	-0.0001	-0.0001	0.0007^{*}	0.0002
(9)	0.0014^{*}	0.0047^{***}	0.00	0.0008	0.0008	0.0040^{***}	0.0021^{**}	0.0070^{***}
(10)	-0.0079^{***}	-0.0048^{***}	-0.0011	-0.0026^{***}	0.0001	-0.003^{***}	-0.0058^{***}	-0.0018^{***}
(11)	0.0042^{*}	-0.0009	-0.0011	-0.0006	0.0094^{***}	0.0001	0.0061^{***}	-0.0081^{***}
(12)	-0.0048^{*}	0.0013	-0.0012	0.0006	-0.0008	-0.0006	0.0027	-0.0056^{***}
	09:00	10:00	11:00	12:00	13:00	14:00	15:00	16:00
(7)	0.0035^{***}	-0.0015^{***}	-0.0017^{***}	0.0003	0.0013^{***}	0.0019^{***}	0.0011^{***}	0.0002
(8)	0.0008^{*}	0.0006	0.0014^{***}	0.0002	0.0009^{**}	-0.0009^{*}	-0.0007	-0.001^{*}
(9)	0.0025^{***}	0.0019^{***}	0.0032^{***}	0.002^{***}	0.0025^{***}	0.0013^{**}	0.0037^{***}	0.0031^{***}
(10)	-0.0085^{***}	0.0002	-0.0043^{***}	-0.0025^{***}	-0.0024^{***}	-0.0058^{***}	-0.0041^{***}	0.0009
(11)	-0.0092^{***}	0.0049^{***}	0.0088^{***}	0.0031^{**}	-0.0019	-0.0073^{***}	-0.0046^{**}	-0.0036^{**}
(12)	-0.009^{***}	-0.0061^{***}	0.0007	0.0026	0.0015	-0.0006	0.001	0.0061^{***}
	17:00	18:00	19:00	20:00	21:00	22:00	23:00	24:00
(7)	-0.002^{***}	-0.0003	0.0049^{***}	0.0018^{***}	0.0003	-0.0007^{**}	0.0013^{***}	0.0011^{***}
(8)	-0.0001	-0.0015^{***}	-0.0034^{***}	-0.0011^{***}	-0.0013^{***}	-0.0008^{**}	0.00	-0.0009^{**}
(9)	0.0050^{***}	0.0020^{***}	0.0147^{***}	0.0034^{***}	0.0003	0.0045^{***}	0.0036^{***}	0.0046^{***}
(10)	-0.0084^{***}	-0.0011^{**}	0.0145^{***}	0.0077^{***}	0.0052^{***}	0.0039^{***}	0.0017^{***}	0.0006
(11)	0.0051^{***}	-0.0110^{***}	0.0035^{***}	0.0033^{**}	0.0029^{*}	-0.0041^{**}	-0.0005	-0.006^{***}
(12)	0.0053^{***}	0.0026	0.0085^{***}	0.008^{***}	0.0033^{**}	0.0083^{***}	-0.0022^{*}	-0.0022

$^{***} = p < 0.01, ^{**} = p < 0.05, ^{*} = p < 0.1$.

Table C.3: Mutivariate OLS robust estimates. Dependent variable: ΔP_t^S. Explanatory variables: Vol_{t-1}^{GF} (1), Vol_{t-1}^{GS} (2), Vol_{t-1}^{FG} (3), Vol_{t-1}^{FS} (4), Vol_{t-1}^{SG} (5), Vol_{t-1}^{SF} (6).

	01:00	02:00	03:00	04:00	05:00	06:00	07:00	08:00
(1)	-0.0001	-0.0003	-0.0001	-0.0002	-0.0002	-0.0002	-0.0015^{***}	-0.0004
(2)	-0.0006	-0.0006	-0.0007	0.0012	-0.0003	-0.0005	0.00	0.0002
(3)	0.0006	0.0005	0.0027^{***}	-0.0014^{**}	0.0002	-0.001	-0.0021^{***}	0.0005
(4)	-0.0018^{**}	0.0024^{**}	-0.0019^{*}	-0.0039^{***}	0.0003	-0.0018^{***}	0.0016	-0.0038^{***}
(5)	0.0005	-0.0001	0.0002	-0.0008	-0.001	0.0025^{***}	0.0018^{**}	0.0014^{**}
(6)	-0.0001	0.0008	0.0004	0.0007	-0.0035^{**}	0.0005	-0.0055^{***}	0.0014
	09:00	10:00	11:00	12:00	13:00	14:00	15:00	16:00
(1)	0.0008^{*}	0.00	0.0006	0.0010^{**}	-0.0002	-0.0015^{***}	0.0017^{***}	-0.0016^{***}
(2)	0.0003	0.0002	-0.0004	0.0039^{***}	0.0008^{***}	0.001^{***}	0.0003	0.0027^{***}
(3)	0.00	-0.0002	-0.0010	0.0011^{**}	-0.0014^{**}	-0.0022^{***}	-0.0027^{***}	-0.0022^{***}
(4)	-0.0018^{**}	-0.0019^{***}	-0.0027^{***}	-0.0063^{***}	0.0017^{***}	0.0021^{***}	-0.0007^{*}	-0.0006^{*}
(5)	0.0004	-0.0008^{*}	-0.0008^{*}	0.0004	0.0012^{**}	0.0029^{***}	0.0008	0.0109^{***}
(6)	-0.0026^{***}	0.0028^{***}	0.0005	0.003^{***}	0.0006	0.0016^{**}	-0.0009	0.0001
	17:00	18:00	19:00	20:00	21:00	22:00	23:00	24:00
(1)	0.0014^{***}	-0.0004	0.0007^{**}	-0.001^{***}	0.0003	0.00	0.0001	0.0014^{**}
(2)	-0.0015^{***}	-0.0002	-0.0006^{**}	0.0015^{***}	-0.0004	0.0002	-0.0001	-0.0004
(3)	-0.0005	0.0002	-0.0001	-0.0004	0.00	0.0003	-0.0003	0.0004
(4)	-0.0016^{***}	0.0010^{*}	0.0027^{***}	-0.0029^{***}	0.0008	-0.0012^{**}	0.0003	-0.0013^{***}
(5)	-0.0039^{***}	-0.0012^{***}	-0.0007^{**}	0.0007^{**}	0.0002	0.0003	0.0007^{*}	-0.0005
(6)	0.0005	-0.0004	0.0014^{**}	-0.0005	-0.0005	-0.0005	0.0010^{*}	-0.0038

$^{***} = p < 0.01, ^{**} = p < 0.05, ^{*} = p < 0.1.$

Table C.4: Mutivariate OLS robust estimates. Dependent variable: ΔP_t^S. Explanatory variables: Vol_{t-1}^{GO} (7), Vol_{t-1}^{OG} (8), Vol_{t-1}^{FO} (9), Vol_{t-1}^{OF} (10), Vol_{t-1}^{SO} (11), Vol_{t-1}^{OS} (12).

	01:00	02:00	03:00	04:00	05:00	06:00	07:00	08:00
(7)	0.0009^{**}	0.0006	0.0006^{*}	-0.0003	-0.0002	0.0009^{***}	0.0007^{**}	-0.0006^{*}
(8)	-0.0013^{**}	-0.0003	-0.0004	0.00	-0.0003	0.0004	0.0002	0.0004
(9)	0.0004	-0.001	-0.0002	0.0029^{***}	0.0057^{***}	-0.001	-0.0026^{***}	-0.0004
(10)	0.0001	-0.0001	0.0002	0.0001	0.00	0.0006	0.0042^{***}	0.00
(11)	0.0002	-0.0010	-0.0036	0.0054^{*}	0.0136^{***}	-0.0021	-0.0029	-0.0016
(12)	-0.0001	-0.0006	-0.0003	-0.003	-0.0014	-0.0019	-0.0035	0.0005
	09:00	10:00	11:00	12:00	13:00	14:00	15:00	16:00
(7)	-0.0019^{***}	0.0002	0.0009^{***}	-0.0047^{***}	-0.0027^{***}	-0.0001	0.0004	-0.001^{***}
(8)	0.0002	0.0014^{***}	0.0024^{***}	0.0002	0.0015^{***}	0.0002	0.00	-0.0023^{***}
(9)	0.0011	0.0016^{**}	0.0001	0.0051^{***}	0.0002	0.0002	-0.0005	0.0004
(10)	0.0004	-0.0006	-0.0001	-0.0015^{**}	0.0010	-0.0013^{*}	0.0001	-0.0032^{***}
(11)	0.0072^{***}	0.0037^{**}	-0.0003	-0.0007	-0.004^{***}	-0.0029^{*}	0.0035^{*}	-0.003^{*}
(12)	-0.0036^{**}	-0.0132^{***}	-0.0002	-0.0003	0.0006	-0.0049^{***}	0.0013	0.0043^{***}
	17:00	18:00	19:00	20:00	21:00	22:00	23:00	24:00
(7)	0.00	0.0008^{***}	-0.0002	0.0012^{***}	0.0002	-0.0001	0.0004	0.0006^{**}
(8)	0.0005	0.0005	0.0008^{**}	0.0005	-0.0001	-0.0005	-0.0006	0.0009^{**}
(9)	0.0017^{***}	-0.0015^{***}	0.0035^{***}	0.0002	0.0012^{**}	-0.0008	0.0002	-0.0002
(10)	0.0044^{***}	-0.0005	-0.0002	-0.0003	-0.0011^{*}	0.0003	0.00	0.0008
(11)	0.003^{*}	-0.0019	0.0025^{*}	0.0035^{**}	0.0001	0.0018	-0.0010	-0.0054^{***}
(12)	0.0013	-0.0036^{**}	0.0075^{***}	-0.0044^{**}	0.0008	-0.0028^{**}	0.0003	-0.0009

$^{***} = p < 0.01, ^{**} = p < 0.05, ^{*} = p < 0.1$.

Table C.5: Mutivariate OLS robust estimates. Dependent variable: ΔP_t^G. Explanatory variables: Vol_{t-1}^{GF} (1), Vol_{t-1}^{GS} (2), Vol_{t-1}^{FG} (3), Vol_{t-1}^{FS} (4), Vol_{t-1}^{SG} (5), Vol_{t-1}^{SF} (6).

	01:00	02:00	03:00	04:00	05:00	06:00	07:00	08:00
(1)	-0.0013^{*}	-0.0012^{*}	0.0005	-0.0002	-0.0001	-0.0022^{***}	-0.0010^{**}	-0.0016^{***}
(2)	0.0068^{***}	0.0012	0.0062^{***}	0.008^{***}	0.0074^{***}	0.0068^{***}	-0.0011^{*}	0.0029^{***}
(3)	-0.0017^{***}	0.00	-0.0043^{***}	-0.0019^{***}	-0.0023^{***}	-0.0005	0.0048^{***}	-0.0003
(4)	-0.003^{***}	-0.0013	0.0034^{***}	-0.0028^{**}	-0.0038^{***}	0.0023^{**}	-0.0041^{***}	0.0001
(5)	-0.0036^{***}	-0.0052^{***}	-0.0039^{***}	-0.0038^{***}	-0.0043^{***}	-0.0056^{***}	-0.0086^{***}	-0.0065^{***}
(6)	-0.0032^{***}	-0.0010	-0.0039^{***}	-0.0072^{***}	-0.0082^{***}	-0.0049^{***}	0.005^{***}	-0.0056^{***}
	09:00	10:00	11:00	12:00	13:00	14:00	15:00	16:00
(1)	-0.0006	-0.0005	-0.0013^{***}	-0.0020^{**}	-0.0013^{***}	0.0039^{***}	0.0088^{***}	0.0054^{***}
(2)	0.0068^{***}	0.0018^{***}	0.0023^{***}	0.0122^{***}	0.0056^{***}	0.0033^{***}	0.0063^{***}	0.0047^{***}
(3)	0.0044^{***}	0.0004	-0.0047^{***}	-0.0053^{***}	-0.0026^{***}	-0.0063^{***}	-0.0076^{***}	-0.0024^{***}
(4)	-0.005^{***}	0.0028^{***}	0.0025^{***}	-0.0033^{***}	-0.0010^{**}	-0.0046^{***}	-0.0015^{***}	0.00
(5)	-0.0054^{***}	-0.0022^{***}	-0.003^{***}	-0.004^{***}	-0.0070^{***}	-0.0033^{***}	0.0007	0.0030^{***}
(6)	-0.0020^{**}	-0.0019^{***}	-0.0024^{***}	-0.0022^{***}	-0.007^{***}	-0.0009	-0.0048^{***}	-0.0109^{***}
	17:00	18:00	19:00	20:00	21:00	22:00	23:00	24:00
(1)	0.0066^{***}	0.0047^{***}	0.0046^{***}	0.0041^{***}	0.0005	0.0027^{***}	-0.0004	0.0009
(2)	0.0046^{***}	0.0029^{***}	0.0032^{***}	0.0045^{***}	0.0043^{***}	0.0056^{***}	0.0044^{***}	0.003^{***}
(3)	-0.0020^{***}	0.0011^{***}	0.0006^{*}	-0.0018^{***}	0.0007^{*}	0.0005	0.0010^{**}	0.0011^{***}
(4)	0.0001	0.0004	0.0024^{***}	0.0020^{***}	0.0069^{***}	0.0003	0.0003	0.0017^{***}
(5)	0.0053^{***}	-0.0047^{***}	-0.0076^{***}	-0.0012^{***}	-0.0040^{***}	-0.0047^{***}	-0.0032^{***}	-0.0051^{***}
(6)	-0.0038^{***}	-0.0051^{***}	-0.0002	-0.0028^{***}	-0.0009	-0.0066^{***}	-0.0056^{***}	-0.0013^{**}

$^{***} = p < 0.01, ^{**} = p < 0.05, ^{*} = p < 0.1$.

Table C.6: Mutivariate OLS robust estimates. Dependent variable: ΔP_t^G. Explanatory variables: Vol_{t-1}^{GO} (7), Vol_{t-1}^{OG} (8), Vol_{t-1}^{FO} (9), Vol_{t-1}^{OF} (10), Vol_{t-1}^{SO} (11), Vol_{t-1}^{OS} (12).

	01:00	02:00	03:00	04:00	05:00	06:00	07:00	08:00
(7)	0.0047^{***}	0.0036^{***}	0.0035^{***}	0.0039^{***}	0.0015^{***}	0.0019^{***}	0.0027^{***}	0.0032^{***}
(8)	-0.0043^{***}	-0.002^{***}	-0.0039^{***}	-0.0033^{***}	-0.0046^{***}	-0.0036^{***}	-0.0027^{***}	-0.0022^{***}
(9)	0.0044^{***}	0.005^{***}	-0.0017^{**}	-0.0064^{***}	0.0036^{***}	0.0013	0.0044^{***}	0.0047^{***}
(10)	-0.0009	-0.0028^{***}	0.0010	-0.0049^{***}	-0.0010	0.0048^{***}	0.0015^{*}	-0.0022^{***}
(11)	-0.0109^{***}	-0.006^{***}	-0.0058^{**}	0.0001	0.0031	0.0061^{***}	-0.0197^{***}	-0.0163^{***}
(12)	-0.0016	-0.0034^{*}	-0.0128^{***}	-0.0021	0.0075^{***}	0.0178^{***}	0.0298^{***}	0.0123^{***}
	09:00	10:00	11:00	12:00	13:00	14:00	15:00	16:00
(7)	0.0054^{***}	0.0035^{***}	0.004^{***}	0.0066^{***}	0.0041^{***}	0.0042^{***}	0.003^{***}	0.0035^{***}
(8)	-0.0066^{***}	-0.0028^{***}	-0.0039^{***}	-0.0048^{***}	-0.0042^{***}	-0.0064^{***}	-0.0103^{***}	-0.0093^{***}
(9)	-0.0041^{***}	-0.0016^{**}	-0.0022^{***}	-0.0056^{***}	-0.0063^{***}	-0.0027^{***}	-0.0029^{***}	0.0031^{***}
(10)	0.0024^{***}	0.0006	0.0094^{***}	-0.0028^{***}	0.0050^{***}	0.0029^{***}	-0.0016^{**}	-0.0022^{***}
(11)	-0.0016	-0.0063^{***}	-0.0184^{***}	-0.0095^{***}	0.0040^{***}	-0.0034^{*}	-0.0068^{***}	-0.0106^{***}
(12)	0.0056^{***}	0.0114^{***}	-0.0003	-0.0095^{***}	-0.0075^{***}	-0.0003	0.0020	0.0044^{***}
	17:00	18:00	19:00	20:00	21:00	22:00	23:00	24:00
(7)	0.0007^{***}	0.0032^{***}	0.0045^{***}	0.0061^{***}	-0.0011^{***}	0.0016^{***}	0.0036^{***}	0.0017^{***}
(8)	-0.0064^{***}	-0.0009^{*}	-0.0038^{***}	-0.0062^{***}	-0.0037^{***}	-0.0017^{***}	-0.0009^{**}	-0.0058^{***}
(9)	-0.0035^{***}	-0.0013^{**}	-0.0031^{***}	-0.0003	0.0016^{***}	0.0027^{***}	0.0038^{***}	-0.0010^{*}
(10)	-0.0023^{***}	-0.0001	0.0014^{***}	-0.0008^{*}	0.0010^{*}	-0.0012^{**}	0.0039^{***}	0.0014^{**}
(11)	-0.0206^{***}	-0.0165^{***}	0.0172^{***}	-0.0167^{***}	-0.0037^{**}	-0.0026	-0.0088^{***}	-0.0237^{***}
(12)	-0.0009	-0.0010	0.0125^{***}	0.0326^{***}	0.0163^{***}	0.0077^{***}	0.0027^{**}	0.0061^{***}

$^{***} = p < 0.01, ^{**} = p < 0.05, ^{*} = p < 0.1$.

Table C.7: Stepwise OLS robust estimates. Dependent variable: ΔP_t^F. Explanatory variables: Vol_{t-1}^{GF} (1), Vol_{t-1}^{GS} (2), Vol_{t-1}^{FG} (3), Vol_{t-1}^{FS} (4), Vol_{t-1}^{SG} (5), Vol_{t-1}^{SF} (6).

	01:00	02:00	03:00	04:00	05:00	06:00	07:00	08:00
(1)	0	0	-0.0016^{***}	0	0	0	0	0
(2)	0	0	0	0	-0.0013^{**}	0	0	0
(3)	0	0	0	0	-0.0012^{**}	0	0	0
(4)	0.0042^{***}	0.0039^{***}	0	0	0.0048^{***}	-0.0022^{**}	0	0.004^{***}
(5)	0	0	0	0	0	0	0	0
(6)	-0.0018^{**}	0	0	0	0	0	0	0
	09:00	10:00	11:00	12:00	13:00	14:00	15:00	16:00
(1)	-0.0016^{**}	0	0	0	0	0	0	0
(2)	0	0	0	0	0	0	0	0
(3)	0	0	0	0	0	0	0	0
(4)	0	0	0	0.0030^{***}	0.0036^{***}	0.0035^{***}	0.0032^{***}	0.0027^{***}
(5)	0	0	0	0	0	0	0	0
(6)	0	-0.0050^{***}	0	0	0	-0.0025^{**}	0	0
	17:00	18:00	19:00	20:00	21:00	22:00	23:00	24:00
(1)	0	0	-0.0026^{***}	0	0	0	0	0
(2)	0	0	0.0016^{***}	0	0	0	0	0
(3)	0	0	0	0	0	0	0	0
(4)	0.0041^{***}	0.0046^{***}	0.0074^{***}	0.0030^{**}	0.0016^{**}	0.0016^{***}	0.0024^{***}	0.0022^{***}
(5)	0	0	0	0	0	0	0	0
(6)	0	-0.0021^{**}	0	-0.0029^{***}	-0.0028^{***}	0	-0.0026^{***}	-0.0022^{***}

$^{***} = p < 0.01, ^{**} = p < 0.05, ^{*} = p < 0.1$.

Table C.8: Stepwise OLS robust estimates. Dependent variable: ΔP_t^F. Explanatory variables: Vol_{t-1}^{GO} (7), Vol_{t-1}^{OG} (8), Vol_{t-1}^{FO} (9), Vol_{t-1}^{OF} (10), Vol_{t-1}^{SO} (11), Vol_{t-1}^{OS} (12).

	01:00	02:00	03:00	04:00	05:00	06:00	07:00	08:00
(7)	0	0	0.0005^{**}	0	0	0	0	0
(8)	0	0	0	0	0	0	0	0
(9)	0	0	0	0	0	0	0	0.0039^{***}
(10)	-0.0025^{**}	-0.0039^{***}	0	0	0	-0.0011^{**}	0	-0.0017^{**}
(11)	0	0	0	0	0	0	0	0
(12)	0	0	0	0	0	0	0	0
	09:00	10:00	11:00	12:00	13:00	14:00	15:00	16:00
(7)	0	0	0	0	0	0	0	0
(8)	0	0	0	0	0	0	0	0
(9)	0.0041^{***}	0	0	0	0.0017^{**}	0	0.0022^{***}	0.0022^{***}
(10)	0	0	-0.003^{**}	-0.0023^{***}	-0.0029^{**}	-0.0028^{**}	0	0
(11)	0	0	0	0.0048^{**}	0	0	0	0
(12)	0	0	0	0	0	0	0	0
	17:00	18:00	19:00	20:00	21:00	22:00	23:00	24:00
(7)	0	0	0	0	0	-0.0009^{***}	0.0008^{**}	0
(8)	0	-0.0013^{**}	0	0.0012^{**}	0	0	0	0
(9)	0.0019^{**}	0.0024^{***}	0	0.0028^{***}	0	0.0038^{***}	0	0.0023^{***}
(10)	0	0	0	-0.0019^{**}	0	-0.0015^{***}	0	0
(11)	0	-0.0072^{***}	0	0	0	0	0	-0.0071^{***}
(12)	0	0	0	0	0	0.0028^{**}	0	0

$^{***} = p < 0.01, ^{**} = p < 0.05, ^{*} = p < 0.1$.

Table C.9: Stepwise OLS robust estimates. Dependent variable: ΔP_t^S. Explanatory variables: Vol_{t-1}^{GF} (1), Vol_{t-1}^{GS} (2), Vol_{t-1}^{FG} (3), Vol_{t-1}^{FS} (4), Vol_{t-1}^{SG} (5), Vol_{t-1}^{SF} (6).

	01:00	02:00	03:00	04:00	05:00	06:00	07:00	08:00
(1)	0.0004^{***}	0	0	0	0	0	-0.0004^{***}	0
(2)	0	0	0	0	0	0	0	0
(3)	0	0	0	0	0	0	0	0
(4)	-0.0006^{***}	0	0	0	0	0	0	0
(5)	0	0	0	0	0	0	0	0
(6)	0	0	0	0	-0.0016^{***}	-0.0012^{**}	0.0017^{***}	0.0025^{***}
	09:00	10:00	11:00	12:00	13:00	14:00	15:00	16:00
(1)	0	0	0.0012^{**}	-0.0019^{***}	0	0	0.0009^{***}	-0.0013^{***}
(2)	0	0	0	0.001^{***}	0	0	0	0
(3)	0	0	0	0	0	0	-0.0007^{**}	0
(4)	-0.001^{**}	0	-0.0021^{***}	0	0	0	-0.0007^{**}	-0.001^{**}
(5)	0	0	0	0	0	0	0	0
(6)	0	0.0028^{**}	0	0	0.0014^{**}	0	0	0
	17:00	18:00	19:00	20:00	21:00	22:00	23:00	24:00
(1)	0	0	0	0	0	0	0	0
(2)	0	0	0	0	0	0	-0.0002^{***}	0
(3)	0	0	0	0	0	0	0	0
(4)	-0.001^{***}	0	0.0015^{***}	0	0	0	-0.0005^{***}	0
(5)	0	-0.0007^{***}	-0.0006^{**}	0	0	0	0	-0.0004^{**}
(6)	0	0.0009^{**}	0	0	0.0005^{***}	0	0.0005^{**}	0

$^{***} = p < 0.01, ^{**} = p < 0.05, ^{*} = p < 0.1.$

Table C.10: Stepwise OLS robust estimates. Dependent variable: ΔP_t^S. Explanatory variables: Vol_{t-1}^{GO} (7), Vol_{t-1}^{OG} (8), Vol_{t-1}^{FO} (9), Vol_{t-1}^{OF} (10), Vol_{t-1}^{SO} (11), Vol_{t-1}^{OS} (12).

	01:00	02:00	03:00	04:00	05:00	06:00	07:00	08:00
(7)	-0.0003^{***}	0	0	0	0	0	0.0002^{**}	-0.0003^{**}
(8)	-0.0003^{**}	0	0	0	0	0	0	0
(9)	0	0	0	0	0.0013^{***}	0	0	-0.0007^{***}
(10)	0	0	0	0	0	0	0	0
(11)	0	0	-0.0018^{***}	0	-0.0028^{***}	0	0	0
(12)	0	0	0	0	-0.002^{***}	0	-0.0017^{**}	0
	09:00	10:00	11:00	12:00	13:00	14:00	15:00	16:00
(7)	0	0	0	0	0	0	0	0
(8)	0	0	0	0	0	0	0	0
(9)	0.0009^{**}	0	0	0.0018^{***}	0	0	0	0
(10)	0	0	0	-0.0012^{**}	0	0	-0.0013^{**}	0
(11)	0	0	0	0	0	0	0	0
(12)	0.0027^{***}	-0.0134^{***}	0	0	0	-0.0051^{***}	0	0
	17:00	18:00	19:00	20:00	21:00	22:00	23:00	24:00
(7)	0	0	-0.0005^{**}	0	0	0	0	0
(8)	0	0	0.0013^{***}	0	0	0	0	0
(9)	0.001^{**}	0	0.0009^{**}	0	0	0	0	0
(10)	0	0	0	0	0	0	0	0.0007^{***}
(11)	0	0	0.0043^{***}	0	0	0	0.0012^{***}	0
(12)	0.0027^{**}	0	0	0	0	0	0	0

$^{***} = p < 0.01, ^{**} = p < 0.05, ^{*} = p < 0.1.$

Table C.11: Stepwise OLS robust estimates. Dependent variable: ΔP_t^G. Explanatory variables: Vol_{t-1}^{GF} (1), Vol_{t-1}^{GS} (2), Vol_{t-1}^{FG} (3), Vol_{t-1}^{FS} (4), Vol_{t-1}^{SG} (5), Vol_{t-1}^{SF} (6).

	01:00	02:00	03:00	04:00	05:00	06:00	07:00	08:00
(1)	0	0	0	0	0	0	0	0
(2)	0.0056^{**}	0	0.0063^{**}	0.0075^{***}	0.0087^{***}	0.0067^{**}	0	0.0042^{***}
(3)	0	0	-0.0047^{**}	0	0	0	0.005^{**}	0
(4)	0	0	0	0	0	0	0	0
(5)	-0.0055^{***}	-0.0079^{***}	-0.006^{**}	0	0	-0.007^{**}	-0.0117^{***}	-0.0068^{***}
(6)	0	0	0	-0.0105^{**}	0	0	0	0
	09:00	10:00	11:00	12:00	13:00	14:00	15:00	16:00
(1)	0	0	0	0	0	0	0	0.005^{***}
(2)	0.0043^{***}	0	0	0	0	0	0.0064^{***}	0
(3)	0	0	0	0	0	0	-0.006^{***}	0
(4)	0	0	0	0	0	0	0	0
(5)	0	-0.0029^{**}	-0.0040^{**}	0	-0.0077^{***}	0	0	-0.0060^{**}
(6)	-0.0108^{***}	0	0	0	-0.0065^{***}	0	0	-0.0076^{***}
	17:00	18:00	19:00	20:00	21:00	22:00	23:00	24:00
(1)	0.0044^{***}	0	0	0	0	0	0	0
(2)	0.0026^{**}	0	0.0044^{***}	0.0048^{***}	0.0038^{***}	0.0041^{***}	0.003^{***}	0.0042^{***}
(3)	0	0	0	0	0	0	0	0
(4)	0	0	0	0	0	0	0	0
(5)	0	-0.0047^{***}	-0.0051^{***}	-0.0052^{***}	-0.0049^{***}	-0.0042^{***}	-0.0037^{***}	-0.0056^{***}
(6)	0	0	0	0	0	-0.0059^{***}	-0.0051^{**}	0

$^{***} = p < 0.01, ^{**} = p < 0.05, ^{*} = p < 0.1$.

Table C.12: Stepwise OLS robust estimates. Dependent variable: ΔP_t^G. Explanatory variables: Vol_{t-1}^{GO} (7), Vol_{t-1}^{OG} (8), Vol_{t-1}^{FO} (9), Vol_{t-1}^{OF} (10), Vol_{t-1}^{SO} (11), Vol_{t-1}^{OS} (12).

	01:00	02:00	03:00	04:00	05:00	06:00	07:00	08:00
(7)	0.0039^{***}	0.0024^{**}	0	0.0035^{***}	0	0	0	0
(8)	-0.0053^{***}	0	-0.0037^{***}	-0.0044^{***}	-0.0041^{***}	-0.0036^{***}	0	-0.0032^{**}
(9)	0	0	0	0	0	0	0	0
(10)	0	0	0	0	0	0	0	0
(11)	0	0	0	0	0	0	0	0
(12)	0	0	0	0	0	0.0169^{**}	0.0248^{**}	0
	09:00	10:00	11:00	12:00	13:00	14:00	15:00	16:00
(7)	0.0048^{***}	0.0031^{***}	0.0045^{***}	0.0058^{***}	0.0047^{***}	0.0058^{***}	0.0052^{***}	0.0048^{***}
(8)	-0.006^{***}	0	0	-0.004^{**}	0	-0.0053^{**}	-0.0068^{***}	-0.0067^{***}
(9)	0	0	0	0	0	0	-0.0038^{**}	0
(10)	0	0	0.006^{**}	0	0	0	0	0
(11)	0	0	-0.0195^{**}	-0.0149^{**}	0	0	0	0
(12)	0	0	0	0	0	0	0	0
	17:00	18:00	19:00	20:00	21:00	22:00	23:00	24:00
(7)	0	0.0045^{***}	0.0054^{***}	0.0041^{***}	0	0.0024^{**}	0.0026^{**}	0
(8)	0	0	0	0	0	0	0	-0.0052^{***}
(9)	0	0	0	0	0	0	0	0
(10)	0	0	0	0	0	0	0	0
(11)	0	-0.0144^{**}	0	0	0	0	0	0
(12)	0	0	0	0.0152^{**}	0	0.0083^{**}	0	0

$^{***} = p < 0.01, ^{**} = p < 0.05, ^{*} = p < 0.1$.

C.2 Proofs

Proof of Prop. 4.4.1

Since the argument of the sup in (4.4.9) is quadratic in $\boldsymbol{\nu}$, and $\omega_k \geq 0 \; \forall \, k \in \{\mathrm{F}, \mathrm{S}, \mathrm{G}\}$, the sup attains a maximum. It is then trivial to obtain the first order condition (FOC) for the vector of controls $\boldsymbol{\nu}$.

Substituting the feedback control forms of $\boldsymbol{\nu}^*$ into (4.4.9), we get

$$
\begin{aligned}
0 &= \partial_t V(t,\mathbf{P}) + \mathcal{L}V(t,\mathbf{P}) \\
&+ \left[\frac{1}{2}\,\boldsymbol{\Upsilon}^{-1}\left(\boldsymbol{H}^\intercal V_P(t,\boldsymbol{P}) + \boldsymbol{B}^\intercal \boldsymbol{P}_t + \boldsymbol{f(t)}\right)\right]^\intercal \left(\boldsymbol{H}^\intercal V_P(t,\boldsymbol{P}) + \boldsymbol{B}^\intercal \boldsymbol{P}_t + \boldsymbol{f(t)}\right) \\
&- \left[\frac{1}{2}\,\boldsymbol{\Upsilon}^{-1}\left(\boldsymbol{H}^\intercal V_P(t,\boldsymbol{P}) + \boldsymbol{B}^\intercal \boldsymbol{P}_t + \boldsymbol{f(t)}\right)\right]^\intercal \boldsymbol{\Upsilon} \left[\frac{1}{2}\,\boldsymbol{\Upsilon}^{-1}\left(\boldsymbol{H}^\intercal V_P(t,\boldsymbol{P}) + \boldsymbol{B}^\intercal \boldsymbol{P}_t + \boldsymbol{f(t)}\right)\right] \;,
\end{aligned}
$$

with

$$
\begin{aligned}
\mathcal{L}V(t,\boldsymbol{P}) = \left(\boldsymbol{\theta} - \boldsymbol{\Phi}\,\mathbf{P}_t\right)^\intercal V_P(t,\boldsymbol{P}) + \frac{1}{2}\mathrm{Tr}\left[\,\boldsymbol{\Omega}\,\mathcal{H}\,\right] \\
+ \sum_{k=1}^{n} \lambda_k \int_{-\infty}^{+\infty} \Delta_k(y) V(t,\mathbf{P}) \frac{1}{\sqrt{2\pi}\xi_k} \mathrm{e}^{\frac{-(y-\psi_k)^2}{2\xi_k^2}}\,\mathrm{d}y \;.
\end{aligned}
$$

Collecting terms in $\left[\frac{1}{2}\,\boldsymbol{\Upsilon}^{-1}\left(\boldsymbol{H}^\intercal V_P(t,\boldsymbol{P}) + \boldsymbol{B}^\intercal \boldsymbol{P}_t\right)\right]^\intercal$, we obtain

$$
\begin{aligned}
0 &= \partial_t V(t,\mathbf{P}) + \mathcal{L}V(t,\mathbf{P}) \\
&+ \frac{1}{4}\left[\boldsymbol{H}^\intercal V_P(t,\boldsymbol{P}) + \boldsymbol{B}^\intercal \boldsymbol{P}_t + \boldsymbol{f(t)}\right]^\intercal \boldsymbol{\Upsilon}^{-1}\left[\boldsymbol{H}^\intercal V_P(t,\boldsymbol{P}) + \boldsymbol{B}^\intercal \boldsymbol{P}_t + \boldsymbol{f(t)}\right] \;.
\end{aligned}
$$

Proof of Prop. 4.4.2

Using the ansatz (4.4.13) into (4.4.11), and collecting terms in powers of P and constant terms, after some computations, we obtain the following system

of 10 ordinary differential equations (ODEs):

$$
\begin{aligned}
0 &= \frac{1}{2}\partial_t E_{11}(t) + \frac{(\eta_1^a(t)+1)^2 + \left(\eta_1^b(t)-1\right)^2}{4(k_1+k_2)} + \frac{(\eta_1^c(t)-1)^2 + \left(\eta_1^d(t)+1\right)^2}{4(k_1+k_3)} \\
&\quad + \frac{\eta_1^e(t)^2 + \eta_1^f(t)^2}{4(k_2+k_3)} - \Phi_{11}E_{11}(t) - \Phi_{21}E_{12}(t) - \Phi_{31}E_{13}(t) \ , \\
0 &= \frac{1}{2}\partial_t E_{22}(t) + \frac{(\eta_2^a(t)-1)^2 + \left(\eta_2^b(t)+1\right)^2}{4(k_1+k_2)} + \frac{\eta_2^c(t)^2 + \eta_2^d(t)^2}{4(k_1+k_3)} \\
&\quad + \frac{(\eta_2^e(t)+1)^2 + \left(\eta_2^f(t)-1\right)^2}{4(k_2+k_3)} - \Phi_{12}E_{12}(t) - \Phi_{22}E_{22}(t) - \Phi_{32}E_{23}(t) \ , \\
0 &= \frac{1}{2}\partial_t E_{33}(t) + \frac{\eta_3^a(t)^2 + \eta_3^b(t)^2}{4(k_1+k_2)} + \frac{(\eta_3^c(t)+1)^2 + \left(\eta_3^d(t)-1\right)^2}{4(k_1+k_3)} \\
&\quad + \frac{(\eta_3^e(t)-1)^2 + \left(\eta_3^f(t)+1\right)^2}{4(k_2+k_3)} - \Phi_{13}E_{13}(t) - \Phi_{23}E_{23}(t) - \Phi_{33}E_{33}(t) \ , \\
0 &= \partial_t D_1(t) + \frac{B_a(t)\left(\eta_1^a(t)+1\right) + B_b(t)\left(\eta_1^b(t)-1\right)}{2(k_1+k_2)} \\
&\quad + \frac{B_c(t)\left(\eta_1^c(t)-1\right) + B_d(t)\left(\eta_1^d(t)+1\right)}{2(k_1+k_3)} + \frac{B_e(t)\eta_1^e(t) + B_f(t)\eta_1^f(t)}{2(k_2+k_3)} \\
&\quad + E_{11}(t)\theta_1 - \Phi_{11}D_1(t) + E_{12}(t)\theta_2 - \Phi_{21}D_2(t) + E_{13}(t)\theta_3 - \Phi_{31}D_3(t) \ , \\
0 &= \partial_t D_2(t) + \frac{B_a(t)\left(\eta_2^a(t)-1\right) + B_b(t)\left(\eta_2^b(t)+1\right)}{2(k_1+k_2)} + \frac{B_c(t)\eta_2^c(t) + B_d(t)\eta_2^d(t)}{2(k_1+k_3)} \\
&\quad + \frac{B_e(t)\left(\eta_2^e(t)+1\right) + B_f(t)\left(\eta_2^f(t)-1\right)}{2(k_2+k_3)} + E_{12}(t)\theta_1 - \Phi_{12}D_1(t) + E_{22}(t)\theta_2 \\
&\quad - \Phi_{22}D_2(t) + E_{23}(t)\theta_3 - \Phi_{32}D_3(t) \ , \\
0 &= \partial_t D_3(t) + \frac{B_a(t)\eta_3^a(t) + B_b(t)\eta_3^b(t)}{2(k_1+k_2)} + \frac{B_c(t)\left(\eta_3^c(t)+1\right) + B_d(t)\left(\eta_3^d(t)-1\right)}{2(k_1+k_3)} \\
&\quad + \frac{B_e(t)\left(\eta_3^e(t)-1\right) + B_f(t)\left(\eta_3^f(t)+1\right)}{2(k_2+k_3)} + E_{13}(t)\theta_1 - \Phi_{13}D_1(t) + E_{23}(t)\theta_2 \\
&\quad - \Phi_{23}D_2(t) + E_{33}(t)\theta_3 - \Phi_{33}D_3(t) \ , \\
0 &= \partial_t E_{12}(t) + \frac{\left(\eta_1^a(t)+1\right)\left(\eta_2^a(t)-1\right) + \left(\eta_1^b(t)-1\right)\left(\eta_2^b(t)+1\right)}{2(k_1+k_2)} \\
&\quad + \frac{\left(\eta_1^c(t)-1\right)\eta_2^c(t) + \left(\eta_1^d(t)+1\right)\eta_2^d(t)}{2(k_1+k_3)} + \frac{\eta_1^e(t)\left(\eta_2^e(t)+1\right) + \eta_1^f(t)\left(\eta_2^f(t)-1\right)}{2(k_2+k_3)} \\
&\quad - \Phi_{11}E_{12}(t) - \Phi_{12}E_{11}(t) - \Phi_{21}E_{22}(t) - \Phi_{22}E_{12}(t) - \Phi_{31}E_{23}(t) - \Phi_{32}E_{13}(t) \ ,
\end{aligned}
$$

$$
\begin{aligned}
0 = {} & \partial_t E_{13}(t) + \frac{\left(\eta_1^a(t)+1\right)\eta_3^a(t) + \left(\eta_1^b(t)-1\right)\eta_3^b(t)}{2(k_1+k_2)} \\
& + \frac{\left(\eta_1^c(t)-1\right)\left(\eta_3^c(t)+1\right) + \left(\eta_1^d(t)+1\right)\left(\eta_3^d(t)-1\right)}{2(k_1+k_3)} \\
& + \frac{\eta_1^e(t)\left(\eta_3^e(t)-1\right) + \eta_1^f(t)\left(\eta_3^f(t)+1\right)}{2(k_2+k_3)} - \Phi_{11}E_{13}(t) - \Phi_{13}E_{11}(t) - \Phi_{21}E_{23}(t) \\
& - \Phi_{23}E_{12}(t) - \Phi_{31}E_{33}(t) - \Phi_{33}E_{13}(t) \ , \\
0 = {} & \partial_t E_{23}(t) + \frac{\eta_3^a(t)\left(\eta_2^a(t)-1\right) + \eta_3^b(t)\left(\eta_2^b(t)+1\right)}{2(k_1+k_2)} \\
& + \frac{\eta_2^c(t)\left(\eta_3^c(t)+1\right) + \eta_2^d(t)\left(\eta_3^d(t)-1\right)}{2(k_1+k_3)} \\
& + \frac{\left(\eta_2^e(t)+1\right)\left(\eta_3^e(t)-1\right) + \left(\eta_2^f(t)-1\right)\left(\eta_3^f(t)+1\right)}{2(k_2+k_3)} - \Phi_{12}E_{13}(t) - \Phi_{13}E_{12}(t) \\
& - \Phi_{22}E_{23}(t) - \Phi_{23}E_{22}(t) - \Phi_{32}E_{33}(t) - \Phi_{33}E_{23}(t) \ , \\
0 = {} & \partial_t A(t) + \frac{B_a(t)^2 + B_b(t)^2}{4(k_1+k_2)} + \frac{B_c(t)^2 + B_d(t)^2}{4(k_1+k_3)} + \frac{B_e(t)^2 + B_f(t)^2}{4(k_2+k_3)} + D_1(t)\theta_1 \\
& + D_2(t)\theta_2 + D_3(t)\theta_3 + \frac{1}{2}E_{11}(t)\lambda_1\left(\sigma_{J_1}^2 + \psi_1^2\right) + \frac{1}{2}E_{22}(t)\lambda_2\left(\sigma_{J_2}^2 + \psi_2^2\right) \\
& + \frac{1}{2}E_{33}(t)\lambda_3\left(\sigma_{J_3}^2 + \psi_3^2\right) + \frac{1}{2}\left(\sigma_{11}^2 + \sigma_{12}^2 + \sigma_{13}^2\right)E_{11}(t) + \frac{1}{2}\left(\sigma_{21}^2 + \sigma_{22}^2 + \sigma_{23}^2\right)E_{22}(t) \\
& + \frac{1}{2}\left(\sigma_{31}^2 + \sigma_{32}^2 + \sigma_{33}^2\right)E_{33}(t) + \left(\sigma_{21}\sigma_{11} + \sigma_{22}\sigma_{12} + \sigma_{23}\sigma_{13}\right)E_{12}(t) \\
& + \left(\sigma_{31}\sigma_{11} + \sigma_{32}\sigma_{12} + \sigma_{33}\sigma_{13}\right)E_{13}(t) + \left(\sigma_{31}\sigma_{21} + \sigma_{32}\sigma_{22} + \sigma_{33}\sigma_{23}\right)E_{23}(t) \ ;
\end{aligned}
$$

where

$$
B_x(t) = \sum_{i=1}^{3} h_i^x D_i(t) \ , \qquad \eta_i^x = \sum_{j=1}^{3} h_j^x E_{ij}(t) \ .
$$

and with terminal condition

$$
A(T) = D_1(T) = D_2(T) = D_3(T) = E_{11}(T) = E_{12}(T) = \cdots = E_{33}(T) = 0 \ .
$$

However, we were not able to find an explicit solution to the system written

in this way. Instead, we decided to re-write the system in matrix form. Thus, we get:

$$V_t = A'(t) + \boldsymbol{D}'^{\intercal}(t)\boldsymbol{P} + \boldsymbol{P}^{\intercal}\boldsymbol{E}'(t)\boldsymbol{P}\,, \tag{C.1}$$

$$\begin{aligned} V_{P_i} &= D_i + \frac{\partial \cdot}{\partial P_i}\sum_{j,k=1}^{n} E_{jk}P_jP_k = D_i + \sum_{j,k=1}^{n} E_{jk}\frac{\partial \cdot}{\partial P_i}(P_jP_i) = \\ &= D_i + \sum_{j,k=1}^{n} E_{jk}\left(\mathbb{1}_{j\neq k=i}P_j + \mathbb{1}_{i=j\neq k}P_k + \mathbb{1}_{i=j=k}2P_i\right) = \\ &= D_i + \sum_{j=1}^{n} E_{ji}P_j + \sum_{k=1}^{n} E_{ik}P_k \end{aligned}$$

$$\Rightarrow V_P = \boldsymbol{D} + (\boldsymbol{E}^{\intercal}(t) + \boldsymbol{E}(t))\boldsymbol{P} = \boldsymbol{D} + 2\boldsymbol{E}(t)\boldsymbol{P}\,, \tag{C.2}$$

$$V_{PP} = \boldsymbol{E}^{\intercal}(t) + \boldsymbol{E}(t) = 2\boldsymbol{E}(t)\,, \tag{C.3}$$

where the last step both in (C.2) and in (C.3) follows from the fact that we are assuming $\mathbf{E}(t)$ to be a symmetric matrix.

Inserting the derivatives (C.1)-(C.3) into the PIDE (4.4.11), we get

$$\begin{aligned} &A'(t) + \boldsymbol{D}'^{\intercal}(t)\boldsymbol{P} + \boldsymbol{P}^{\intercal}\boldsymbol{E}'(t)\boldsymbol{P} + \mathcal{L}V(t,\boldsymbol{P}) \\ &+ \frac{1}{4}\left[\boldsymbol{H}^{\intercal}V_P(t,\boldsymbol{P}) + \boldsymbol{B}^{\intercal}\boldsymbol{P}_t + \boldsymbol{f(t)}\right]^{\intercal}\boldsymbol{\Upsilon}^{-1}\left[\boldsymbol{H}^{\intercal}V_P(t,\boldsymbol{P}) + \boldsymbol{B}^{\intercal}\boldsymbol{P}_t + \boldsymbol{f(t)}\right] = \\ &= A'(t) + \boldsymbol{D}'^{\intercal}(t)\boldsymbol{P} + \boldsymbol{P}^{\intercal}\boldsymbol{E}'(t)\boldsymbol{P} + \mathcal{L}V(t,\boldsymbol{P}) \\ &+ \frac{1}{4}\left\{\boldsymbol{H}^{\intercal}\left[\boldsymbol{D} + (\boldsymbol{E}^{\intercal}(t) + \boldsymbol{E}(t))\boldsymbol{P}\right] + \boldsymbol{B}^{\intercal}\boldsymbol{P} + \boldsymbol{f(t)}\right\}^{\intercal}\boldsymbol{\Upsilon}^{-1}\cdot \\ &\cdot\left\{\boldsymbol{H}^{\intercal}\left(\boldsymbol{D} + (\boldsymbol{E}^{\intercal}(t) + \boldsymbol{E}(t))\boldsymbol{P}\right) + \boldsymbol{B}^{\intercal}\boldsymbol{P} + \boldsymbol{f(t)}\right\} = 0\,, \end{aligned} \tag{C.4}$$

where $\mathcal{L}$ is the infinitesimal generator obtained under the optimal control,

corresponding to

$$\begin{aligned}\mathcal{L}V(t,\boldsymbol{P}) &= (\boldsymbol{\theta}-\boldsymbol{\Phi}\,\mathbf{P}_t)^{\intercal}\,V_P(t,\boldsymbol{P})+\frac{1}{2}\mathrm{Tr}\left[\,\boldsymbol{\Omega}^{\intercal}\mathcal{H}\,\boldsymbol{\Omega}\,\right]+\int_{-\infty}^{+\infty}J\cdot\Delta V(t,\boldsymbol{P})\,\mathrm{d}y=\\ &=(\boldsymbol{\theta}-\boldsymbol{\Phi}\,\mathbf{P}_t)^{\intercal}\left[\boldsymbol{D}+(\boldsymbol{E}^{\intercal}(t)+\boldsymbol{E}(t))\boldsymbol{P}\right]+\frac{1}{2}\mathrm{Tr}\left[\,\boldsymbol{\Omega}\,(\boldsymbol{E}^{\intercal}(t)+\boldsymbol{E}(t))\,\right]\\ &+\int_{-\infty}^{+\infty}J\cdot\Delta V(t,\boldsymbol{P})\,\mathrm{d}y=\\ &=(\boldsymbol{\theta}^{\intercal}-\mathbf{P}_t^{\intercal}\,\boldsymbol{\Phi}^{\intercal})\,(\boldsymbol{D}+2\boldsymbol{E}(t)\boldsymbol{P})+\mathrm{Tr}\left[\,\boldsymbol{\Omega}\,\boldsymbol{E}(t)\,\right]+\int_{-\infty}^{+\infty}J\cdot\Delta V(t,\boldsymbol{P})\,\mathrm{d}y\ ,\end{aligned}$$

where, with a slight abuse of notation,

$$\int_{-\infty}^{+\infty}J\cdot\Delta V(t,\boldsymbol{P})\,\mathrm{d}y=\sum_{i=1}^{n}\lambda_i\int_{-\infty}^{+\infty}\Delta_i(y)V(t,\mathbf{P})\frac{1}{\sqrt{2\pi}\xi_i}\mathrm{e}^{\frac{-(y-\psi_i)^2}{2\xi_i^2}}\,\mathrm{d}y\,.$$

Jump part:

$$\Delta_i(y)V(t,\mathbf{P})=V(t,\mathbf{P}+y\mathbb{1}_i)-V(t,\mathbf{P})\quad\forall\,i\in\{1,...,n\}\ ,$$

where the indicator function $\mathbb{1}_i$ is defined as

$$\mathbb{1}_1=(1,0,\cdots,0)^{\intercal}\ ,\qquad\mathbb{1}_2=(0,1,\cdots,0)^{\intercal}\ ,\ \cdots\ ,\ \mathbb{1}_n=(0,0,\cdots,1)^{\intercal}\ .$$

Thus, we have:

$$\begin{aligned}V(t,\mathbf{P}+y\mathbb{1}_i)=A(t)+\boldsymbol{D}^{\intercal}(t)\mathbf{P}+D_i(t)\,y+\mathbf{P}^{\intercal}\boldsymbol{E}(t)\mathbf{P}+\\ +y\mathbb{1}_i^{\intercal}\boldsymbol{E}(t)\mathbf{P}+\mathbf{P}^{\intercal}\boldsymbol{E}(t)y\mathbb{1}_i+y^2\mathbb{1}_i^{\intercal}\boldsymbol{E}(t)\mathbb{1}_i\,,\end{aligned}$$

and

$$\begin{aligned}\Delta_i(y)V(t,\mathbf{P})&=D_i(t)y+\sum_{j=1}^{n}P_jE_{ij}(t)y+\sum_{j=1}^{n}P_jE_{ji}(t)y+E_{ii}(t)y^2=\\ &=D_i(t)y+2\sum_{j=1}^{n}P_jE_{ij}(t)y+E_{ii}(t)y^2\ ,\end{aligned}\tag{C.5}$$

where the last step follows from the fact that we are assuming $\mathbf{E}$(t) to be a

symmetric matrix. Thus,

$$\int_{-\infty}^{+\infty} J \cdot \Delta V(t, \boldsymbol{P})\, \mathrm{d}y = \sum_{i=1}^{n} \lambda_i \int_{-\infty}^{+\infty} \Delta_i(y) V(t, \mathbf{P}) \frac{1}{\sqrt{2\pi}\xi_i} \mathrm{e}^{\frac{-(y-\psi_i)^2}{2\xi_i^2}}\, \mathrm{d}y = \\ = \sum_{i=1}^{n} \lambda_i \left[\left(D_i(t) + 2 \sum_{j=1}^{n} P_j E_{ij}(t) \right) \psi_i + E_{ii}(t) \left(\xi_i^2 + \psi_i^2 \right) \right], \tag{C.6}$$

where the last step follows from $\mathbb{E}(Y) = \int_{-\infty}^{+\infty} y f(y)\, \mathrm{d}y = \psi$, and from $\mathbb{E}(Y^2) = Var(Y) + \mathbb{E}(Y)^2 = \xi^2 + \psi^2$. Finally, we get:

$$\int_{-\infty}^{+\infty} J \cdot \Delta V(t, \boldsymbol{P})\, \mathrm{d}y = \left[\boldsymbol{D}^\intercal(t) + 2\boldsymbol{P}^\intercal \boldsymbol{E}(t) \right] (\boldsymbol{\lambda} \circ \boldsymbol{\psi}) + \boldsymbol{\psi}^\intercal diag(\boldsymbol{E}(t)) (\boldsymbol{\lambda} \circ \boldsymbol{\psi}) \\ + \boldsymbol{\xi}^\intercal diag(\boldsymbol{E}(t)) (\boldsymbol{\lambda} \circ \boldsymbol{\xi}), \tag{C.7}$$

where $\circ$ denotes the Hadamard product between two vectors, and $diag(\boldsymbol{E}(t))$ is a matrix with the elements on the main diagonal equal to those on the main diagonal of $\boldsymbol{E}(t)$, and with all other elements equal to zero, such that

$$diag(\boldsymbol{E}(t)) = \begin{pmatrix} E_{11}(t) & 0 & \cdots & 0 \\ 0 & E_{22}(t) & 0 & \vdots \\ \vdots & 0 & \ddots & 0 \\ 0 & \cdots & 0 & E_{nn}(t) \end{pmatrix}. \qquad \square$$

Now, collecting quadratic and linear terms of P and constant terms in

(C.4), we obtain the following three equations:

$$
\begin{aligned}
0 &= \boldsymbol{E}'(t) + \frac{1}{2}\boldsymbol{E}^{\intercal}(t)\boldsymbol{H}\,\boldsymbol{\Upsilon}^{-1}\boldsymbol{B}^{\intercal} + \frac{1}{2}\boldsymbol{B}\,\boldsymbol{\Upsilon}^{-1}\boldsymbol{H}^{\intercal}\boldsymbol{E}(t) - 2\boldsymbol{\Phi}^{\intercal}\boldsymbol{E}(t) + \boldsymbol{E}^{\intercal}(t)\boldsymbol{H}\,\boldsymbol{\Upsilon}^{-1}\boldsymbol{H}^{\intercal}\boldsymbol{E}(t) \\
&\quad + \frac{1}{4}\boldsymbol{B}\,\boldsymbol{\Upsilon}^{-1}\boldsymbol{B}^{\intercal} \\
&= \boldsymbol{E}'(t) + \frac{1}{2}\boldsymbol{E}^{\intercal}(t)\boldsymbol{H}\,\boldsymbol{\Upsilon}^{-1}\boldsymbol{B}^{\intercal} + \left(\frac{1}{2}\boldsymbol{H}\,\boldsymbol{\Upsilon}^{-1}\boldsymbol{B}^{\intercal}\right)^{\intercal}\boldsymbol{E}(t) - \boldsymbol{\Phi}^{\intercal}\boldsymbol{E}(t) - \boldsymbol{\Phi}^{\intercal}\boldsymbol{E}(t) \\
&\quad + \boldsymbol{E}^{\intercal}(t)\boldsymbol{H}\,\boldsymbol{\Upsilon}^{-1}\boldsymbol{H}^{\intercal}\boldsymbol{E}(t) + \frac{1}{4}\boldsymbol{B}\,\boldsymbol{\Upsilon}^{-1}\boldsymbol{B}^{\intercal} \\
&= \boldsymbol{E}'(t) + \boldsymbol{E}^{\intercal}(t)\left(\frac{1}{2}\boldsymbol{H}\,\boldsymbol{\Upsilon}^{-1}\boldsymbol{B}^{\intercal} - \boldsymbol{\Phi}\right) + \left(\frac{1}{2}\boldsymbol{H}\,\boldsymbol{\Upsilon}^{-1}\boldsymbol{B}^{\intercal} - \boldsymbol{\Phi}\right)^{\intercal}\boldsymbol{E}(t) \\
&\quad + \boldsymbol{E}^{\intercal}(t)\boldsymbol{H}\,\boldsymbol{\Upsilon}^{-1}\boldsymbol{H}^{\intercal}\boldsymbol{E}(t) + \frac{1}{4}\boldsymbol{B}\,\boldsymbol{\Upsilon}^{-1}\boldsymbol{B}^{\intercal}\ ; \qquad \text{(C.8)}
\end{aligned}
$$

$$
\begin{aligned}
0 &= \boldsymbol{D}'(t) + \boldsymbol{E}^{\intercal}(t)\boldsymbol{H}\,\boldsymbol{\Upsilon}^{-1}\left(\boldsymbol{H}^{\intercal}\boldsymbol{D}(t) + \boldsymbol{f}(t)\right) + \frac{1}{2}\boldsymbol{B}\,\boldsymbol{\Upsilon}^{-1}\left(\boldsymbol{H}^{\intercal}\boldsymbol{D}(t) + \boldsymbol{f}(t)\right) \\
&\quad + 2\boldsymbol{E}(t)(\boldsymbol{\theta} + \boldsymbol{\lambda}\circ\boldsymbol{\psi}) - \boldsymbol{\Phi}^{\intercal}\boldsymbol{D} \\
&= \boldsymbol{D}'(t) + \left(\frac{1}{2}\boldsymbol{H}\,\boldsymbol{\Upsilon}^{-1}\boldsymbol{B}^{\intercal} - \boldsymbol{\Phi}\right)^{\intercal}\boldsymbol{D}(t) + \boldsymbol{E}^{\intercal}(t)\boldsymbol{H}\,\boldsymbol{\Upsilon}^{-1}\boldsymbol{H}^{\intercal}\boldsymbol{D}(t) \\
&\quad + 2\boldsymbol{E}(t)(\boldsymbol{\theta} + \boldsymbol{\lambda}\circ\boldsymbol{\psi}) + \boldsymbol{E}^{\intercal}(t)\boldsymbol{H}\boldsymbol{\Upsilon}^{-1}\boldsymbol{f}(t) + \frac{1}{2}\boldsymbol{B}\boldsymbol{\Upsilon}^{-1}\boldsymbol{f}(t)\ ; \qquad \text{(C.9)}
\end{aligned}
$$

$$
\begin{aligned}
0 &= A'(t) + \frac{1}{4}\left(\boldsymbol{D}^{\intercal}(t)\boldsymbol{H} + \boldsymbol{f}^{\intercal}(t)\right)\boldsymbol{\Upsilon}^{-1}\left(\boldsymbol{H}^{\intercal}\boldsymbol{D}(t) + \boldsymbol{f}(t)\right) + \mathrm{Tr}\left[\boldsymbol{\Omega}\,\boldsymbol{E}(t)\right] \\
&\quad + \boldsymbol{D}^{\intercal}(t)\left(\boldsymbol{\theta} + \boldsymbol{\lambda}\circ\boldsymbol{\psi}\right) + \boldsymbol{\psi}^{\intercal}diag(\boldsymbol{E}(t))\left(\boldsymbol{\lambda}\circ\boldsymbol{\psi}\right) + \boldsymbol{\xi}^{\intercal}diag(\boldsymbol{E}(t))\left(\boldsymbol{\lambda}\circ\boldsymbol{\xi}\right), \qquad \text{(C.10)}
\end{aligned}
$$

with terminal condition

$$A(T) = \boldsymbol{D}(T) = \boldsymbol{E}(T) = 0\ .$$

The last step in (C.8) is where we need the restriction on $\boldsymbol{\Phi}$ we previously imposed when defining the price dynamics. In fact, if and only if $\boldsymbol{\Phi}$ is a symmetric matrix, we can apply Gombani and Runggaldier (2013) and solve the matrix Riccati equation (C.8), writing the solution to $E(t)$ as follows:

$$E(t) = Y(t)X(t)^{-1}\,, \qquad \text{(C.11)}$$

where X and Y satisfy the following linear differential equation:

$$\frac{\partial}{\partial t}\begin{pmatrix} X \\ Y \end{pmatrix} = \begin{pmatrix} \frac{1}{2}\boldsymbol{H}\boldsymbol{\Upsilon}^{-1}\boldsymbol{B}^{\intercal} - \boldsymbol{\Phi} & \boldsymbol{H}\boldsymbol{\Upsilon}^{-1}\boldsymbol{H}^{\intercal} \\ -\frac{1}{4}\boldsymbol{B}\boldsymbol{\Upsilon}^{-1}\boldsymbol{B}^{\intercal} & -\left(\frac{1}{2}\boldsymbol{H}\boldsymbol{\Upsilon}^{-1}\boldsymbol{B}^{\intercal} - \boldsymbol{\Phi}\right)^{\intercal} \end{pmatrix}\begin{pmatrix} X \\ Y \end{pmatrix}, \tag{C.12}$$

with final condition

$$\begin{pmatrix} X(T) \\ Y(T) \end{pmatrix} = \begin{pmatrix} I \\ E(T) \end{pmatrix}. \tag{C.13}$$

We thus get

$$\begin{pmatrix} X(t) \\ Y(t) \end{pmatrix} = \exp\left[(T-t)\begin{pmatrix} -\frac{1}{2}\boldsymbol{H}\boldsymbol{\Upsilon}^{-1}\boldsymbol{B}^{\intercal} + \boldsymbol{\Phi} & -\boldsymbol{H}\boldsymbol{\Upsilon}^{-1}\boldsymbol{H}^{\intercal} \\ \frac{1}{4}\boldsymbol{B}\boldsymbol{\Upsilon}^{-1}\boldsymbol{B}^{\intercal} & \left(\frac{1}{2}\boldsymbol{H}\boldsymbol{\Upsilon}^{-1}\boldsymbol{B}^{\intercal} - \boldsymbol{\Phi}\right)^{\intercal} \end{pmatrix}\right]\begin{pmatrix} X(T) \\ Y(T) \end{pmatrix}. \tag{C.14}$$

We thus have the solution for $E(t)$, and, using a corollary in Gombani and Runggaldier (2013), we can also compute the solution of $D(t)$, which is given by

$$D(t) = X^{\intercal}(t)^{-1}D(T) + \int_0^t \left[X(t)^{-1}\right]^{\intercal} X^{\intercal}(s)\left[2\boldsymbol{E}(s)(\boldsymbol{\theta} + \boldsymbol{\lambda}\circ\boldsymbol{\psi}) + \boldsymbol{E}(s)\boldsymbol{H}\boldsymbol{\Upsilon}^{-1}\boldsymbol{f}(s) + \frac{1}{2}\boldsymbol{B}\boldsymbol{\Upsilon}^{-1}\boldsymbol{f}(s)\right]\mathrm{d}s\,.$$

Finally, we can solve (C.10):

$$A(t) = A(T) + \int_t^T \frac{1}{4}\left(\boldsymbol{D}^{\intercal}(s)\boldsymbol{H} + \boldsymbol{f}^{\intercal}(s)\right)\boldsymbol{\Upsilon}^{-1}\left(\boldsymbol{H}^{\intercal}\boldsymbol{D}(s) + \boldsymbol{f}(s)\right) + \mathrm{Tr}\left[\boldsymbol{\Omega}\,\boldsymbol{E}(s)\right] + \boldsymbol{D}^{\intercal}(s)\left(\boldsymbol{\theta} + \boldsymbol{\lambda}\circ\boldsymbol{\psi}\right) + \boldsymbol{\psi}^{\intercal}diag(\boldsymbol{E}(s))\left(\boldsymbol{\lambda}\circ\boldsymbol{\psi}\right) + \boldsymbol{\xi}^{\intercal}diag(\boldsymbol{E}(s))\left(\boldsymbol{\lambda}\circ\boldsymbol{\xi}\right)\mathrm{d}s\,. \tag{C.15}$$

Bibliography

Abadie, L. M. , Chamorro, J. M., and González-Eguino, M. (2011). *Optimal abandonment of EU coal-fired stations*. The Energy Journal, 32 (**3**): 175–207, 2011.

Alfonsi, A., Fruth, A., Schied, A. (2010) *Optimal execution strategies in limit order books with general shape functions*. Quantitative Finance, vol. 10(2): 143-157.

Autorità di Regolazione per Energia Reti e Ambiente ARERA (2018). *Modifiche e integrazioni ai criteri e alle condizioni per la disciplina del sistema di remunerazione della disponibilità di capacità produttiva di energia elettrica introdotto dall'autorità con deliberazione arg/elt 98/11*. Resolution 261/2018/R/EEL, issued on April 11.

Benth, F. E., Kallsen, J., Meyer-Brandis, T. (2007) *A non-Gaussian Ornstein-Uhlenbeck process for electricity spot price modeling and derivatives pricing*. Applied Mathematical Finance 14(2): 153-169.

Benth, F. E., Šaltytė Benth, J., and Koekebakker, S. (2008). *Stochastic Modelling of Electricity and Related Markets*. Advanced Series on Statistical Science & Applied Probability, 11, World Scientific Publishing Co. Pte. Ltd., Hackensack, NJ, 2008.

Benth, F. E., Kiesel, R., and Nazarova, A. (2012). *A critical empirical study of three electricity spot price models*. Energy Economics, 34 (5): 1589–1616.

Benth, F. E., Piccirilli, M., Vargiolu, T. (2017) *Additive energy forward curves in a Heath-Jarrow-Morton framework*. Working paper.

Biondi, T. and Moretto, M. (2015). *Solar Grid Parity dynamics in Italy: a real option approach*. Energy, 80: 293–302, 2015.

Bjork, T. (1998). *Arbitrage Theory in Continuous Time*. Oxford University Press 1998.

Brauneis, A., Mestel, R. and Palan, S. (2013). *Inducing low-carbon investment in the electric power industry through a price floor for emissions trading*. Energy Policy, 53: 190–204, 2013.

Carmona, R. and Durrleman, V. (2003). *Pricing and Hedging Spread Options*. SIAM Review **45 (4)**: 627–685, 2003.

Carr, P. and Madan, D. B. (1999). *Option valuation using the fast Fourier transform*. Journal of Computational Finance, 2: 61–73, 1999.

Cartea, Á., Figueroa, M. (2005) *Pricing in Electricity Markets: a mean reverting jump diffusion model with seasonality*. Applied Mathematical Finance, 12(4): 313–335.

Cartea, Á., González-Pedraz, C. (2012) *How much should we pay for interconnecting electricity markets? A real option approach*. Energy Economics, 34: 14–30.

Cartea, Á., Jaimungal, S. (2016a) *Algorithmic Trading of Co-Integrated Assets*. International Journal of Theoretical and Applied Finance, vol. 19, issue 6.

Cartea, Á., Jaimungal, S. (2016b) *Incorporating order-flow into optimal execution*. Mathematics and Financial Economics, vol. 10(3): 339–364.

Cartea, Á., Jaimungal, S., Penalva, J. (2015) *Algorithmic and high frequency trading* (1st ed.) Cambridge: Cambridge University Press.

Cartea, Á., Jaimungal, S., Qin, Z. (2016) *Speculative trading of electricity contracts in interconnected locations*. Available at SSRN 2870814.

Chevallier, J. (2012). *Time-varying correlations in oil, gas and CO2 prices: an application using BEKK, CCC and DCC-MGARCH models*. Applied Economics, 44 (**32**): 4257–4274, 2012.

Cramton, P., Ockenfels, A., and Stoft, S. (2013). *Capacity Market Fundamentals*. Economics of Energy & Environmental Policy, **2(2)**: 28–48.

Cramton, P., and Stoft, S. (2007). *Colombia Firm Energy Market*. Proceedings of the Hawaii International Conference.

Creti, A., and Fontini, F. (2018). *Electricity Economics*. Cambridge University Press, forthcoming.

Dixit, A. K., and Pindyck, R. S. (1994). *Investment under Uncertainty*. Princeton University Press, Princeton, N.J., 1994.

EC, European Commission (2018). *State Aid SA.42011 (2017/N) - Italy - Italian Capacity Mechanism*. Document C(2018) 617 final, published on February 7, 2018 but released to the general public in April 2018.

Edoli, E., Gallana, M., and Vargiolu, T. (2017). *Optimal intra-day power trading with a Gaussian additive process*. Journal of Energy Markets **10 (4)**: 23–42.

Edwards, D. W., (2009). *Energy Trading and Investing: Trading, Risk Management, And Structuring Deals In The Energy Markets*. McGraw-Hill Education.

Engle, R., Dufour, A. (2000) *Time and the price impact of a trade*. The Journal of Finance, 55 (6): 2467–2498.

Engle, R., Granger, C. (1987) *Co-integration and error correction: representation, estimation and testing*. Econometrica, 55: 251–276.

Federal Energy Regulatory Commission (2014). *Order on Tariff Filing and Instituting Section 206 Proceeding*. Docket No. ER14-1050-000, issued on May 30.

Finlay, R. (2009). *The Variance-Gamma (VG) model with Long Range Dependence*. School of Mathematics and Statistics, University of Sydney, 2009.

Fleming, W., Soner, M. (1993), *Controlled Markov Processes and Viscosity Solutions*. New York: Springer-Verlag.

Fraunhofer ISE (2015). *Current and Future Cost of Photovoltaics. Long-term Scenarios for Market Development, System Prices and LCOE of Utility-Scale PV Systems. Study on behalf of Agora Energiewende*. Fraunhofer ISE, 2015.

Geman, H., Roncoroni, A. (2006) *Understanding the fine structure of electricity prices*. The Journal of Business, 79 (3): 1225–1261.

Gombani, A., Runggaldier, W. J. (2013) *Arbitrage-free multifactor term structure models: a theory based on stochastic control*. Mathematical Finance, 23(4): 659–686.

Grüll, G. and Kiesel, R. (2012). *Quantifying the CO_2 permit price sensitivity*. Zeitschrift für Energiewirtschaft, 36(**2**): 101–111.

Grüll, G. and Taschini, L. (2011). *Cap-and-trade properties under different hybrid scheme designs*. Journal of Environmental Economics and Management, 61(**1**): 107–118, 2011.

GSE (2017). *Rapporto Statistico "Energia da Fonti Rinnovabili in Italia - 2015"*. Gestore Servizi Energetici (GSE), 2017.

Hasbrouck, J. (1991). *Measuring the information content of stock trades*. The Journal of Finance, 46(1): 179–207.

IEA (2008). *Energy Efficieny Indicators for Public Electricity Production from Fossil Fuels*. OECD IEA, Paris, 2008.

IEA (2014a). *Technology Roadmap: Solar Photovoltaic Energy*. OECD IEA, Paris, 2014.

IEA (2014b). *World Energy Investment Outlook 2014*. OECD/IEA, Paris, 2014.

IEA (2016). *Re-powering Markets – Market design and regulation during the transition to low-carbon power systems*. OECD/IEA, Paris, 2016.

IEA (2017a). *Renewable Information: Overview (2017 edition)*. OECD/IEA, Paris, 2017.

IEA (2017b). *IEA World Energy Balances 2017*. OECD IEA, Paris, 2017.

IEA (2018). *IEA World Energy Balances: Overview 2018*. OECD IEA, Paris, 2018.

IPCC (2006). *2006 IPCC Guidelines for National Greenhouse Gas Inventories*. IPCC, 2006.

Kiesel, R. and Paraschiv, F. (2016). *Econometric analysis of 15-minute intraday electricity prices*. Energy Economics, 64: 77–90, 2016.

Laurikka, H. and Koljonen, T. (2006). *Emissions trading and investment*

decisions in the power sector — a case study in Finland. Energy Policy, 34(**9**): 1063–1074, 2006.

Lee, R. W. (2004). *Option pricing by transform methods: extensions, unification, and error control*. Journal of Computational Finance, 7(**3**): 51–86, 2004.

Lei, Y., Xu, J. (2015) *Costly arbitrage through pairs trading*. Journal of Economic Dynamics and Control, 56: 1-19.

Leung, T., Li, X. (2015) *Optimal mean reversion trading with transaction costs and stop-loss exit*. International Journal of Theoretical and Applied Finance, 18(03).

Lintilhac, P. S., Tourin, A. (2017) *Model-based pairs trading in the bitcoin markets*. Quantitative Finance, 17(05): 703-716.

Longstaff, F. A. and Schwartz, E. S. (2001). *Valuing American options by simulation: a simple least-squares approach*. Review of Financial Studies, 14(**1**): 113–147, 2001.

Lucia, J. J., Schwartz, E. S. (2002) *Electricity prices and power derivatives: Evidence from the Nordic power exchange*. Review of Derivatives Research, 5: 5-50.

Lutz, B. (2010). *Pricing of Derivatives on Mean-Reverting Assets*. Lecture Notes in Economics and Mathematical Systems, **630**, Springer-Verlag Berlin Heidelberg 2010.

Madan, D. B., Carr, P. P., and Chang, E. C. (1998). *The Variance Gamma process and option pricing*. European Finance Review, 2: 79–105, 1998.

Mastropietro, P., Fontini, F., Rodilla, P., Batlle, C. (2017). *The Italian Capacity Remuneration Mechanism: Description and Open Questions*. Working Paper IIT-17-034A.

Mastropietro, P., Herrero, I., Rodilla, P., Batlle, C. (2016). *A model-based analysis on the impact of explicit penalty schemes in capacity mechanisms*. Applied Energy, 168: 406–417.

McDonald, R., Siegel, D. (1985). *Investment and the valuation of firms when there is an option to shut down*. International Economic Review **26 (2)**: 331–349.

Mudchanatongsuk, S., Primbs, J. A., Wong, W. (2008) *Optimal pairs trading: a stochastic control approach*. American Control Conference, June 11-13 2008: 1035–1039.

Øksendal, B., Sulem, A. (2007) *Applied stochastic control of jump diffusions*. 2nd ed., Springer.

Pascucci, A. (2011). *PDE and Martingale Methods in Option Pricing*. Springer-Verlag, Bocconi & Springer series, 2011.

Pilipovic, D. (1998) *Energy risk: valuing and managing energy derivatives*. New York: McGraw-Hill.

Protter, P. (2003) *Stochastic Integration and Differential Equations* 2^{nd} *edn*. Berlin Heidelberg: Springer.

Rodilla, P., Batlle, C. (2013). *Security of generation supply in electricity markets*. In: Regulation of the Power Sector, 2013, Springer, Perez-Arriaga, Ignacio J. (Ed.).

Roncoroni, A. (2002) *A class of marked point processes for modeling electricity prices*. PhD, Université Paris IX Dauphine.

Rosenberg, M., Bryngelson, J.D., Baron, M., Papalexopoulos, A.D. (2010) *Transmission valuation analysis based on real options with price spikes*. In: Rebennack S., Pardalos P., Pereira M., Iliadis N. (eds) Handbook of Power Systems II. Energy Systems. Springer, Berlin, Heidelberg.

Seifert, J., Uhrig-Homburg, M. (2007) *Modelling jumps in electricity prices: theory and empirical evidence*. Review of Derivatives Research, 10: 59–85.

Single Electricity Market Committee, SEM (2015). *Integrated Single Electricity Market (I-SEM) - Capacity Remuneration Mechanism Detailed Design - Decision Paper 1*. Decision Paper SEM-15-103, released on December 16.

Single Electricity Market Committee, SEM (2016a). *Integrated Single Electricity Market (I-SEM) - Capacity Remuneration Mechanism Detailed Design - Decision Paper 3*. Decision Paper SEM-16-039, released on July 8.

Single Electricity Market Committee, SEM (2016b). *Integrated Single Electricity Market (I-SEM) - Capacity Remuneration Mechanism Detailed Design - Decision Paper 2*. Decision Paper SEM-16-022, released on May 10.

Szolgayova, J., Fuss, S. and Obersteiner, M. (2008). *Assessing the effects of CO_2 price caps on electricity investments - A real options analysis.* Energy Policy, 36: 3974–3981, 2008.

Terna (2017a). *Schema di proposta di disciplina del sistema di remunerazione della disponibilità di capacità produttiva di energia elettrica.* Proposal, released in January 2017. Available at http://download.terna.it/terna/0000/0842/24.PDF.

Terna (2017b). *Relazione tecnica sullo schema di proposta di disciplina del sistema di remunerazione della disponibilità di capacità produttiva di energia elettrica.* Technical report accompanying the proposal, released in January 2017. Available at http://download.terna.it/terna/0000/0842/32.PDF.

Terna (2017c). *Metodologia per il calcolo del prezzo di esercizio.* Annex to Terna (2017a), released in January 2017. Available at http://download.terna.it/terna/0000/0842/29.PDF.

Tourin, A., Yan, R. (2013) *Dynamic pairs trading using the stochastic control approach.* Journal of Economic Dynamics and Control, 37(10): 1972-1981.

Vázquez, C., Rivier, M., Perez-Arriaga, I.J. (2002). *A Market Approach to Long-Term Security of Supply.* IEEE Transactions on Power Systems 17**(2)**: 349–357.

Weber, T. A. and Neuhoff, K. (2010). *Carbon markets and technological innovation.* Journal of Environmental Economics and Management, 60(**2**): 115–132, 2010.

Weron, R. (2007) *Modeling and forecasting electricity loads and prices: a statistical approach.* Volume 403, John Wiley & Sons.

Wood, P. J. and Jotzo, F. (2011). *Price floors for emissions trading.* Energy Policy, 39(**3**): 1746–1753, 2011.

Yang, M., Blyth, W., Bradley, R., Bunn, D., Clarke, C. and Wilson, T. (2008). *Evaluating the power investment options with uncertainty in climate policy.* Energy Economics, 30: 1933–1950, 2008.